THE ROLES OF CYCLIC ADENOSINE MONOPHOSPHATE (cAMP) AND APOLIPOPROTEIN A1 (ApoA1) IN AVIAN EYE GROWTH – A PROTEOMIC APPROACH

CHUN KA MAN

Ph.D

The Hong Kong Polytechnic University

2010

The Hong Kong Polytechnic University

School of Optometry

The roles of cyclic adenosine monophosphate (cAMP) and apolipoprotein A1 (ApoA1) in avian eye growth -a proteomic approach

Chun Ka-Man

A thesis submitted in partial fulfillment of the requirements for the Degree of Doctor of Philosophy

November 2009

CERTIFICATE OF ORIGINALITY

I hereby declare that this thesis is my own work and that, to the best of my knowledge and belief, it reproduces no material previously published or written, nor material that has been accepted for the award of any other degree or diploma, except where due acknowledgement has been made in the text.

_____ (Signed)

Chun Ka-Man (Name of student)

Abstract

The prevalence of myopia, as well as high myopia, in some Asian countries has been increasing in recent decades. High myopia is one of the leading causes of visual impairments due to its associated sight threatening conditions, such as retinal detachment and glaucoma. At present, the underlying mechanism of the development of myopia is still unclear.

The origin of myopia signals is thought to reside in the retina which will initiate biochemical changes and accelerate eye growth. Profiling the retinal proteomes of myopic chick may help to capture such changes in terms of protein expressions during myopic growth. The current study employed two-dimensional fluorescence difference gel electrophoresis (2-D DIGE) to profile the retinal proteins in lens-induced myopia (LIM) and form deprivation myopia (FDM). With the aid of a nano-liquid chromatography coupled tandem mass spectrometry (LC-MS/MS), a number of differentially expressed retinal proteins related to myopic growth were identified.

In eyes with three days of LIM, phosphoglycerate mutase 1 (brain) (PGAM) was up-regulated whereas apolipoprotein A1 (ApoA1) was decreased in expressions in myopic retinas. In terms of differentially expressed retinal proteins in three days of FDM by diffusers, there were six protein spots showing alternation in expressions. Only two of them were successfully identified. Up-regulation of destrin and down regulation of ApoA1 was shown in three days of FDM retinas by diffusers. Besides,

there was also up-regulation of destrin after three days of myopia induced by occluders.

After seven days of LIM and FDM, only six protein spots showed differential expressions and three of them were successfully identified. They belonged to destrin and PGAM that were both up-regulated in myopic retinas.

Since ApoA1 was the common protein spot found to be down-regulated consistently after three days of LIM and FDM, the role of ApoA1 in the development of myopia was further studied.

Intravitreal injections of nicotinic acid and bezafibrate, which could increase ApoA1 protein expression, were tested for their efficacies in reducing LIM. Nicotinic acid (60mM) was effective in reducing vitreous chamber depth and increasing the retinal ApoA1 expressions in LIM.

Localizations of retinal ApoA1 after LIM and lens-induced hyperopia (LIH) were carried out using immunohistochemistry. ApoA1 was more evident in the photoreceptor layer of myopic retina. In hyperopic eyes, ApoA1 was mainly located in inner limiting membrane and RPE. This is the first report showing differences in immunoreactivity of retinal ApoA1 in LIM and LIH.

Since cyclic adenosine monophosphate (cAMP) is one of the modulators of ApoA1 expression, the effect of cAMP on myopia development was explored. Intravitreal

injection of cAMP (1mM) analog was found to inhibit refractive errors and elongation of vitreous chamber depth in LIM. There was also an increase in retinal ApoA1 expression with intravitreal injection of cAMP. The results indicated cAMP may affect myopia development through ApoA1 expression.

In the last part of this study, the level of retinal cAMP under LIM and LIH was measured using enzyme immunoassay. There was no change in retinal cAMP in myopic eyes but the retinal cAMP level was raised significantly in LIH. Concurrently, the expression of retinal ApoA1 was also increased in LIH. The data suggested that cAMP may play a significant role in the cascade of reactions leading to produce the "STOP" signal in eye growth.

In conclusion, the present study profiled the changes in protein expressions in myopic retinas using 2-D DIGE. The data suggested that cAMP may modulate ApoA1 expression in chick retina and together they play an important and inhibitory role in the eye growth and development of myopia.

List of selected presentation and publications:

Conference presentations:

1. CHUN R.K.M., Li K.K., LAM T.C. and TO C.H. Proteome analysis of myopic chick sclera. Presented at 11th International Myopia Conference, Singapore, August 2006.
2. LAM T.C., CHUN R.K.M., LI K.K., DO C.W., LO S.C.L., GUGGENHEIM J.A. and TO C.H. A global retinal proteins expressions involving compensated myopia by proteomic approach. Presented at 11th International Myopia Conference, Singapore, August 2006.
3. CHUN R.K.M., Li K.K., LAM T.C. and TO C.H. Apolipoprotein A1 expression in form deprived chick retina. Presented at the Association for Research in Vision and Ophthalmology (ARVO), United States, May 2007.

Publication:

LAM, T. C., CHUN, R.K.M., LI, K. K. and TO, C. H. Application of proteomic technology in eye research: a mini review. Clin Exp Optom vol. 91, no. 1, pp. 23-33 (2008)

Acknowledgements

I would like to express my gratitude to my supervisor, Prof. Chi-ho To for his guidance and mentoring in my research study. He always showed his enthusiasm in research and gave lots of helpful suggestions on my thesis.

My special thanks to Prof. Patrizia Tarugi from Department of Biomedical Sciences, University of Modena and Reggio Emilia, Italy, who have donated the primary antibodies of apolipoprotein A1 generously. This project could not be possible without his generous help.

I am grateful in working with my lab-mates and colleagues Thomas, KK, Lung, Samantha, Sing and Dennis. They are always helpful and willing to share their ideas and suggestions. It is my pleasure working with them in the laboratory.

Finally, I would like to give sincere thanks to my husband Forrest and my family for their love, patience, prayers and understandings throughout these years.

TABLE OF CONTENTS

Lists of Figures

Chapter 1

Chapter 2

Chapter 3

Chapter 4

Chapter 5

Chapter 6

List of Tables

Chapter 2

Chapter 3

Chapter 4

Chapter 5

Abbreviations

℃	Degree in Celsius
2-DE	Two-dimensional electrophoresis
2-D DIGE	Two-dimensional fluorescence difference gel electrophoresis
AChE	Acetylcholinesterase
ADF	Actin depolymerizing factor
AP	Alkaline phosphatase
ApoA1	Apolipoprotein A1
ASB14	Myristic amidosulphobetaine
ABCA1	ATP binding cassette transporter 1
BSA	Bovine serum albumin
cAMP	Cyclic adenosine monophosphate
CCD	Charged-coupled device
CHAPS	3-[(3-Cholamidopropyl)dimethylammonio]-1-propanesulfonate
CHO	Choroid
D	Dioptre
DAB	3,3'-Diaminobenzidine
DAPI	4',6-diamidino-2-phenylindole
DOPAC	Dihydroxyphenylacetic acid
DTT	Dithiothreitol
Egr-1 / ZENK	Early growth response 1
EIA	Enzyme immunoassay
ELISA	Enzyme linked immunosorbent assay
Epac	Exchange protein directly activated by cAMP
ESI	Electrospray ionization
FDM	Form deprivation myopia
FG	Formoguanamine
g	Grams
GI	GenInfo Identifier
HDL	High density lipoprotein
HRP	Horseradish peroxidase
IEF	Isoelectric focusing
IHC	Immunohistochemistry
ILM	Inner limiting membrane
INL	Inner nuclear layer
IPL	Inner plexiform layer
IPGs	Immobilized pH gradients
LC-MS/MS	Nano liquid chromatography with tandem mass spectrometry
LE	Left eye
LIH	Lens-induced hyperopia
LIM	Lens-induced myopia
M	Molar
MALDI-TOF	Matrix-assisted laser desorption/ionization time of flight
MMPs	Matrix metalloproteinases
mRNA	Messenger ribonucleic acid
MS	Mass spectrometry/ mass spectrometer

Mw	Molecular weight
m/z	Mass-to-charge ratio
NIH	National Institute of Health
NO	Nitric oxide
ONL	Outer nuclear layer
OPL	Outer plexiform layer
PBS	Phospate buffered saline
PGAM	Phosphoglycerate mutase 1 (brain)
pI	Isoelectric point
PKA	Protein kinase A
PTM	Post translational modification
PVDF	Polyvinylidene difluoride
RA	Retinoic acid
RAR	Retinoic acid receptor
RE	Right eye
RET	Retina
RPE	Retinal pigment epithelium
SCL	Sclera
SDS-PAGE	Sodium dodecyl sulfate polyacrylamide gel electrophoresis
SE	Spherical equivalent
SMA	Smooth muscle actin
TCA	Trichloroacetic acid
TEMED	Tetramethylethylenediamine
TFA	Trifluoroacetic acid
TGF	Transforming growth factor
Tris	Tris (hydroxymethyl) aminomethane
TTX	Tetrodotoxin
VIP	Vasoactive intestinal peptide

m	milli- (10^{-3})
μ	micro- (10^{-6})
n	nano- (10^{-9})
p	pico- (10^{-12})

Chapter 1: Literature review

1.1 Myopia

1.1.1 Background

Myopia, or nearsightedness, is the most common refractive errors among human. The word, myopia, is derived from a Greek word, implying a closed or contracted eye as the myopes frequently squints to create a pinhole effect by closing the eyelids (Lawrence and Azar 2002). In myopia, the incident light rays are focused in front of the retina, instead of on the retina. Therefore the distant objects appear blurry in myopic eye. Myopia can be corrected by optical devices in the form of spectacles or contact lenses. Concave or negative lenses are used for redirecting the light rays and focusing on the retina. The degree of myopia is expressed in terms of dipoter (D) and it is the reciprocal of focal length measured in metres. High myopia is usually defined when the refractive error is more negative than -6.00 D (Percival 1987).

The prevalence of myopia has been escalating in recent years, especially in some Asian regions (Matsumura and Hirai 1999). It increased from 36.7% to 61% of aged 12 Taiwan children in 20 years since 1983 (Lin et al. 2004). More than 70% of 17 year-old youngsters in Hong Kong are myopic (Edwards and Lam 2004). Myopia also affected about 74% of high school students in Singapore (Quek et al. 2004) and Guangzhou (He et al. 2004). Myopic prevalence is rapidly increasing even in preschool children in Hong Kong. Over 40% of 7 year-old children became myopic in 5 years according to a longitudinal study (Fan et al. 2004). The prevalence of myopia in these Asian regions were higher than that in Europe, Australia and North

America (Kleinstein et al. 2003; Robaei et al. 2006; Czepita et al. 2007). The problem of myopia is now becoming a public health issue. Although vision can be improved by optical correction, high myopes have a high risk of having sight threatening diseases, such as retinal degeneration and glaucoma (Grossniklaus and Green 1992). These diseases may lead to permanent loss of vision. High myopia was amongst the leading causes of registered blindness in the developed countries (Rosenberg and Klie 1996). In addition to inconvenience caused by optical correction, heavy cost in treating and rehabilitating these myopia related sight threatening diseases may be incurred (Seet et al. 2001).

The majority of myopia is resulted from an excessive elongation of eyeball, so called axial myopia (Smith and Hung 2000). Myopia may also arise from refractive anomaly of cornea and lens.

Myopia is frequent suggested as a result of failure of the emmetropization process. Emmetropization is a vision dependent process that produces normal vision by matching the axial length of the eye to the optical power (Morgan 2003). The process is particularly active in young animals when the visual system is still plastic.

1.1.2 Excessive accommodation and myopia development

Excessive accommodation has long been suggested as a reason for excessive eye growth in myopia. This notion is initially supported by the fact that blocking the accommodation by atropine reduced the excessive elongation of eyeball in human

(Gruber 1985) and monkeys (Raviola and Wiesel 1985). However, McBrien et al. found that atropine prevented form deprivation myopia (FDM) in chicks through a non-accommodative mechanism as the accommodation of chicks was not blocked after the administration of atropine (McBrien et al. 1993). Since atropine is a non selective muscarinic antagonist, the use of more specific muscarinic antagonists is applied to investigate the site of action of atropine. Further study has shown M1 selective antagonist, pirenzepine, but not M2 or M3 antagonists reduced lens-induced myopia (LIM) in chicks (Rickers and Schaeffel 1995; Luft et al. 2003). Besides M1 receptors, the role of M4 receptors in preventing myopia was also suggested. Intravitreal injection of M4 selective antagonists, himbacine, in chicks was effective in inhibiting the development of myopia and it implicates the role of M4 receptors (Cottriall et al. 2001).

Moreover, studies on reading glasses or progressive addition lenses aiming to relax accommodation in human was unsuccessful in controlling the myopic progression (Shih et al. 2001; Edwards et al. 2002). Although some studies showed significant difference in retarding myopic progression, the difference was only 0.25 D (Leung and Brown 1999; Hasebe et al. 2008; Yang et al. 2009) which is not very clinically significant in terms of myopia control. In animal studies, blocking accommodation by cutting the ciliary or optic nerve did not prevent FDM (Troilo et al. 1987; Schmid and Wildsoet 1996; Wildsoet 2003). LIM was still present after elimination of accommodation through lesion of Edinger-Westphal nucleus in chicks (Troilo 1990).

Therefore, the role of excessive accommodation does not appear to be major in myopia development.

Clinical study has its limitations in exploring the underlying mechanism of myopia development as there are multiple factors that can contribute to myopia development in human. Socioeconomical status, outdoor activity, amount of near work may all play a role in myopia progression (Kinge et al. 2000; Saw et al. 2000). These parameters are relatively difficult to control and assess quantitatively in human studies. Animal myopia model offers an alternative for investigating the mechanism of myopia, since a variety of factors can be controlled so that their contributions can be teased out separately.

1.1.3 Animal models of myopia

A numbers of species have been used as animal models for myopia research. The most commonly used animals are chicks, albeit they were not the first animal being used (Wallman et al. 1978). Rabbits were the first animal being induced experimental myopia in 1966 (Maurice and Mushin 1966). Other species have also been used as animal models such as monkey (Wiesel and Raviola 1977), marmoset (Graham and Judge 1999), tree shrew (Sherman et al. 1977), guinea pig (McFadden et al. 2004), mouse (Tejedor and de la Villa 2003) and fish (Shen et al. 2005). Chicks have several advantages over the other species as an animal myopia model. Chicks have good optical opponents and visual acuity developed within 48 hours of hatchling (Over and Moore 1981). They are able to distinguish colors (Osorio et al.

1999). Their eyes are displaced laterally with independent accommodation. It is beneficial for investigating the mechanism of myopia development as it minimizes the interaction between two eyes. The growth rate of chicks is fast and the rearing cost is low compared to other species, especially primates. Moreover, chicks can detect and compensate for small focusing error of 1D (Schmid and Wildsoet 1997). These characteristics have made chicks a popular animal model for understanding myopia development. It is also prudent to test new hypothesis on chicks first before primates.

1.1.4 Form deprivation and lens-induced myopia

Myopia can be introduced to the chicks by deprivation of vision through negative lenses or translucent goggles (Fig.1.1). Typically, young chicks can emmetropize in the first six weeks after hatchling (Wallman et al. 1981). During this period, myopia can be induced by attachment of negative lenses and this is called lens-induced myopia (LIM). The amount of myopia induced depends on the refractive power of the lenses. The chick eye can completely compensate optical lenses between +15D to -10D (Irving et al. 1992).

Myopia can also be resulted from wearing translucent goggles or lid suture in chicks (Zhu et al. 1995) and tree shrews (Norton 1990). Deprivation of vision may cause myopia not only in animal model, but also in human. The corneal opacity in children acted as translucent goggle to deprive the children from vision. Different degree of

myopia were found depends on the age of onset of corneal opacity (Meyer et al. 1999). Similar observations was found in infants with neonatal ptosis and cataracts (Hoyt et al. 1981). The myopia induced in these circumstances is called form deprivation myopia (FDM). The plasticity or sensitivity to FDM or LIM declines with age (Irving et al. 1992).

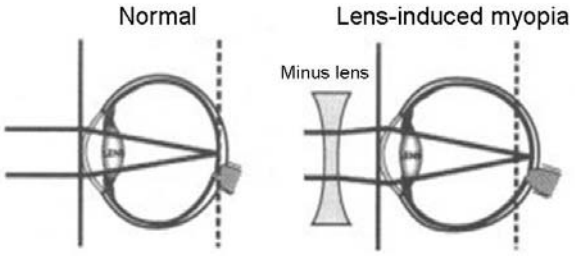

Fig.1.1 Schematic diagram of formation of lens-induced myopia (Modified and adopted from (Norton 1999).

1.1.5 Anatomical changes in form deprivation and lens-induced myopia

In both the FDM and LIM, the vitreous chamber depth of chick eye increases with myopia (Wallman et al. 1995). The retinas become thinner and the scleral thickness decreases significantly after two week of FDM or LIM (Beresford et al. 2001). The thickness of choroid also becomes thinner in myopic chicks. When positive lenses (+10D) were attached on the eyes, the choroid expanded in ten minutes in response to the myopic defocus applied (Zhu et al. 2005). The increase in choroidal thickness was also observed when myopic chicks stopped wearing the negative lenses or translucent goggles. The thickness of choroid was found to be increased by 10-fold in 72 hours after removal of two-week FDM (Liang et al. 2004). During recovery, the eyes received myopic defocus, as in lens-induced hyperopia (LIH) (Junghans et

al. 1999), and the vitreous chamber depth decreased and the eyes became less myopic.

Besides the alteration of choroidal thickness during myopia or recovery from myopia, the choroidal blood flow also varied with different visual manipulations. The choroidal blood flow was reduced by about 30% after two weeks of form deprivation (Shih et al. 1993). It was increased after FDM was removed from the chicks. It was found that the increase in choroidal blood flow preceded the thickening of choroidal thickness during the recovery form myopia (Fitzgerald et al. 2002). Therefore, it is plausible to speculate that the choroidal blood flow may have initiated the choroidal thickening during recovery from myopia.

Experimentally, the changes in choroidal blood flow can be eliminated by choroidal nerve sections. However, in eyes with choroidal nerve section, FDM could not be completely prevented (Shih et al. 1994). Since FDM could still be induced, it argues against a major role of choroidal blood flow in myopia development. Choroidal blood flow may play a role in facilitating the changes in choroidal thickness, rather than initiating the changes.

Protein concentrations of suprachoroidal space in myopia and recovery from myopia have also been intensely investigated as a possible cause of choroidal thickening. Suprachoroidal space is the space between the choriocapillaries and sclera. It contains many thin-walled, endothelial-lined vessels that are similar to lymphatic vessels. It contains clear fluid that is deprived of blood cells (De Stefano and

Mugnaini 1997). The amount of protein in suprachoroidal space decreased significantly in myopic eye and it increased again during the recovery from myopia (Pendrak et al. 2000).

However, only the changes in total protein concentrations were reported and the types of proteins in suprachoroidal space have not been identified.

Sclera underwent a numbers of changes during the development of myopia. In chicks, the thickness of fibrous sclera decreased which was associated with a reduced rate of proteoglycan synthesis and collagen accumulation (Rada et al. 2006). There was an increase in matrix metalloproteinase-2 (MMP-2) expression in sclera. MMP-2 is a member of neutral proteinase that initiates the degradation of collagens and other extracellular matrix components (Woessner 1994). As far as the biomechanics of sclera was concerned, the scleral elasticity was increased in myopic eye. The creep rate, which indicates tissue extension with time, increased during myopia development (McBrien et al. 2009).

1.1.6 The origin of signals in myopia development

The signals initiated for myopia development were thought to be generated locally in the retina. FDM was still present in the eyes with ciliary or optic nerve section (Troilo et al. 1987). Application of tetrodotoxin (TTX) did not prevent the development of FDM in chicks and tree shrews (Norton 1990; Wildsoet and Wallman 1995). TTX is able to block action potential of optic nerve and it acts on voltage-gated sodium channels in the retina. These evidences supported that central

nervous system is not necessary for development of myopia. Moreover, when half of occluder was applied to the chick eye, the ocular growth was localized to the corresponding region (Wallman et al. 1987). Ocular growth control appeared to be localized and mediated in the retina.

The retina is the nervous layer in the eyes. It consists of outer pigmented layer and an inner neurosensory layer. The retina has a uniform structure in all the vertebrates including mammals, birds, fishes, reptiles and amphibians. They all have the same layers and neurons across the retina. The outer pigmented layer of the retina is the retinal pigment epithelium (RPE) consisting of a single layer of cells. There are multiple microvilli from apical surface of the RPE projecting to and enclosing the photoreceptors in the retina. Melanin granules are present in these microvilli.

There are several groups of neurons present in the inner neurosensory layer of the retina. It includes photoreceptors, bipolar cells, ganglion cells, horizontal cells and amacrine cells. The photoreceptors, rods and cones, are responsible for converting the visual stimuli to action potentials. Bipolar cells have synapses with photoreceptors and ganglion cells helping to amplify the signal across the retina. The ganglion cells synapse with the bipolar and amacrine cells and transmit the action potentials to the brain. Generally, horizontal and amacrine cells provide feedback and modulate retinal electrical responses (Fig.1.2).

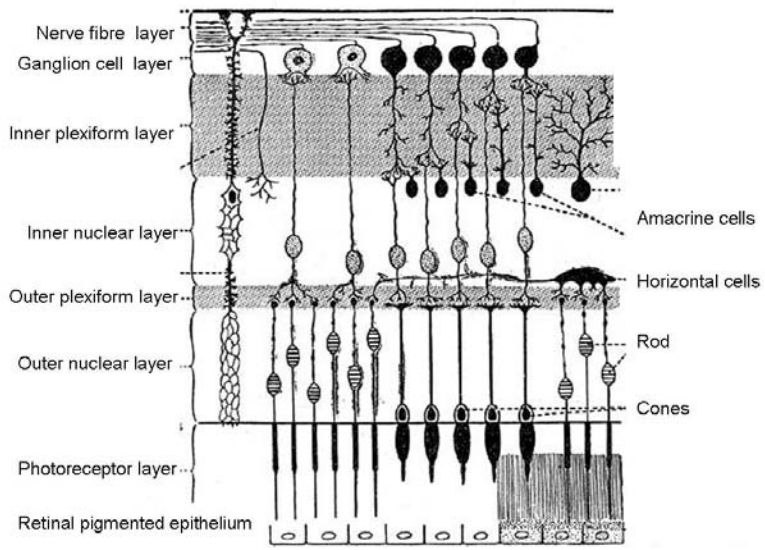

Fig.1.2 Schematic representation of the retinal layers in vertebrates.
Modified from URL: http://embryology.med.unsw.edu.au/Notes/eye11.htm (assessed 24th Nov 2009)

1.1.7 Biochemical signals involved in the myopia development

Many studies have suggested that signals are present to activate (GO) and suppress (STOP) the rate of eye growth (Morgan 2003; Bertrand et al. 2006). GO signals are prompted when hyperopic defocus is projected to the eyes through negative lens or translucent diffuser. On the other hand, STOP signals are formed when myopic defocus is imposed by positive lens (Morgan 2003). It is believed that recovery from FDM or LIM generates similar kind of STOP signals in the eyes. Myopia is thought to be an imbalance between the GO and STOP signals as these signals guided the direction of eye growth. When there are stronger GO signals, and/or deficits in STOP signals, excessive axial length elongation will be observed (Bertrand et al.

2006). Interestingly, the time required to initiate the GO and STOP signals are different. Only a short duration (10 minutes to 2 hours) of myopic defocus per days, which generated STOP signals, was able to block the excessive eye growth induced by long period of LIM (Nickla et al. 2005; Zhu et al. 2005). It suggested that STOP signals produced by positive lens were more robust than that by negative lens.

Although the exact identities of GO or STOP signals are not yet fully annotated, a numbers of possible candidates have been suggested.

1.1.7.1 Dopamine

Dopamine is one of the possible candidates for myopia signal and it has been studied intensely. Dopamine is a hormone and neurotransmitter in vertebrates and invertebrates. It is involved in the control of movement, signaling of error in prediction of reward, motivation and cognition. One of the key problems of Parkinson's disease is the shortage of cerebral dopamine (Arias-Carrion and Poppel 2007). Dopamine dysfunction has also been found to be associated with autism, attention deficit hyperactivity disorder and schizophrenia (Salgado-Pineda et al. 2005; Micheli and Heidbreder 2006).

The release of dopamine in the eye is affected by light (Megaw et al. 2006) and stroboscopic illumination (Rohrer et al. 1995). Retinal dopamine level is high during daytime and low at night (Zawilska et al. 2003). In the eye, the vitreal level of dihydroxyphenylacetic acid (DOPAC) can reflect the release of dopamine in the retina (Megaw et al. 2001). In FDM, the production of DOPAC (metabolites of

dopamine) was decreased which suggests the metabolism of dopamine is affected (Pendrak et al. 1997). The amount of tyrosine hydroxylase, the rate-limiting enzyme for synthesis of dopamine, was also reduced in myopic eyes (Iuvone et al. 1989). It indicated that synthesis of dopamine has also been reduced. Furthermore, retinal dopamine was found to be reduced in FDM chicks (Stone et al. 1989; Rohrer et al. 1993) and it was restored to the control level after recovery from myopia. These changes in retinal dopamine suggest a possible role in myopia development. A number of experiments have been carried out to manipulate dopamine in eye and studied the effect on myopia development in animal.

Intravitreal injection of dopamine was found to suppress eye growth induced by FDM in rabbits (Gao et al. 2006). A non-specific dopaminergic agonist, apomorphine, can activate dopamine receptors and mimic the effect of dopamine. Daily application of apomorphine intravitreally prevented FDM in chicks and primates (Stone et al. 1989; Iuvone et al. 1991; Rohrer et al. 1993). Another non-specific dopamine agonist, 2-amino-6,7-dihydroxy-1,2,3,4-tetrahydronaphthalene hydrobromide (ADTH), showed similar inhibitory effect on FDM and was likely mediated by D2 receptors (Rohrer et al. 1993; McCarthy et al. 2007).

In contrast, injection of dopaminergic neurotoxin 6-hydroxydopamine (6-OHDA) acting to deplete dopamine, blocked the development of FDM, rather than stimulating the eye growth (Li et al. 1992; Hoffmann and Schaeffel 1996). Sulpiride is a specific D2 antagonist that can induce up-regulation of retinal dopamine.

Surprisingly, sulpiride increased myopia and axial elongation, rather than inhibiting myopia as predicted (Schaeffel et al. 1995). Moreover, in fish with complete depletion of dopamine, the eyes could still respond to imposed hyperopic or myopic defocus (Kroger et al. 1999). Therefore, studies using dopaminergic agents on myopia development have uncertain and inconsistent results. The role of dopamine in myopia development is still unclear and required further investigation.

1.1.7.2 Vasoactive intestinal peptide

Vasoactive intestinal peptide (VIP) has been thought to play a role in myopia development. VIP is a 28-amino acid neuropeptide involved in controlling circadian rhythms in physiological, endocrine and metabolic functions in body. It was shown that VIP promoted growth of retinal neuron and RPE during development (Casini 2005). VIP was found in amacrine cells and inner plexiform layer in chick retina (Seltner and Stell 1995). It was able to stimulate cyclic adenosine monophosphate (cAMP) signaling pathway by stimulating retinal adenylate cyclase in rabbit (Longshore and Makman 1981; Koh 2000).

In an early primate study, an increase in retinal VIP was found in the lid-sutured primates (Stone et al. 1988). However, there was no change in retinal VIP after 1,2, 6 and 24 hours of form deprivation in mouse (Mathis and Schaeffel 2007). The gene expression of retinal VIP in chicks after FDM was investigated using gene microarray. The retinal VIP showed a decrease in expression after 3 days of FDM (McGlinn et al. 2007). These findings suggested that there may be species

differences in the expression of VIP in response to induced myopia. It was also puzzling that both VIP's analog and antagonists inhibited FDM (Seltner and Stell 1995). However, recent study showed intravitreal injection of VIP had no effect in FDM in chicks (Vessey et al. 2005). Therefore, it is unclear how VIP contributes to the myopia development at present.

1.1.7.3 Retinoic acid

Retinoic acid (RA) is the acidic form of vitamin A. The role of vitamin A is well characterized in the process of photochemical reaction which leads to the excitation of photoreceptors in response to light.

RA has been implicated in the control of ocular growth and development of myopia (Seko et al. 1998; Mertz and Wallman 2000; McFadden et al. 2004). In chicks and guinea pigs, the retinal RA increased during FDM and LIM, while it decreased in lens-induced hyperopia. The changes of RA in choroid during myopia were opposite to that of the retina (Seko et al. 1998; Mertz and Wallman 2000). Besides apparent changes of RA during myopia, the mRNA of retinal aldehyde dehydrogenase 2 was also elevated after 3 days of LIM (Bitzer et al. 2000). Aldehyde dehydrogenase 2 is an enzyme mediating the RA synthesis in the retina. It was suggested that an increase in retinal RA during myopia may be due to elevation of mRNA of retinal aldehyde dehydrogenase 2 (Bitzer et al. 2000). Furthermore, intravitreal injection of RA synthesis inhibitor prevented FDM in chicks (Bitzer et al. 2000). These findings demonstrated a possible role of RA in myopia development.

A recent study on oral administration of RA raised the doubt of its role in myopia development (McFadden et al. 2006). Oral administration of RA induced an increase in axial length and vitreous chamber depth in lens-induced myopic chicks. Although the increase was greater than that induced by negative lens alone, its refractive errors of RA treated chicks remained similar to the control eye (McFadden et al. 2006). Unexpectedly, it did not induce greater amount of myopia in RA treated chicks and the refractive errors did not correlate with changes of axial length and vitreous chamber depth. The exact reason for the discrepancies to the expected role of RA remains unclear. The way in administrating RA orally may have partly contributed to such phenomenon since both the retinal and choroidal RA levels were elevated by oral administration. It may have disturbed the signaling pathway that would have induced opposite changes in RA levels in the retina and choroids as shown in myopic or hyperopic animal eyes. Intravitreal injection of RA will likely produce a more direct effect on the retina but avoiding its effect on the choroid. Nevertheless, the bidirectional effect of RA on the retina and choroid is intriguing and required further experiments to elucidate its relevance to eye growth.

1.1.7.4 Early growth response 1

Early growth response 1 (Egr-1) is also known as the transcription factor ZENK. Transcription factor is protein in nature that can bind to short DNA sequences. The binding is able to regulate the transcription of genes that lead to mRNA and proteins production (Latchman 1997). ZENK has been found to be differentially expressed during myopia development. The retinal ZENK protein and mRNA were declined in

expression with ocular elongation in myopia (Brand et al. 2005). On the other hand, retinal ZENK protein and mRNA was up-regulated in response to lens-induced hyperopia or recovery from FDM (Fischer et al. 1999; Ashby et al. 2007). In addition, increased axial length and myopia were reported in ZENK knockout mice (Schippert et al. 2007).

ZENK is expressed in glucagon amacrine cells in chick retina. Interestingly, glucagon amacrine cells also express VIP which may be part of the crosstalk that is involved in myopia development (Mathis and Schaeffel 2007). However, the interaction between ZENK and VIP in myopia development remains unclear.

Besides the interplay between VIP and ZENK, ZENK also affects the activity of transforming growth factor beta (TGF-β). The expression of TGF-β was found to be decreased in sclera in tree shrew during myopia (Jobling et al. 2004). Other studies have shown that TGF-β could be transcriptionally activated by ZENK which is associated with growth inhibition (Liu et al. 1999; Chen et al. 2006). It was also showed that both the TGF-β and ZENK mRNA decreased after exposing to 15 minutes of hyperopic defocus with negative lenses (Simon et al. 2004) and it was speculated that the defocus could act on TGF-β and ZENK simultaneously to trigger other signaling pathways that lead to eye growth. These findings indicate that there may be a close and yet undefined interaction between TGF-β and ZENK in myopia development.

1.2 Analytical techniques used in this study

1.2.1 Two-dimensional electrophoresis

1.2.1.1 Background

Two-dimensional electrophoresis (2-DE) is an analytical technique for examining differential protein expressions between samples using fluorescence or other staining methods as visualization tools (Patton 2002). Before performing 2-DE, samples are prepared so as to solubilize the maximum amount of proteins in the sample. The aim of the sample preparation is to solubilize all the cellular proteins in the sample. This results in disaggregation, denaturation and reduction of proteins in the sample. The cells in the sample are necessary to be lysed and disrupted during sample preparation. There are several methods to disrupt the cells using chemical and mechanical approaches.

1.2.1.2 Mechanical approaches of solubilization

Mechanical methods are frequently used with chemical approaches of solubilization. The tissue sample is homogenized using mechanical methods, such as sonication, grinding by pestle and mortar or homogenizers. These methods are more potent way to lyse the tissue as compared to chemical approaches. Sonication has drawbacks on homogenizing the tissue as it generated heat by ultrasonic waves in the process. It leads to an increase in the rate of proteolysis and degradation of proteins in the tissues. Sonication is more suitable and effective for cells suspension than tissues. In the current study, homogenization of chick retinas is preformed in a motorized homogenizer. It enables the frozen sample to be homogenized into fine powder in a

few minutes. This low temperature approach reduces decomposition of proteins during the process. The homogenization is achieved by shaking the frozen sample with a chromium steel ball in the telfon chamber. It shakes at a very high frequency of 1600 revolutions per minute. All procedures are performed at low temperature using liquid nitrogen.

During the homogenization, proteases are released once the cells are disrupted. The presence of proteases degrades the cellular proteins. This contributes to undesirable variations in separating proteins during electrophoresis. Since the activity of proteases is reduced under low temperature, the samples are kept cold during the process of homogenization in the present study. In addition, protease inhibitors are added to the sample solution to further suppress its activities.

1.2.1.3 Solubilization solutions

Homogenization of tissues is usually achieved with solubilization solutions. Typically, it contains a variety of components serving different functions in solubilization. For example, denaturant, detergent, reductant and carrier ampholytes are usually included in the solution (Weiss and Gorg 2008). Urea and thiourea are frequently used as a denaturant which is chaotropic in nature. They disrupt the noncovalent bonds in the proteins and thereby unfold protein's conformation. As a result, it increases the solubilization of proteins in solutions.

Detergent enables solubilization of the cellular membranes and releases the cytoplasmic contents of cells. It prevents aggregation through hydrophobic interactions and minimizes protein-lipid interactions which are important for subsequent protein separation as in isoelectric focusing in the first dimension of electrophoresis. Examples of detergents are CHAPS and ASB-14 which are effective zwitterionic detergents.

Solubilization can be increased by disrupting the disulfide bonds in the proteins. It is carried out by a reductant, such as 2-mercaptoethanol and dithiothreitol (DTT). They prevent the phenolic oxidation which may modify proteins through oxidative reactions. The reducing agents help maintain the proteins in fully reduced state. Carrier ampholytes are included in the solubilization solution and it can increase the stability of proteins by minimizing protein aggregation due to charge-charge interactions.

Different tissues or cell suspensions require different combinations of above components to solubilize the proteins. The concentrations of different reagents used are frequently varied in different proteomic studies. Although the combinations of reagents are different, the aim of sample preparation remains the same. They all aim at solubilizing the proteins optimally in order to obtain reproducible protein extracts from samples.

1.2.1.4 Isoelectric focusing

When the proteins are extracted and solubilized, the proteins are ready to be separated by isoelectric focusing. Isoelectric focusing, also known as electrofocusing, separates the proteins in a gel according to its isoelectric point. Each protein has its own net charge depending on the total charges on amino acid chains, amino- and carboxyl terminals. The charges vary with different pH values. The isoelectric point of a protein is the pH value at which the net charge of the protein is zero.

The pH gradient of gel strips are maintained by carrier ampholytes. They have high buffering capacity near their isoelectric point. They migrate under electrical current and form a pH gradient along the gel. However, the variations in pH gradient among different batches of gel strips can be large. Gradient drift may be present when carrier ampholytes are employed in setting the gradient pH. Nowadays, the precast immobilized pH gradient (IPG) strips are commonly used in isoelectric focusing (Righetti and Bossi 1997). IPG strips are formed by buffering acrylamide derivatives with either a free carboxylic acid or a tertiary amino group which is copolymerized with acrylamide. Therefore, an immobilized pH gradient is created. In addition to the pH gradient, the electric field strength is also important and it will determine the resolution of isoelectric focusing. Isoelectric focusing is usually performed at high voltage (exceed 1000V) for a constant number of voltage-hours. A cooling system is required to keep the temperature low and steady because a high voltage is applied and also because the pH of the proteins will vary with temperature.

1.2.1.5 Second dimension of two-dimensional electrophoresis

After isoelectric focusing, the focused IPG strip is equilibrated with buffer solution containing urea, glycerol, sodium dodecyl sulfate (SDS) and DTT. These chemicals help to reduce electroendosmotic effect and facilitate transfer of proteins from isoelectric focusing to the second dimension (Yan et al. 1999). Moreover, it allows the proteins to fully interact with SDS in the second dimension. A further equilibration step using iodoacetamide instead of DTT is necessary. Iodoacetamide is used to alkylate the free DTT which can cause point streaking in the gels. Iodoacetamide is imperative for mass spectrometry as it alkylates sulfhydryl groups and prevents their re-oxidation during electrophoresis.

After equilibration, the focused IPG strips are placed on the SDS polyacrylamide gels. SDS in polyacrylamide gels acts as an anionic detergent which forms a complex with proteins. The SDS-protein complex has constantly negative charges so it migrates across the gel on the basis of molecular weight only. The smaller the molecular weight of a protein, the faster is its migration rate. Therefore smaller proteins usually can be found at the lower part of a vertical SDS-PAGE gel. SDS also functions as a reductant which breaks the disulfide bonds in proteins. SDS polyacrylamide gel is formed by polymerization of acrylamide in the presence of tetramethylethylenediamine (TEMED) and ammonium persulfate. The gel is electrical neutral and therefore eliminates the electroendosmotic flow effects of its components. The pore size of the gel can be readily changed by adjusting the concentrations of the monomer.

1.2.1.6 Detection of protein profiles

There are several methods for visualizing the proteins after second dimension of electrophoresis (Sasse and Gallagher 2004). Silver staining is one of the commonly used methods. It is highly sensitive and is able to detect the protein below one nanogram. However, its linear dynamic range for quantifying protein concentration is limited (Steinberg 2009). This affects the quantitative measurements and comparison between protein spots. Furthermore, the protocol of silver staining is quite complex when compared to other methods such as fluorescent staining. The conventional silver staining method has to be modified in order to be compatible with mass spectrometry.

The other visualization methods are made use of organic dyes such as Coomassie brilliant blue, fluorescent labeling such Sypro dyes, and metal ions such as negative staining with zinc imidazole. Except Sypro dye, all these staining methods are not more sensitive than silver staining.

1.2.1.7 Merits and limits of two dimensional electrophoresis

Two dimensional electrophoresis (2-DE) techniques enable separation and visualization of the proteins in a sample in one gel. They separate thousands of cellular proteins according to their charges and molecular weights in the form of a protein map. It further allows the protein of interest be studied by other proteomic methods such as mass spectrometry. However, 2-DE does not resolve all the proteins presented in the sample, especially those with high molecular weights. Those high molecular weight proteins are usually hydrophobic and are difficult to

solubilize during the sample preparation process. They tend to aggregate and precipitate in aqueous media and do not allow good separation in isoelectric focusing. These proteins are usually expressed in low copy numbers which render them very difficult to detect. There is no ideal method for solubilizing these proteins at present. New approaches are needed to better solubilize and optimize them in proteomic study.

1.2.2 Two-dimensional fluorescence difference gel electrophoresis (2-D DIGE)

1.2.2.1 Background

Two-dimensional fluorescence difference gel electrophoresis **(**2-D DIGE) is an advanced method for analyzing differential protein expressions based on conventional 2-DE method (Unlu et al. 1997). It labels the solubilized proteins with fluorescent dyes before separating them in isoelectric focusing. The dyes used are CyDye^{TM} DIGE Fluor minimal dyes (GE Healthcare Life Science, Sweden). It consists of three minimal dyes as Cy2, Cy3 and Cy5. These three minimal dyes have narrow and different excitation and emission wavelengths which allow multi-color detection. As they have three distinct fluorescent dyes, it can be used to label three different samples. These samples are allowed to be separated in a single gel. By exciting the dyes with different wavelengths, three gel images can be generated. These images can then be overlaid on each other to calculate the differential protein expressions among different samples.

1.2.2.2 Merits of two-dimensional fluorescence difference gel electrophoresis

One of the major advantages of 2-D DIGE is that the treated and control samples are run in the same gel under the same experimental procedure and condition. This greatly reduces gel-to-gel variations which may be due to slightly different in running conditions during electrophoresis and staining (Marouga et al. 2005). Besides, it shortens the laborious conventional staining procedures for visualizing the protein maps. Typically, the conventional silver staining takes around three hours to accomplish while 2-D DIGE only needs 30 minutes to obtain a high resolution gel image. More importantly, the sensitivity of 2-D DIGE is higher than that of other conventional staining methods. It is able to detect protein as low as 125 pg while the detection limit of silver staining is around 1 ng. The linear range of the minimal dyes in 2-D DIGE is up to five orders of magnitude. In comparison, the linear response of protein concentration in silver staining is less than a two orders of magnitude.

1.2.2.3 Application of internal standard

Although three different samples can be labeled using these three minimal dyes, Cy2 is used as an internal standard for the experiment. This internal standard is a mixture of all samples involved in the experiment so that all the proteins (from both the control and experimental samples) are present. The internal standard is run in all gels in the experiment and it acts to normalize data across gels. Relative changes of protein spots against its internal standard in each gel are calculated and used for normalizing across different gels so as to minimize experimental variations.

Therefore, the quantification of differential protein expression will be more accurate. The internal standard also guides spot matching and improves success in matching spots between gels. As a result, the confidence in qualitative and quantitative measurement is greatly enhanced (Marouga et al. 2005).

1.2.2.4 Properties of CyDye^{TM} DIGE Fluor minimal dyes

The CyDye^{TM} DIGE Fluor minimal dyes have an N-hydroxysuccinimidyl (NHS) ester reactive group which binds the lysine residues of the proteins covalently to form an amide linkage. It works best at pH 8.5. These minimal dyes are charged-matched in which it replaces the lysine's single positive charge with its own. The pI of protein is not affected after the labeling of Cydye. In order not to affect the molecular weight of the protein too much, the dyes are reacted with proteins in a minimally. Around 1-2% of lysines are labeled with the minimal dyes. Although the labeling is kept at minimum, it still slightly affects the molecular weight of proteins. It increases the molecular weight of the protein by approximately 500 Da.

1.2.3 Mass spectrometry

1.2.3.1 Background

Mass spectrometry (MS) is a technique widely used in proteomic research nowadays to determine the molecular masses and structure of proteins through fragmentation. The concept of MS began at the end of 19th century when positive gas phase ions in the gas discharge that travelled away from the anode under low pressure were discovered. Further investigation discovered that positive rays can be separated

according to their mass to charge ratios under parallel electric and magnetic fields. The first MS instrument to produce a mass spectrograph was made subsequently in 1974 (Patterson and Aebersold 2003).

The use of MS has expanded quickly since the development of matrix-assisted laser desorption ionization (MALDI) and electrospray ionization (ESI). These techniques help the generation of peptide ions in a simple and sensitive way.

Before MS, the proteins of interest are cleaved by sequence specific endopeptidase such as trypsin or GluC. Trypsin cleaves the peptide bonding at the carboxyl side of lysine and arginine acid residues whereas GluC cleaves the carboxyl side of aspartic and glutamic acid residues. Peptides of appropriate mass are suitable for subsequent MS analysis. However, it is known that if high abundance peptides are present in the sample, it will mask the detection of low abundance peptides and greatly decreases the sensitivity in protein identification. Therefore, in order to produce the best results, the peptides in a sample cannot be too complex. The complexity of peptide can be reduced by pre-fractionation so that different types of proteins are separated. In this study, reversed phase liquid chromatography (RP-LC) is performed before MS as a pre-fractionation step. RP-LC is made use of non polar stationary phase for separation and performing chromatography. The separation is based on the hydrophobic interaction of alkyl chain using agents such as C_{18} which is coated within the column. The peptides are eluted by gradient changes of water plus water miscible organic solvent like acetonitrile according to their hydrophobicities. The eluted peptides are MS compatible without further treatment.

MS typically consists of three modules including ions sources, mass analyzer and detection. The first step involves the ionization of peptides in the liquid/ gas phase. There are two common methods of ionization, namely the matrix-assisted laser desorption ionization (MALDI) and electrospray ionization (ESI).

1.2.3.2 Matrix-assisted laser desorption ionization (MALDI)

MALDI was first discovered in 1988 (Chen 2008). MALDI is made use of a matrix which absorbs the energy from laser sources. The peptide solution is firstly co-crystallized with a matrix on the MALDI plate. The matrix, such as 2,5-dihydroxybenzoic acid (DHB), can promote ionization of peptides but is large enough not to be evaporated by laser. It has strong absorption of UV so that the laser energy can be absorbed very rapidly. The matrix absorbs the laser radiation and acts as a proton source, causing desorption and ionization of peptides.

1.2.3.3 Electrospray ionization (ESI)

ESI generates ions in gas phase from liquid droplets at atmospheric pressure. Analytes in liquid phase are ejected from a small diameter electrospray emitter needle while a high voltage is applied to the metal coated emitter tip. The analytes are charged in the process and are ready to transfer to the mass analyzer for determining the masses. ESI has several advantages over MALDI. It allows continuous flow of analytes and it can tolerate different types of solvents. Its flow rate can be varied as required to cater for different detection needs. It is also able to generate intact multiple charged ions from different sources.

1.2.3.4 ESI tandem mass spectrometry (ESI-MS/MS)

After the formation of charged peptides by ESI, the charged peptides are directed to a mass analyzer to produce a MS/MS spectrum. First, the mass of intact peptides, known as precursor ions, are determined. The ions are trapped in the device consisting of two convex end cap electrodes and a ring electrode. The masses of ions can be determined by varying the radio frequency voltage and direct current in the ion trap. As a result, only selected ions with specific mass to charge ratio can pass through the ion trap.

The selected ions are further processed in the next fragmentation step. The selected ions are fragmented by the method of collision induced dissociation (CID). The ions are allowed to collide with the inert gas atom or molecules, such as helium, argon. During CID, two ions are formed after cleavage of bonding between carboxyl oxygen and amide nitrogen. They are y-ions and b-ions. Y-ions indicate that the positive charge is retained on the C-terminal of original peptide ions, while b-ions exhibit the charge on the N-terminal of original peptide ions (Frohlich and Arnold 2006).

Finally, the protein is identified from using the information of the MS/MS spectra. The mass of precursor peptide, the masses of fragmented peptide and the type of enzyme used for digestion are required to input for data analysis. The results are generated from comparison of spectra to sequence databases. The spectra from database are performed in computer using search algorithms, so called *in silico*. The frequently used search algorithm is MASCOT (Matrix Science, Boston, MA, USA).

MASCOT is a search engine for identifying protein using mass spectrometry data from protein sequence databases. The common protein sequence databases are the National Centre for Biotechnology Information (NCBI) and SwissProt databases (http://www.expasy.org/sprot/). The numbers of protein entry are different among databases. Non redundant (Nr) database of NCBI contains proteins predicted from the genome while SwissProt focuses on the indentified proteins and its related information.

1.2.4 Western Blotting

1.2.4.1 Background

Western blotting enables detection of specific proteins in the tissue lysates using antibodies and antigen reaction. The tissue lysates are first separated in SDS-polyacrylamide gel electrophoresis **(**SDS-PAGE) according to its molecular masses. Different percentage of acrylamide is used for the gel depending on the size of proteins of interest. Lower percentage of acrylamide in gels such as 7% enables higher resolution of the proteins with molecular weights above 100kDa.

1.2.4.2 Transfer of proteins

The proteins are then immobilized onto the membrane, such as nitrocellulose or polyvinylidene difluoride (PVDF) membrane. PVDF membrane is used in this study because it is of higher tensile strength and it is also easier to handle as compared with traditional nitrocellulose membrane. Although PVDF is more hydrophobic and

difficult to wet, it can be improved by prewetting with methanol before use. The transfer of proteins is carried out by electroblotting at a constant voltage.

The time required for the transfer process depends on the protein size, gel to membrane contact and gel composition. Large proteins usually require longer transfer time. The efficiency of transfer can be examined by staining the gels after transfer process. Blocking of the membrane before incubating with the primary antibodies is necessary. This reduces the non-specific binding of proteins onto the membrane and increases the signal to noise ratio.

1.2.4.3 Detection of signals

After protein blotting, the PVDF membrane is incubated with the primary antibody against the target protein. After several washes, secondary antibody with enzyme conjugated is applied onto the membrane. The commonly used enzymes are alkaline phosphatase (AP) and horseradish peroxidase (HRP). The signal can be visualized by colorimetric or chemiluminence methods. For example, by adding peroxide buffer and luminol into HRP, luminol oxidizes and forms an excited product that emits light. The light is captured by a charged-coupled device (CCD) camera, rather than using film. Film has the problem of lower dynamic range and the bands are easily saturated. This causes incorrect quantifications of the signals. Western blotting shares similar characteristics with other methods using antibodies in which high affinity and specificity of the antibodies are crucial to the success of binding the target proteins. Furthermore, using optimal concentrations of both the primary

and secondary antibodies is imperative in producing the good results in Western blotting.

1.2.5 Immunohistochemistry

1.2.5.1 Background

Immunohistochemistry (IHC) is a technique making use of antibodies to locate the proteins in cells of tissue section under a microscope. It bases on the specificity of antibodies to antigens present in the cells in a tissue section. By visualizing the antibodies-antigen binding, the distribution and location of specific proteins can be observed.

There are two ways of detecting target proteins in IHC, namely the direct and indirect methods. They differ in the types of antibodies used in incubating tissue sections.

1.2.5.2 Direct immunohistochemistry

In the direct method, only one antibody is incubated with tissue sections. The antibodies are labeled with fluorophore and directly probed the antigens in tissue sections. This method allows direct visualization of proteins in tissue sections. However, the sensitivity is weak due to a lack of signal amplification. As a result, it is not commonly used in IHC.

1.2.5.3 Indirect immunohistochemistry

Indirect method uses two types of antibodies, primary and secondary antibodies. The sections are first incubated with primary antibody which is specific to the target protein. The secondary antibody is then applied on the sections. The secondary antibody is raised against the IgG of the animal species in which the primary antibody is raised. They are conjugated with a fluorescent dye or enzyme such as horseradish peroxidase (HRP). It will react with 3,3'-Diaminobenzidine (DAB) to form a brown staining for visualization under a microscope. Alternatively, the secondary antibody can be linked with fluorophore, such as Alexa Fluor or rhoadmine. They can be excited using different excitation wavelengths under a fluorescent microscope. The indirect method has greater sensitivity than the direct one due to signal amplification through several secondary antibodies reacting with different sites on primary antibody. As a result, it amplifies the interaction between the primary antibody and its antigen. Therefore, indirect method is more frequently used in IHC.

The major requirement for success in IHC is the specificity of the primary antibodies. The antibodies need to be sufficiently specific to the interested proteins. Otherwise, false positive results may be generated. It is therefore important to verify the results using positive and negative controls for antibody. Positive control is used to confirm the specificity of antibodies by incubating the antibodies with tissues known to have the corresponding antigens. Negative control is performed by incubating the tissue sections with the secondary antibodies only.

1.2.6 Enzyme immunoassay (EIA)

Enzyme immunoassay (EIA), also called enzyme linked immunosorbent assay (ELISA), is an assay for measuring the level of antigens or antibodies using antibody-antigen reaction. EIA is usually performed in a microtiter plate so that the results can be read out easily by a spectrophotometer. The antibodies used in EIA are linked to an enzyme, reacting with a substrate in the developing reagent, will give out a visible or coloured signal.

1.2.6.1 Competitive enzyme immunoassay

Fixed amount of antibodies are immobilized in the wells of microtiter plate. Sample and fixed amount of enzyme-linked antigens are incubated in the well simultaneously. A competition between free antigens in the sample and known amount of enzyme-linked antigens is performed. Both of them will compete for the limited number of antibody binding sites coated on the plate.

After incubation, unbound antigens and samples are washed away. Substrates are then added to the plate and the enzyme, bound to the antibody binding sites, catalyses the reaction to give a coloured product. The intensity of colour is then measured by a spectrophotometer. The intensity of the colour is proportional to the amount of enzyme-linked antigens, which is inversely proportional to the amount of free antigen present in the sample.

1.3 Research goals and objectives

In the current study, the goal was to investigate the differential protein expressions of chick retina during LIM and FDM. Identification of differentially expressed proteins may help in understanding the biochemical signals and processes involved in myopia development. The profiling of retinal proteomes of both myopic and control eyes were carried out by two-dimensional fluorescence difference gel electrophoresis **(**2-D DIGE). The proteins with altered expressions were identified by a nano liquid chromatography with tandem mass spectrometry (LC-MS/MS).

Among a number of differentially expressed proteins found in this study, one of these candidate proteins (apolipoprotein A1) was selected for further investigation in terms of its effect on myopia development and its localization in the retina of lens-induced myopic and hyperopic eyes.

The role of cyclic adenosine monophosphate (cAMP) in development of myopia in chicks was studied by intravitreal injection. Western blotting and EIA was employed to measure the expression of apolipoprotein A1 and cAMP respectively.

Chapter 2: Differential protein expressions in myopic chick retinas using two-dimensional fluorescence difference gel electrophoresis

2.1 Introduction

High prevalence of myopia is evident in many Asian countries (Edwards 1999; Matsumura and Hirai 1999; Saw et al. 2000). Myopia can be optically corrected by spectacles and low myopia is often without major health hazards. However, high myopia can lead to a number of ocular changes that may impair vision permanently. High myopia (more than six dioptors) is associated with sight threatening diseases such as retinal detachment, macular degeneration and glaucoma (Grossniklaus and Green 1992; Chihara et al. 1997; Iwase et al. 2006). This could eventually create socio-economical problems in terms of losing workforce and burdening the health care system in the future. Therefore, there is an urgent need to better understand the mechanism of myopia development so as to combat the raising trend of myopia in the community.

Signals involved in developing myopia have been thought to reside in the retinas (Wallman et al. 1987). Previous literatures have demonstrated that blockage of control from higher centre did not prevent form deprivation myopia (FDM) (McBrien et al. 1995; Wildsoet and Wallman 1995). This can be achieved by sectioning of optic nerve or application of tetrodotoxin (TTX) (Wildsoet and

Wallman 1995). TTX is able to block retinal cell action potentials (McBrien et al. 1995). The results implied that development of myopia is not controlled by the central nervous system. It is interesting to note that when half of the occluders were applied to the eye, only the corresponding part of the eye elongated (Troilo et al. 1987). In other words, the eye is capable of having differential regional growth. Thus, signals and biochemical processes involved in myopic growth appears to be regionally localized in the retinas.

Proteome is the protein complement expressed by genome from an organism or cell types (Wilkins et al. 1996). Exploring the proteomes is increasingly applicable in understanding the disease states such as cancers and developmental processes (Chambers et al. 2000; Dongre et al. 2001). Concurrently, genomic approach provides information on transcription and mRNA expressions which are the initiation of biological processes. Ultimately the genetic information is translated into proteins to elicit various physiological responses. However, protein expressions do not always quantitatively agree with its mRNA expression because of the complexity in the translation process due to post translational modifications (PTM) (Patterson and Aebersold 2003). Therefore, proteomic information is very important in substantiating genetic data in terms of better describing up or down regulations in a variety of physiological processes (Dongre et al. 2001).

The current study employed two-dimensional fluorescence difference gel electrophoresis (2-D DIGE) to investigate the proteomes of myopic chick retinas. 2-

D DIGE is a modified method based on conventional two-dimensional electrophoresis (2-DE). 2-D DIGE makes use of three CyDye^{TM} DIGE Fluor minimal dyes (GE Healthcare Life Science, Sweden) with three distinct fluorescent wavelengths. The three dyes can minimally label the different samples so that they can be run in the same gel. It improves the gel to gel variations present in the conventional 2-DE. One of the CyDye^{TM} DIGE Fluor minimal dyes (GE Healthcare Life Science, Sweden) acts as an internal standard to label a mixture of each sample involved in the experiment. The internal standard is employed in normalizing protein quantity across the gels. This further enhances the accuracy in identifying differential expressed proteins between samples. This technique provides a broader dynamic range, greater reproducibility and higher sensitivity than conventional 2-DE.

2.2 Objectives

The aim of this experiment was to identify the differential protein expressions in the retinas under FDM and lens-induced myopia (LIM) using 2-D DIGE. Those differentially expressed proteins were identified using a nano-liquid chromatography with tandem mass spectrometry (LC-MS/MS).

2.3 Materials and methods

White leghorn chicks (Gallus gallus domesticus) were bred from Specific Pathogen Free (SPF) eggs (SPFEGG, Jinan, China). The care and use of the animals in these experiments were in accordance with the ARVO resolution on the Use of Animals in

Research and in compliance with university guidelines set forth by the Animal Subjects Research Ethnic Subcommittee (ASEC). Newly hatched white-leghorn chicks were reared under 12/12hr light/dark diurnal cycle. Food and water were provided *ad libitum*.

2.3.1 Sample preparation

The experiments were carried out on chicks at the age of two days after hatching. Six groups of animals were used and each group contained four chicks. Refractive errors and ocular parameters were measured before and after experiments. Ocular parameters were examined by high-frequency A-scan ultrasound system with a 30-MHz transducer sampled at a rate of 100 MHz while refractive errors were measured by streak retinoscopy. Refractive errors were presented in terms of spherical equivalent which was the sum of spherical power and half of cylindrical power.

Two groups of chicks wore -10D and plano lenses on their right and left eyes respectively for three or seven days. Another two group wore diffusers and plano lenses on their right and left eyes respectively for three or seven days. Occluders and plano lenses were used in the last two groups of chicks for three or seven days.

After treatment, the chicks were sacrificed by carbon dioxide overdose and the eyes were enucleated. Extraocular muscles were removed and eye was hemisected near the equator. Vitreous were removed carefully. The retinas were then separated from retinal pigment epithelium (RPE) with forceps. It was immediately frozen in liquid nitrogen and kept under -80 ℃ for further use.

2.3.2 Homogenization of retina

A frozen retinal sample with 300 μl lysis buffer was homogenized in a liquid nitrogen-cooled Teflon freezer mill (Mikrodismembrator Braun Biotech, Germany) for a total of 6 minutes at 1600 revolutions per minute. Lysis buffer contained 7 M urea, 2 M thiourea, 40 mM Tris, 0.2% (v/v) Biolytes, 2% (w/v) CHAPS, 1% (w/v) ASB14 (Calbiochem, San Diego, CA, USA) and 1 tablet of Complete, Mini protease inhibitor cocktail (Roche Applied Science, Switzerland) in 10ml buffer. The pH of the lysis buffer was maintained at pH8.0-9.0 so as to facilitate the labeling of proteins with CyDyes. The sample was collected and incubated at room temperature for 20 minutes and then centrifuged at 16100 g for 20 minutes at 4 ℃. The supernatant, the soluble protein extract, was collected while the pellet was discarded.

2.3.3 Protein quantification

Three microlitres of supernatant was extracted to measure its protein concentration by 2D Quant Kit (GE Healthcare Life Science, Sweden). The kit makes use of principle of protein precipitation to measure the protein amount. After precipitation and co-precipitation of protein, the cupric (Cu^{2+}) ions were added to bind to the polypeptide backbones of proteins. A colorimeter agent reacting with unbound cupric ions was applied. The color density is inversely related to the concentration of protein. Protein concentration was then calculated by comparison to a standard curve. The standard curve was performed using bovine serum albumin (BSA). The absorbance was measured with a UV/VIS Spectrophotometer SP-300 Plus (Optima, Japan) at 480 nm.

2.3.4 Labeling of proteins

Each CyDye DIGE Fluor minimal dyes (25nmol) were first reconstituted in 25 µl anhydrous N,N-dimethyformamide (DMF) to give a final concentration of 1000 pmol/µl.

Fifty micrograms of proteins from the right and left retinas were labeled with 400 pmol of Cy3 and Cy5 in random. Cy2 was used to label the same amount of internal standard which was drawn from pooling aliquots of all retinal samples. The labeling was processed on ice in the dark for 30 minutes. The labeling reaction was quenched by 1µl of 10mM lysine for 10 minutes. After labeling, the separated internal standard, right and left retinal samples from the same chick were combined with an equal volume of lysis buffer with 2% (w/v) DTT and 0.4% (v/v) Biolytes. They were incubated at dark for 10 minutes at 4℃. The mixture was then complemented to 300 µl with rehydration buffer (7 M urea, 2 M thiourea, 0.2% (w/v) Biolytes, 1% (w/v) DTT, 2% (w/v) CHAPS, 1% (w/v) ASB14 (Calbiochem, San Diego, CA, USA)) and trace amount of bromophenol blue before isoelectric focusing.

2.3.5 Isoelectric focusing

Isoelectric focusing was performed using ReadyStrip linear immobilized pH gradient (IPG) strips (17cm, pH5-8) (BioRad, San Diego, CA, USA). Labeled sample with rehydration buffer was added to the slot of focusing tray. The strips were then applied into the slot with its gel side down. Active rehydration at 50 V

was applied to the strips in PROTEAN IEF Cell (BioRad, San Diego, CA, USA) through focusing tray under constant temperature 20 ℃ for 12 hours. The IPG strip was then focused for a total of 42000 Voltage-hour (Vh) using linear voltage ramp: 100 V for 2 hours (hrs), 500 V for 1 hr, 1000 V for 1 hr, 4000 V for 2 hrs and 8000 V for 6 hrs. The IPG strips were kept at dark during isoelectric focusing.

2.3.6 Second dimension of electrophoresis

Before performing electrophoresis, the focused IPG strips were required to go through equilibration steps. Dithiothreitol (DTT) was used in the first step in equilibration steps. It can preserve the fully reduced state of denatured, unalkylated proteins. Iodoacetamide was added in the second part of equilibration. It alkylates the thiol group of proteins so as to prevent the reoxidation during electrophoresis.

The focused IPG strips were incubated in the equilibration buffer (6 M urea, 30% glycerol, 50 mM Tris and 2% SDS) containing 0.5% DTT for 10 minutes and then 2.5% iodoacetamide for another 10 minutes. The focused IPG strips were raised with Milli-Q H_2O and placed with 1% agarose on the top of a 1.5mm thick, 18cm x 16cm SDS-PAGE gel for second dimension. The 12% sodium dodecyl sulfate (SDS) polyacrylamide gels were casted in between low fluorescence Pyrex glass plate in order to reduce the high background signals. Constant current of 40mA per gel was applied. A cooling system using water was continuously utilized during electrophoresis.

Proteins were further separated according to their masses using SE600 cooled vertical electrophoresis unit (Hoefer, Holliston, MA, USA). All the procedures were kept in a dark environment.

2.3.7 Acquisition of gel image using Typhoon 9400 Variable Mode Imager

After electrophoresis, labeled proteins were visualized using Typhoon 9400 Variable Mode Imager (GE Healthcare Life Science, Sweden). The imager was required to warm up for 30 minutes before scanning. The glass plate sandwiching the gels was removed from SE600 cooled vertical electrophoresis unit (Hoefer, Holliston, MA, USA). They were cleaned to remove all the lint on its surface, which scattered light and affected the image quality. The imager was remote controlled by The Typhoon Scanner Control Software (GE Healthcare Life Science, Sweden). Scan area, orientation of gels and mode of acquisition was selected appropriately.

Images of CyDye were scanned by different excitation wavelength and emission filter. Cy2 images were scanned using 488nm excitation and 520BP40 (band pass) emission filter; Cy3 images were scanned using 532nm excitation and 580BP30 emission filter; Cy5 images were scanned using 633nm excitation and 670BP30 emission filter.

A pre-scan of gel image was preformed at 1000 μm pixel resolution so as to adjust the strength of each scan wavelength. Its strength was adjusted by varying the photomultiplier tube (PMT) voltage. PMT voltages were required to maintain to the level that minimal saturated images can be obtained.

All gels were scanned at 100 μm pixel resolutions for analysis. Area of interest in gel images were defined using ImageQuant^{TM} v.5.2 (GE Healthcare Life Science, Sweden). All the images were saved as *.gel files which were directly used in DeCyder Differential Analysis Software.

2.3.8 Protein visualization by silver staining

The gels were visualized with MS compatible silver staining method. The procedure included fixation, sensitization, silver impregnation, developing and washing steps. The gels were first fixed in 10% acetic acid and 40% methanol in double distilled water (DDH_2O) overnight with gentle shaking. After fixation, the gels were undergone sensitization step and the gel was incubated in sensitivity enhancers. Sensitization solution included 0.2% (w/v) sodium thiosulfate and 30% methanol in DDH_2O. The gels were soaked in sensitization solution for 1 hour with gentle shaking and they were then washed with DDH_2O for 5 times, 10 minutes each. The gels were incubated with silver impregnation solution (0.25% silver nitrate in DDH_2O) for 1 hour with gentle shaking. The gels were further washed with DDH_2O for 5 times, 10 minutes each. The protein in gels were visualized and developed by treatment with silver reductant which reduced the silver ions to metallic silver for signal visualization. Formaldehyde was used as a silver reductant. The gels were developed in the solution containing 2.5% (w/v) sodium carbonate, 0.04% formaldehyde in DDH_2O. This developing solution was freshly made prior to staining. The incubation time for developing solution was about 4 to 6 minutes. The

development of color was stopped by 5% acetic acid in DDH_2O for 30 minutes. The stained gels were washed in DDH_2O for 3 times, 5 minutes each.

The stained gels were then scanned as uncompressed "TIFF" images at 200 dpi (pixels per inch) resolutions with an Epson perfection V100 Photo flatbed scanner (Nagano, Japan).

2.3.9 Biological variation analysis by DeCyder Differential Analysis Software

DeCyder Differential Analysis Software (DeCyder) (GE Healthcare Life Science, Sweden) was employed to analyze the differential protein expressions between myopic and control retinas. DeCyder enables the detection, quantification, matching and analysis of protein spots. It consists of Differential In-gel Analysis (DIA) and Biological Variation Analysis (BVA) in DeCyder.

Gel images were first analyzed in DIA module. Protein spots in images from a single gel were co-detected and quantified with respect to its internal standard. Cy3 and Cy5 images were assigned an experimental condition, either control or treated (myopic). All Cy2 images were assigned as internal standard. Ratio of protein abundances of each spot in internal standard and sample (control/ treated) within the same gel was determined. As the internal standard was the same across gels running in the experimental design, the calculated ratio was normalized among gels. This process is called in-gel normalization. The estimated number of spots for each co-detection procedure was set to 1800.

The analysis was further performed in BVA module. BVA processed the matching of protein spots among multiple gels. The protein abundances were then compared

and quantified across multiple gels. Statistical analysis was carried out in DeCyder and paired T-test was employed in this study. Standardized abundance of a protein spot was used in BVA to direct comparison among gels. Standardized abundance is defined as abundance relative to standard images in a function of ratio as calculated in DIA module.

2.3.10 Protein identification by mass spectrometry (MS)

Identifications of interested proteins were determined by a nano-liquid chromatography with tandem mass spectrometry (LC-MS/MS). Protein spots of interest (about $1mm^3$) were cut from the gels. Precaution in handling the gel plugs was necessary in order to prevent contamination of keratins. The gel plugs were washed with milli-Q H_2O for 15 minutes and then 50mM ammonium bicarbonate/ acetonitrile (NH_4HCO_3/ ACN, 1:1, v/v) for another 15 minutes. The gel plugs were destained using Farmers silver reducing solution (60mM potassium ferricyanide, 130mM sodium thiosulfate) for 3 minutes. 25mM NH_4HCO_3 were used to wash the destained gel plug for 2 times. The gel plugs were air dried by ACN.

Gel plugs were soaked in 2 μl 20ng/μl trypsin (Promega, WI, USA) with 25mM NH_4HCO_3 at 4℃ for 30 minutes for in gel digestion of proteins. The gel plugs were further incubated in 2 μl 25mM NH_4HCO_3 at 37℃ overnight. The digested peptides were collected after sonication with 5 μl acetonitrile/ 2% trifluoroacetic acid (ACN/ 2% TFA, 1:1; v/v) for 2 times, 10 minutes each. The collected digested peptides

were dried by Savant SVC 100H Speed Vac Concentrator (Savant, USA). The extracted peptides were re-dissolved in 20 µl 0.1% formic acid.

The peptides were separated in an Ultimate 3000 nano-liquid chromatography system (LC Packings, Dionex, Sunnyvale, CA, USA) and analyzed by HCT Ultra ion trap mass spectrometer (Bruker Daltonics, Billerica, Massachusetts, USA) equipped with an online nanospray source. Samples (17µl) were injected into a reversed-phase pre-column (C_{18} PepMap, 300µm inner diameter (i.d.), 5mm, LC Packings, Dionex, Sunnyvale, CA, USA) and then eluted and separated in a nano reversed phase column (C_{18} PepMap, 75µm i.d., 150mm, LC Packings, Dionex, Sunnyvale, CA, USA) with linear gradient from 96% mobile phase A/ 4% mobile phase B to 50% mobile phase A /50% mobile phase B in 10 minutes. Mobile phase A contained 0.1% (v/v) formic acid in water and mobile phase B contained 0.08% formic acid in water-ACN (20:80, v/v%).

The column was connected to an electrospray emitter, distal coating, 20µm i.d. with 10µm opening (New Objective, Woburn, MA, USA). The peptides were detected in the positive ion mode and fragmented by collision-induced dissociation using helium as the collision gas. The voltage applied to the capillary cap was -1500V and the temperature of the capillary were set to 150℃. Precursor selection was set as 300-1500 mass to charge ratio (m/z). Two most abundant precursor ions were selected for MS/MS. Three scans were averaged to obtain an MS/MS mass spectrum.

The MS/MS spectra were then matched with theoretical MS/MS spectra calculated from sequence database.

The MS and the MS/MS data were searched using the NCBInr protein database (NCBIni_20081017) by MASCOT search engine. Trypsin was designated as the enzyme and one missed cleavage was allowed. Carbamidomethylation of cysteines was set as fixed modification and oxidation of methionine residues as variable modification. The mass tolerances were 1.2Da for MS and 0.6Da for MS/MS. The proteins were considered identified when the peptide ion score was above 25.

2.4 Results

2.4.1 Treatment with negative lenses

In eyes wearing -10D lenses for 3 days, they became significantly myopic (in terms of spherical equivalent) (-4.63D ± 0.48, mean ± SEM, $p<0.01$ by Student's t-test) (Fig.2.1A). Increase in vitreous chamber depth and axial length were seen after 3 days of -10D lens wear (Fig.2.2).

When -10D lenses were wore for 7 days, the eyes became more myopic than those wearing -10D lenses for 3 days. The mean refractive error was -7.83D ± 0.76 (Fig. 2.1B). The increase in vitreous chamber depth and axial length were also greater than those wearing -10D lenses for 3 days. The vitreous chamber depths of the 3-day and 7-day LIM eyes were increased by 0.38mm and 0.58mm respectively (Fig.2.2).

A.

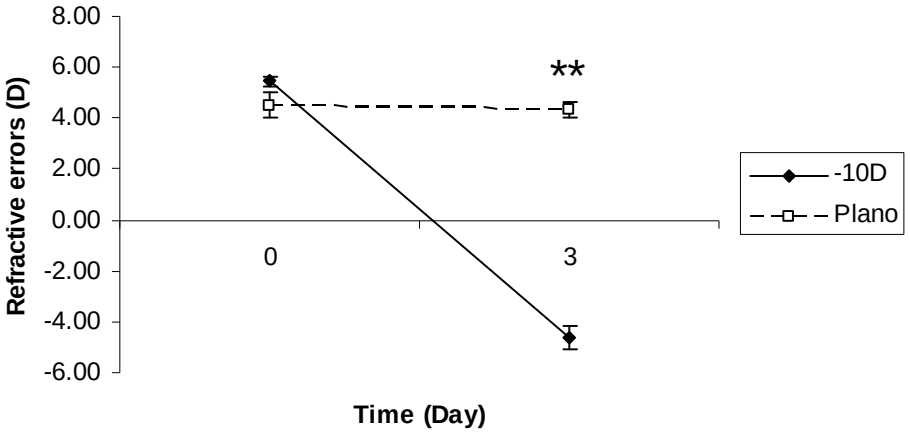

B.

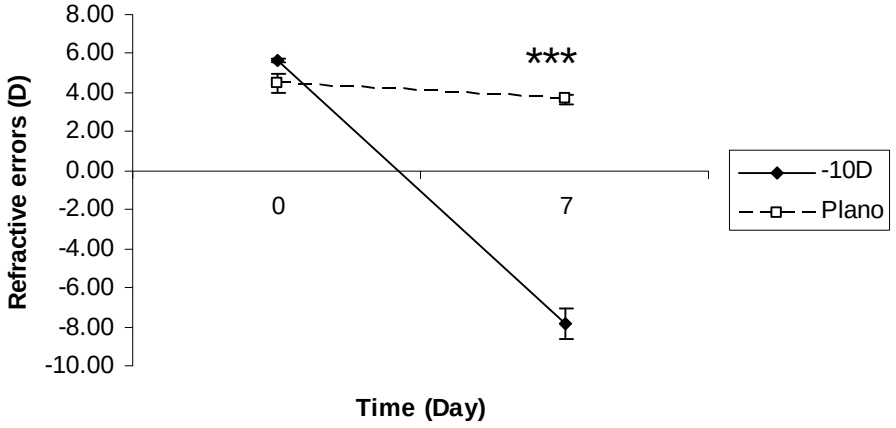

Fig.2.1 The development of refractive error (spherical equivalent) under 3-day (A) and 7-day (B) lens-induced myopia.
Negative (-10D) and plano lenses were worn by the right and left eyes respectively for 3 or 7 days. Each data point represents the mean refractive error ± SEM (n=4), *asterisks* over bars indicate paired, two-tailed Student's *t*-tests comparing the data from right and left eye. * P<0.05, ** P<0.01, *** P<0.001.

A.

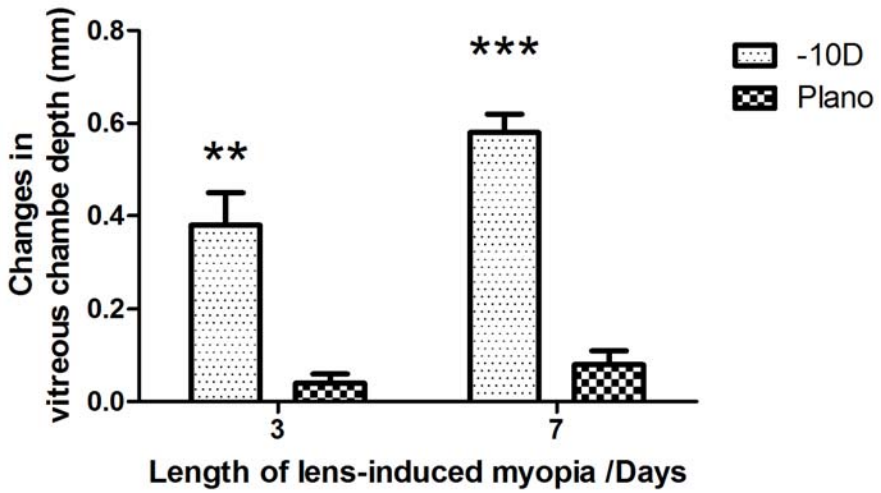

B.

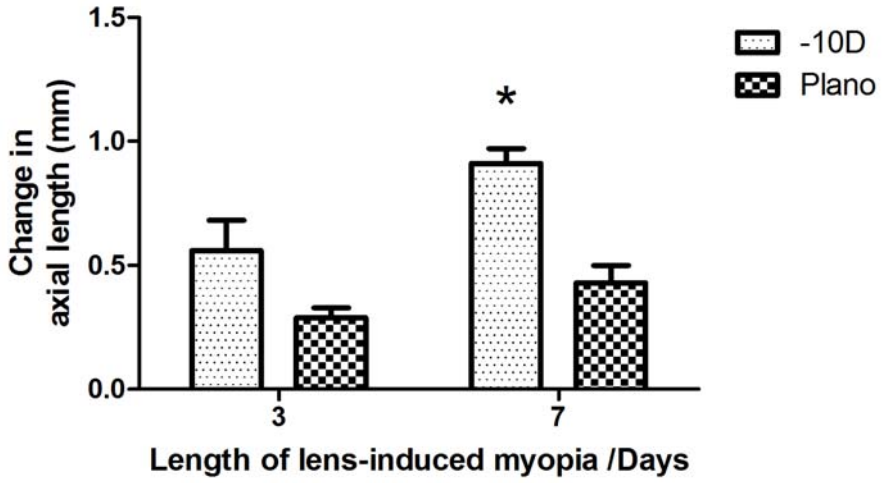

Fig.2.2 Changes in vitreous chamber depth (A) and axial length (B) after 3 and 7 day of lens-induced myopia by -10D lenses.
Each data point represents mean change ± SEM (n=4), *asterisks* over bars indicate paired, two-tailed Student's *t*-tests comparing data from right and left eye. * P<0.05, ** P<0.01, *** P<0.001.

The retinal proteome from 3-day lens-induced myopia (LIM) were shown (Fig.2.3). Proteins are visualized as spots in the polyacrylamide gel according to their isoelectric points and molecular weights. There were approximately 1800 protein spots detected in soluble extract from the retinas.

In the current study, differentially expressed proteins are defined according to a number of criteria. The differential protein expressions must be present in all four samples. They must all be in the same direction of regulation, either up-regulated or down-regulated. The abundance ratio between myopic and control eye must be at least 1.2-fold with statistically significance ($p<0.05$, paired Student t-test). Only the proteins fulfilling these requirements were regarded as differentially expressed proteins in the current study.

When comparing the retinal proteomes between 3-day LIM and control eyes, there were four differentially expressed proteins (Fig.2.3). Of these spots, three of them showed an increase in expressions in myopic eye whereas one spot showed a decrease in expressions (Fig.2.4). These spots were subsequently identified by LC-MS/MS.

Among the three up-regulated protein spots, two spots could be identified which is phosphoglycerate mutase 1 (PGAM). The spot showing a decrease in expression was found to be apolipoprotein A1 (ApoA1) (Table 2.1).

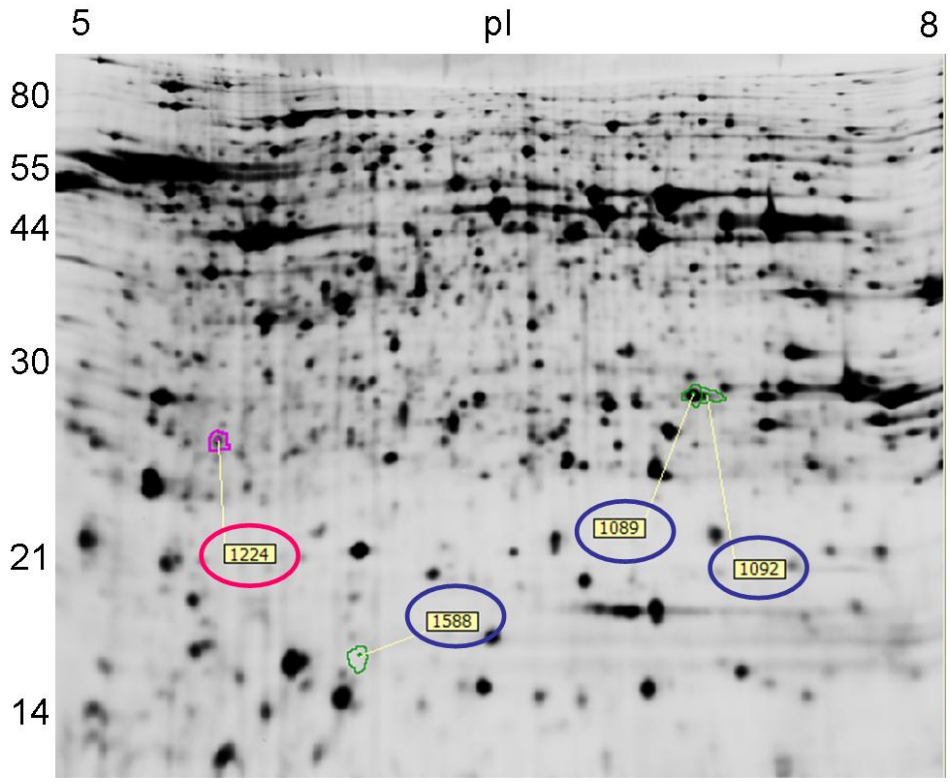

Fig.2.3 Identification of differential protein expressions after 3 days of lens-induced myopia.
The gel image is a representative DIGE gel. Approximate molecular weights and isoelectric points are indicated. Spots in red circle indicate down-regulated proteins while those in blue circle are up-regulated proteins in myopic retinas.

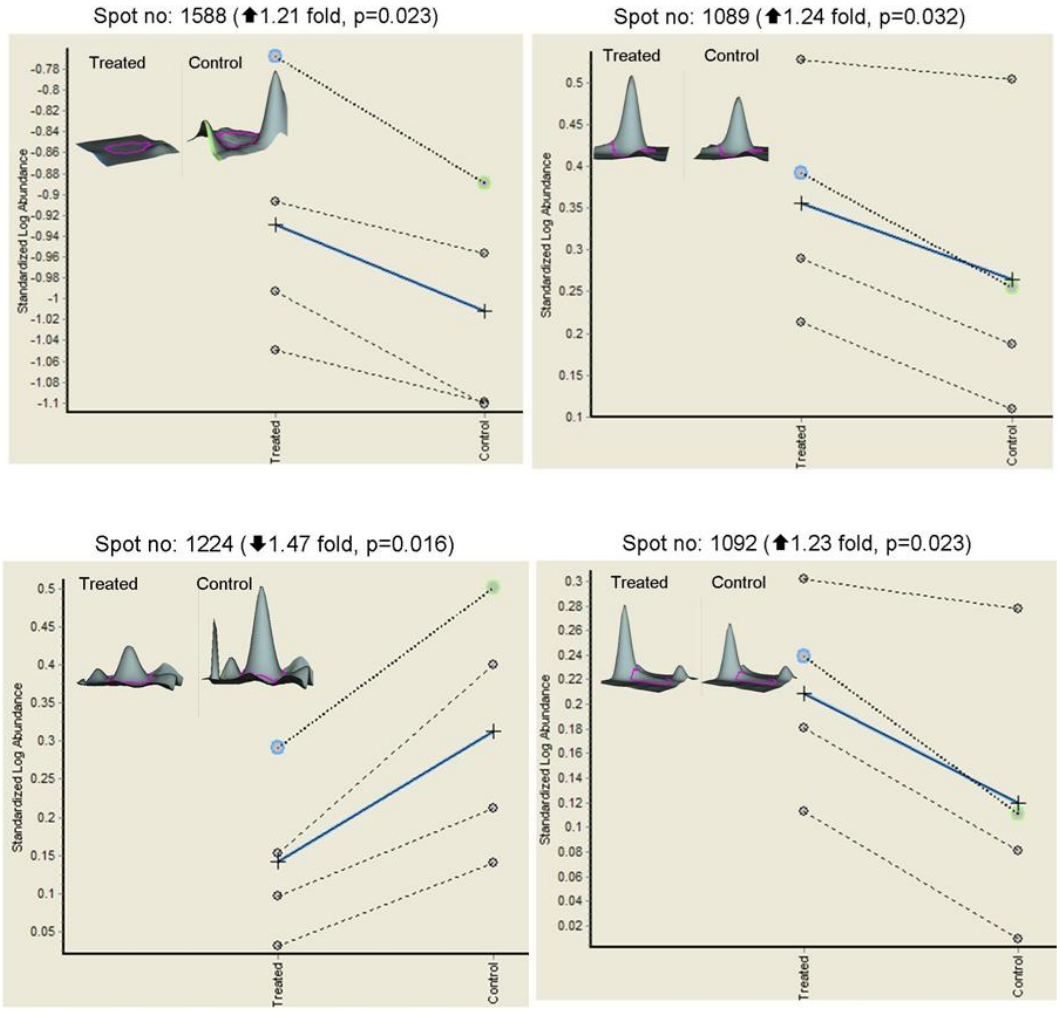

Fig.2.4 Differential protein expressions of individual spots found by DeCyder Differential Analysis Software.
Fold-changes and paired t-test values were shown. The graphs show the standardized log abundance of spot volume in each protein spot (y-axis) against the treated and control groups. The treated eyes were under 3 days of LIM. 3-D views of protein abundance for each individual spots are also shown.

Table 2.1. Differentially expressed proteins after 3 days of lens-induced myopia.

DIGE spot no.	NCBI GI no. [a]	Mascot protein name	Mowse Score [b]	Sequence coverage	Mascot pI [c]	Mascot Mw /kDa [d]	No. of peptides [e]	Organism [f]
1224	211159	Apolipoprotein A1	376.4	28.8%	5.46	30.67	9	Gallus gallus
1089	71895985	Phosphoglycerate mutase 1 (brain)	133.1	12.6%	7.82	29.05	12	Gallus gallus
1092	71895985	Phosphoglycerate mutase 1 (brain)	63.1	12.6%	7.82	29.05	5	Gallus gallus

a. A GI number (GenInfo Identifier) was assigned to each nucleotide and protein sequence accessible through The National Center for Biotechnology Information (NCBI)
b. Score was calculated by Mowse scoring algorithm in the Mascot system
c,d. The theoretical isoelectric point and molecular weight calculated using the databases in Mascot system
e. Number of peptides used for sequencing
f. Species of the identified protein

In terms of the retinal proteome of 7-day LIM, DIGE detected two spots that were differentially expressed in the myopic retinas (Fig.2.5). Both of them were up-regulated in myopic retina (Fig.2.6). Only one of them was identified using mass spectrometry. The spot identified was found to be destrin (Table 2.2).

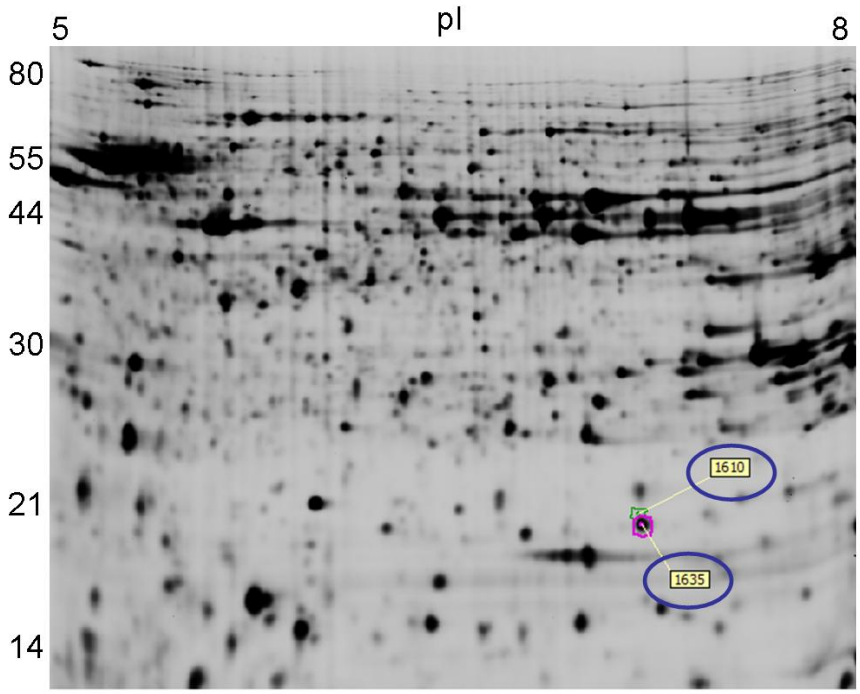

Fig.2.5 Identification of differential protein expressions after 7 days of lens-induced myopia.
The gel image is a representative DIGE gel. Approximate molecular weights and isoelectric points are indicated. Spots in red circle indicate down-regulated proteins while those in blue circle are up-regulated proteins in myopic retinas.

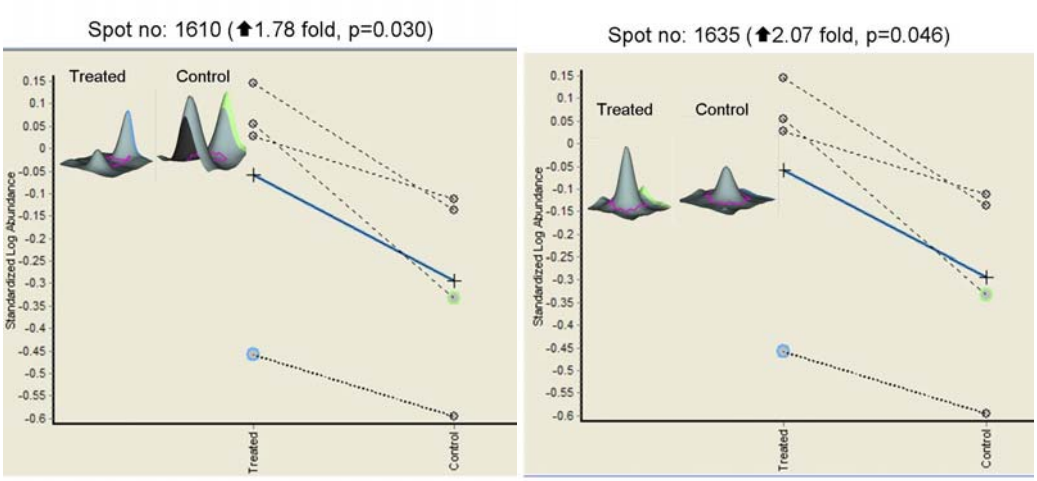

Fig.2.6 Differential protein expressions of individual spots found by DeCyder Differential Analysis Software.
Fold-changes and paired t-test values were shown. The graphs show the standardized log abundance of spot volume in each protein spot (y-axis) against the treated and control groups. The treated eyes were under 7 days of LIM. 3-D views of protein abundance for each individual spots are also shown.

Table 2.2 Differentially expressed proteins after 7 days of lens-induced myopia.

DIGE spot no.	NCBI GI no. [a]	Mascot protein name	Mowse Score [b]	Sequence coverage	Mascot pI [c]	Mascot Mw /kDa [d]	No. of peptides [e]	Organism [f]
1635	45382979	Destrin	84	16%	7.52	18.9	3	Gallus gallus

a. A GI number (GenInfo Identifier) was assigned to each nucleotide and protein sequence accessible through The National Center for Biotechnology Information (NCBI)
b. Score was calculated by Mowse scoring algorithm in the Mascot system
c,d. The theoretical isoelectric point and molecular weight calculated using the databases in Mascot system
e. Number of peptides used for sequencing
f. Species of the identified protein

2.4.2 Treatment with diffusers

Significant amount of myopia was induced using translucent diffusers for 3 days ($p<0.001$). The mean refractive error was -6.31D ± 0.76 (Fig.2.7A). Significant increases in the vitreous chamber depth and axial length were also observed ($p<0.01$) (Fig.2.8).

Expectedly, higher amounts of myopia (-8.69D ± 2.34, mean ± SEM) were obtained after wearing diffusers for 7 days (Fig.2.7B) than 3 days, and so were the vitreous chamber depth (0.685mm versus 0.335mm, mean change) and axial length measurements (Fig.2.8).

A.

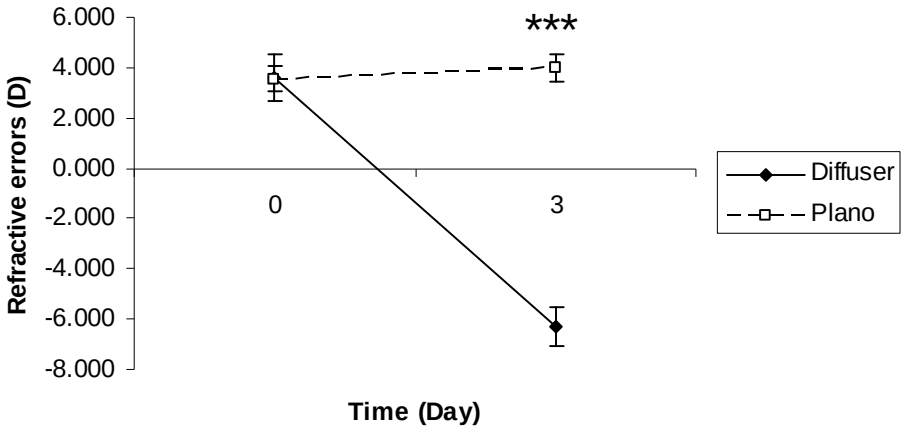

B.

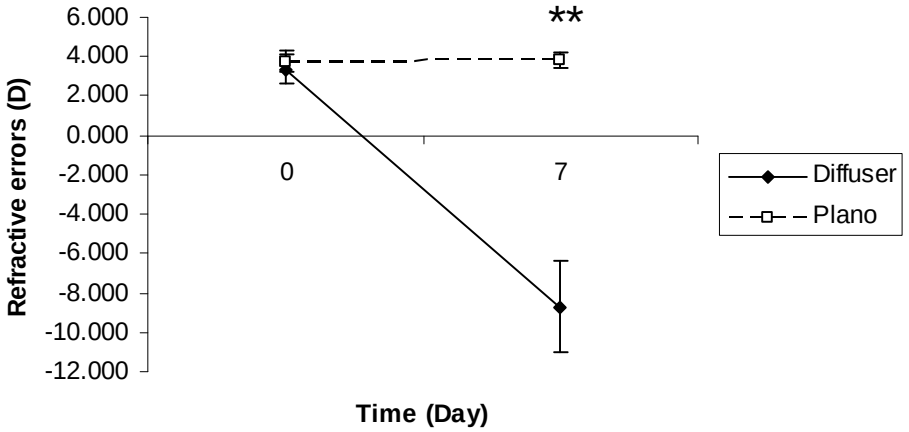

Fig.2.7 The development of refractive error (spherical equivalent) under 3-day (A) and 7-day (B) form deprivation myopia by diffusers.
Diffuser and plano lenses were worn on the right and left eyes respectively for 3 or 7 days. Each data point represents mean refractive error ± SEM (n=4), *asterisks* over bars indicate paired, two-tailed Student's *t*-tests comparing data from right and left eye. * P<0.05, ** P<0.01, *** P<0.001.

A.

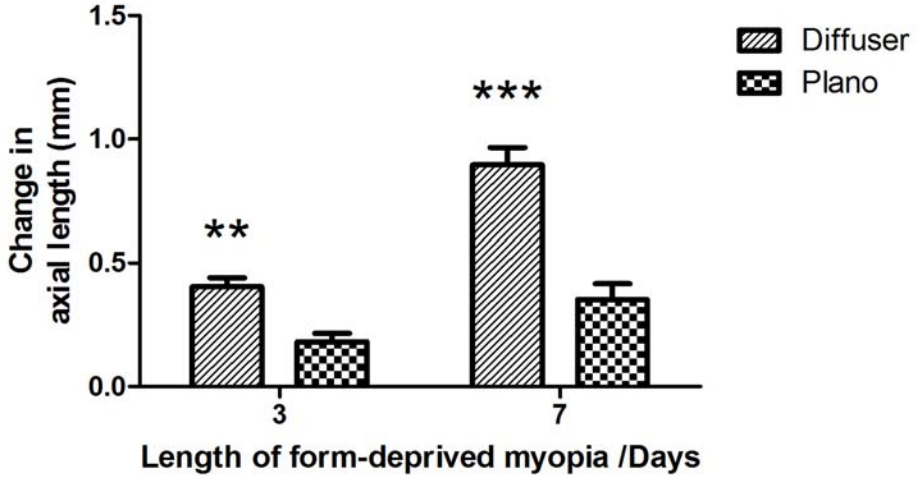

B.

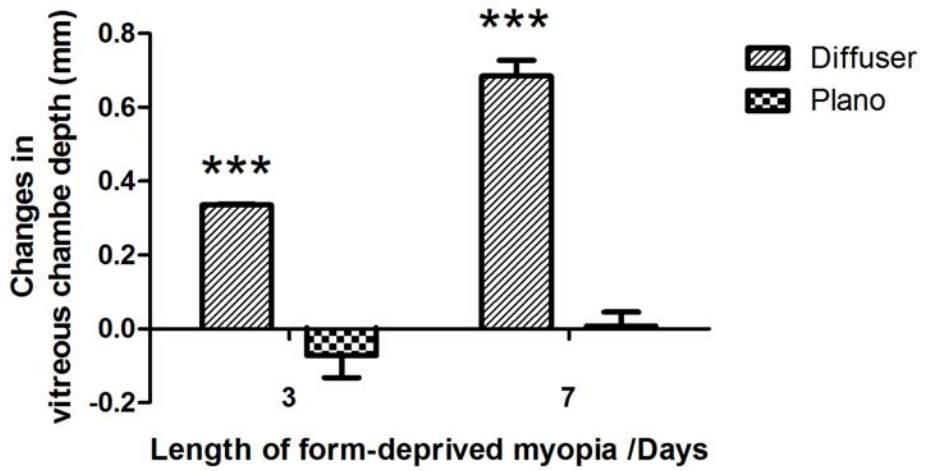

Fig.2.8 Changes in axial length (A) and vitreous chamber depth (B) after 3 and 7 day of form deprivation myopia by diffuser.
Each data point represents mean change ± SEM (n=4), *asterisks* over bars indicate paired, two-tailed Student's *t*-tests comparing data from right and left eye. * P<0.05, ** P<0.01, *** P<0.001.

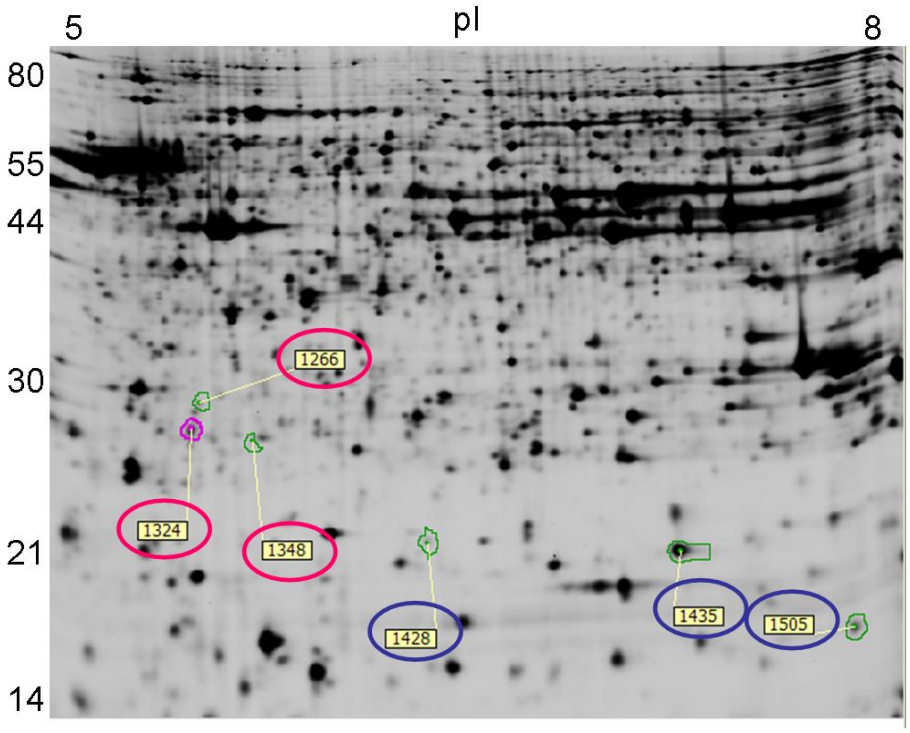

Fig.2.9 Identification of differential protein expressions after 3 days of form deprivation myopia by diffusers.
The gel image is a representative DIGE gel. Approximate molecular weight and isoelectric points are shown. Protein spots in red circle indicate down-regulated proteins while those in blue circle are up-regulated proteins in myopic retinas.

In eyes with diffusers for 3 days, 6 protein spots were found to be differentially expressed in the myopic retinas (Fig.2.9). Three of them showed up-regulation while another three spots demonstrated down regulation (Fig.2.10). Two spots were identified using mass spectrometry. ApoA1 was the down regulated protein spot having a 1.98 fold change while destrin was identified as one of the up regulated protein spots (Table 2.3).

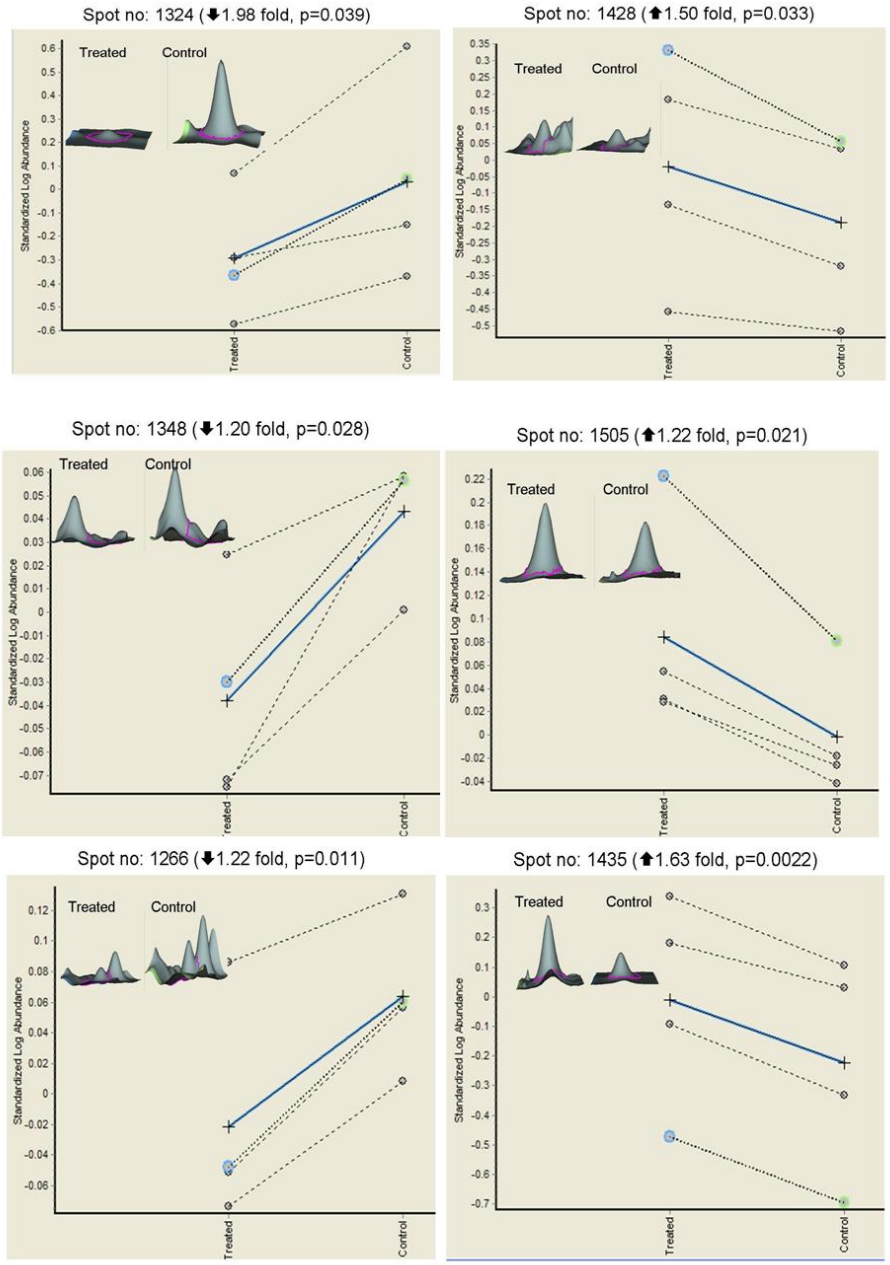

Fig.2.10 Differential protein expressions of individual spots found by DeCyder Differential Analysis Software.
Fold-changes and paired t-test values are shown. The graph shows the standardized log abundance of spot volume of each protein spot (y-axis) against the treated and control groups. The treated eyes were under 3 days of form deprivation myopia by diffuser. A 3-D view of protein abundance is also shown for each individual spots.

Table 2.3. Differentially expressed proteins after 3 days of form deprivation myopia by diffusers.

DIGE spot no.	NCBI GI no. [a]	Mascot protein name	Mowse Score [b]	Sequence coverage	Mascot pI [c]	Mascot Mw /kDa [d]	No. of peptides [e]	Organism [f]
1324	211159	Apoliprotein A1	376.4	28.8%	5.46	30.67	9	Gallus gallus
1435	45382979	Destrin	84	16%	7.52	18.9	3	Gallus gallus

a. A GI number (GenInfo Identifier) was assigned to each nucleotide and protein sequence accessible through The National Center for Biotechnology Information (NCBI)
b. Score was calculated by Mowse scoring algorithm in the Mascot system
c,d. The theoretical isoelectric point and molecular weight calculated using the databases in Mascot system
e. Number of peptides used for sequencing
f. Species of the identified protein

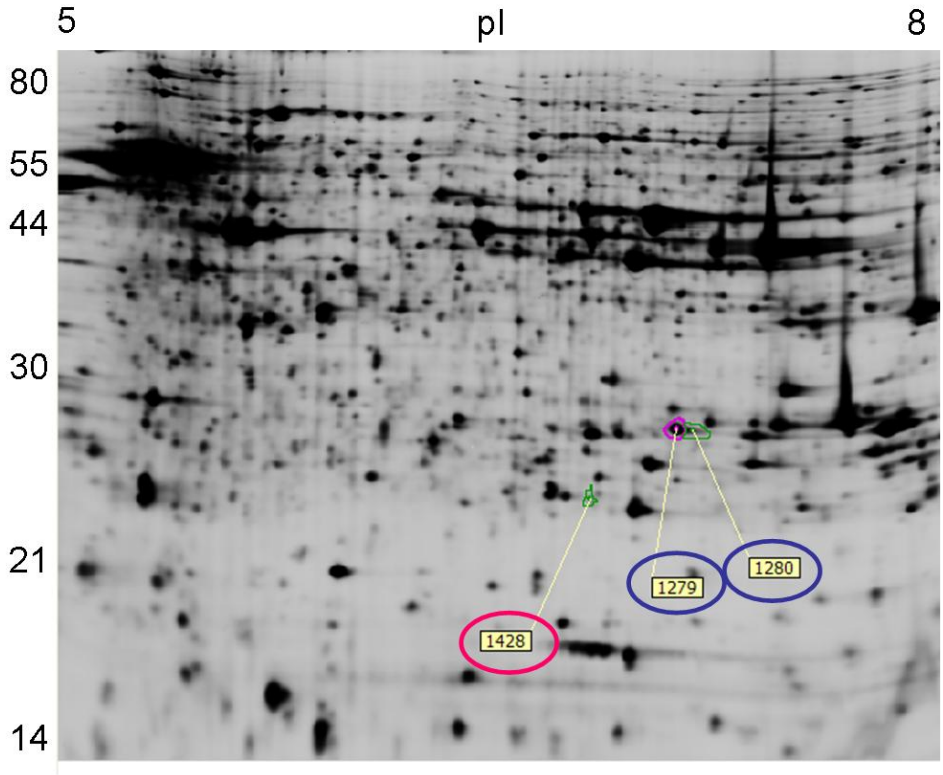

Fig.2.11 Identification of differential protein expressions after 7 days of form deprivation myopia by diffusers.
The gel image is a representative DIGE gel. Approximate molecular weight and isoelectric points are indicated. Protein spots in red circle indicate down-regulated proteins while those in blue circle are up-regulated proteins in myopic retinas.

In the retinal proteome of 7-day FDM by diffusers, fewer protein spots were found to be differentially expressed. Three spots showed a difference in expression after 7 days of FDM by diffusers (Fig.2.11). Of these spots, two showed an increase in expression and one spot showed a decrease in expression (Fig.2.12). These two up-regulated protein spots were identified as the same protein - phosphoglycerate mutase 1 (brain) (Table.2.4).

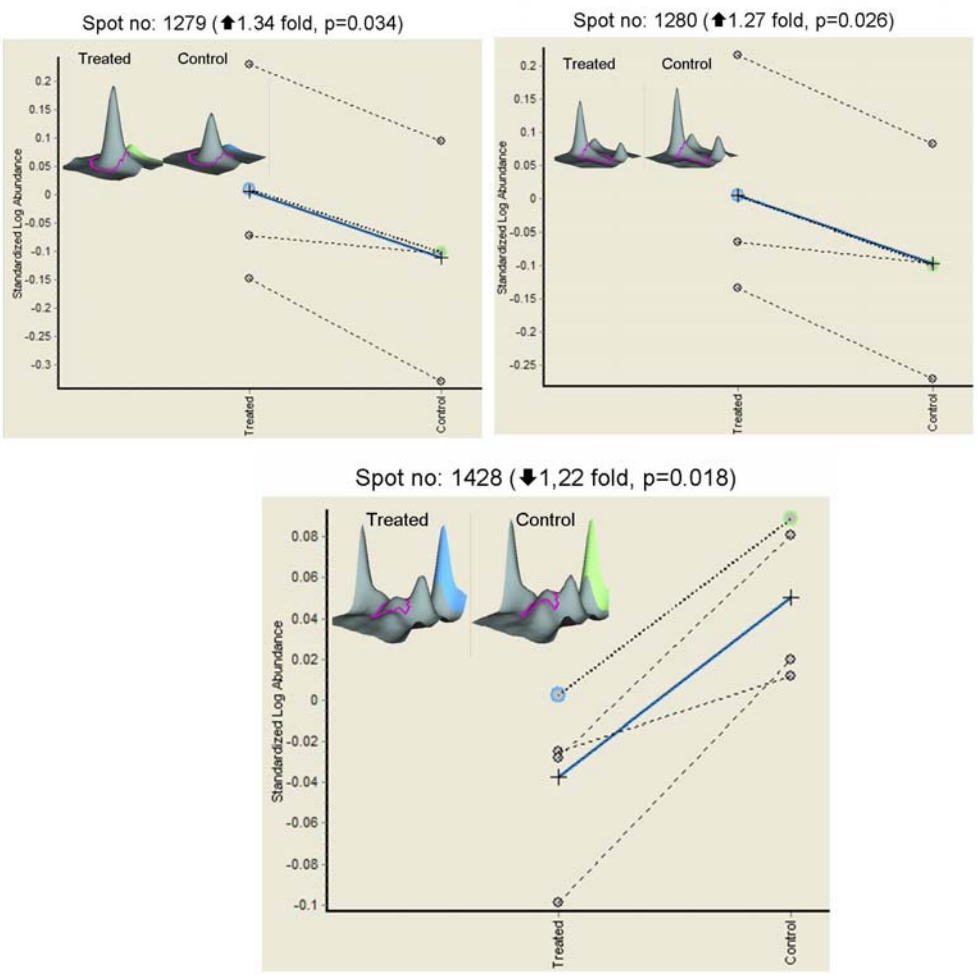

Fig.2.12 Differential protein expressions of individual spots found by DeCyder Differential Analysis Software.
Fold-changes and paired t-test value are shown. The graph shows the standardized log abundance of spot volume of each protein spot (y-axis) against the treated and control groups. The treated eyes were under 7 days of form deprivation myopia by diffuser. 3-D view is also shown for each individual spots.

Table 2.4. Differentially expressed proteins after 7 days of form deprivation myopia by diffusers.

DIGE spot no.	NCBI GI no. [a]	Mascot protein name	Mowse Score [b]	Sequence coverage	Mascot pI [c]	Mascot Mw /kDa [d]	No. of peptides [e]	Organism [f]
1279	71895985	Phosphoglycerate mutase 1 (brain)	133.1	12.6%	7.82	29.05	12	Gallus gallus
1280	71895985	Phosphoglycerate mutase 1 (brain)	63.1	12.6%	7.82	29.05	5	Gallus gallus

a. A GI number (GenInfo Identifier) was assigned to each nucleotide and protein sequence accessible through The National Center for Biotechnology Information (NCBI)
b. Score was calculated by Mowse scoring algorithm in the Mascot system
c,d. The theoretical isoelectric point and molecular weight calculated using the databases in Mascot system
e. Number of peptides used for sequencing
f. Species of the identified protein

2.4.3 Treatment with occluders

Myopia was also significantly induced in eye wearing occluders for 3 days ($p<0.01$). The mean refractive error was -5.58D ± 0.94 (Fig.2.13A). Elongation of axial length and vitreous chamber depth were also observed after myopia induced by occluders (Fig.2.14).

The amount of myopia was larger (-9.50D ± 1.02) after 7 days of myopia induced by occluders (Fig.2.13B). Concurrently, there was a significant increase in the vitreous chamber depth and axial length ($p<0.001$, paired Student's t-test). The vitreous chamber depth was increased by 0.286mm and 0.724mm after wearing occluders for 3 and 7 days respectively (Fig.2.14).

A.

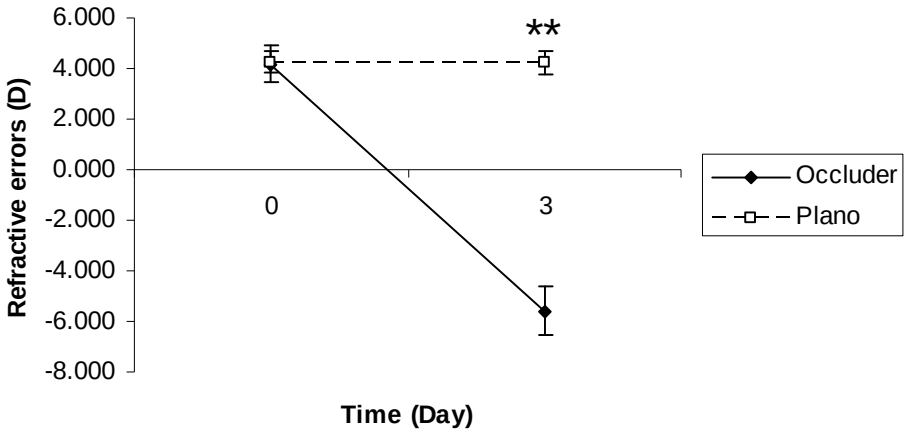

B.

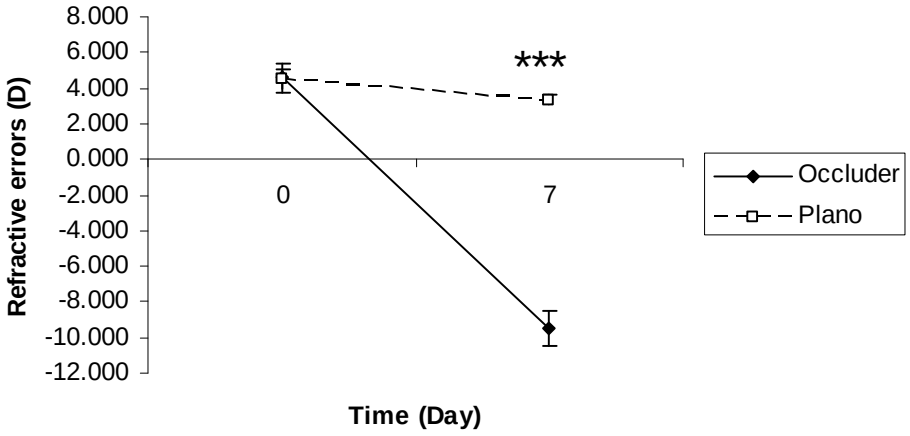

Fig.2.13 The development of refractive error (spherical equivalent) after 3 days (A) and 7 days (B) of myopia induced by occluders.
Occluders and plano lenses were worn on the right and left eyes respectively for 3 or 7 days. Each data point represents the mean refractive error ± SEM (n=4), *asterisks* over bars indicate paired, two-tailed Student's *t*-tests comparing data from right and left eye. * P<0.05, ** P<0.01, *** P<0.001

A.

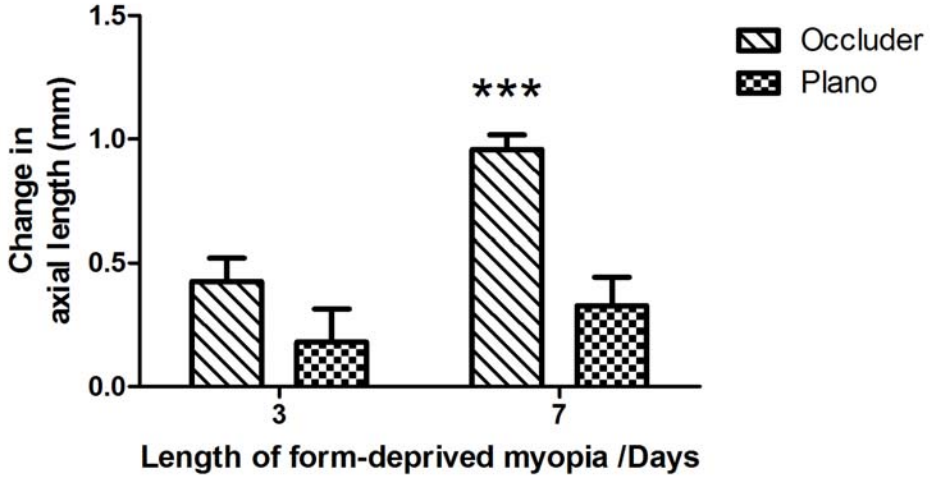

B.

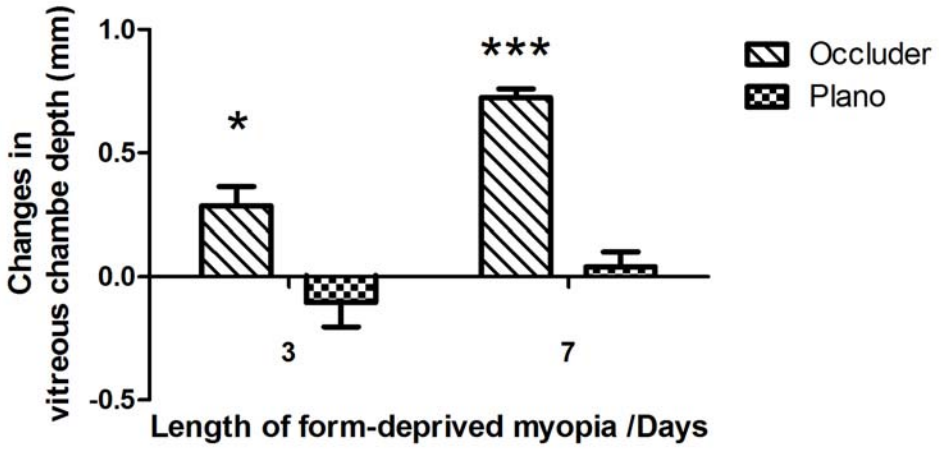

Fig.2.14 Changes in axial length (A) and vitreous chamber depth (B) after 3 and 7 days of myopia induced by occluders.
Each data point represents mean change ± SEM (n=4), *asterisks* over bars indicate paired, two-tailed Student's *t*-tests comparing data from right and left eye. * P<0.05, ** P<0.01, *** P<0.001.

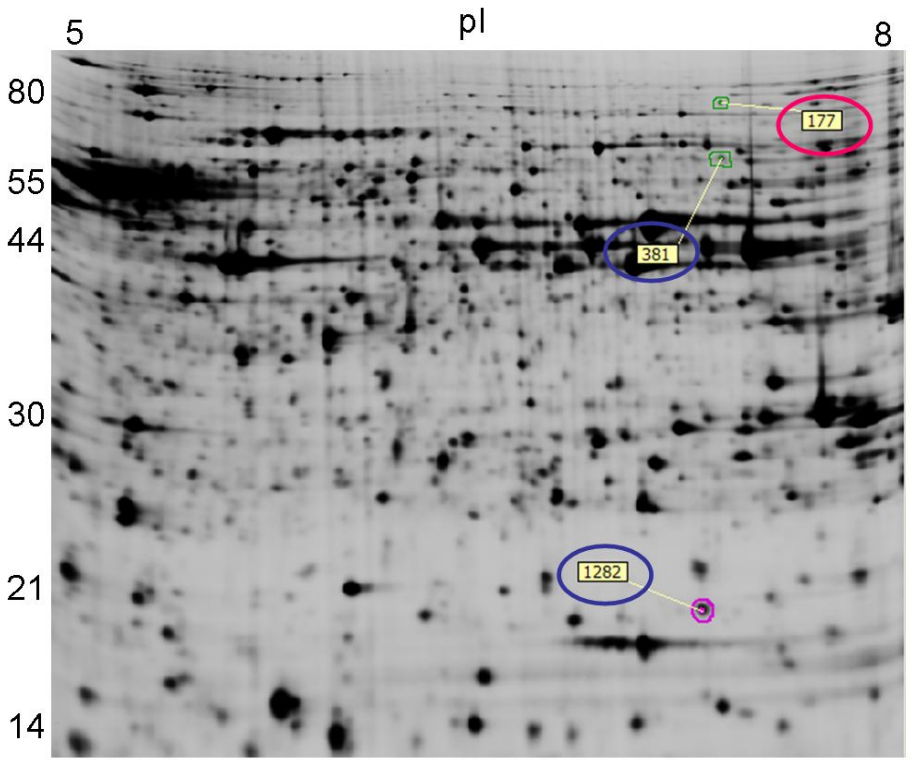

Fig.2.15 Identification of differential protein expressions after 3 days of myopia induced by occluders.
The gel image is a representative DIGE gel. Approximate molecular weights and isoelectric points are indicated. Spots in red circle indicate down-regulated proteins while those in blue circle are up-regulated proteins in myopic retinas.

After wearing occluders for three days, three protein spots were differentially expressed in myopic retinas (Fig.2.15). Two of them were up-regulated while one spot was down regulated (Fig.2.16). Destrin was identified as the protein spot showing with up regulation of 1.81 folds. Another two spots could not be identified as the amounts of peptide extracted from them were not sufficient for identification (Table 2.5).

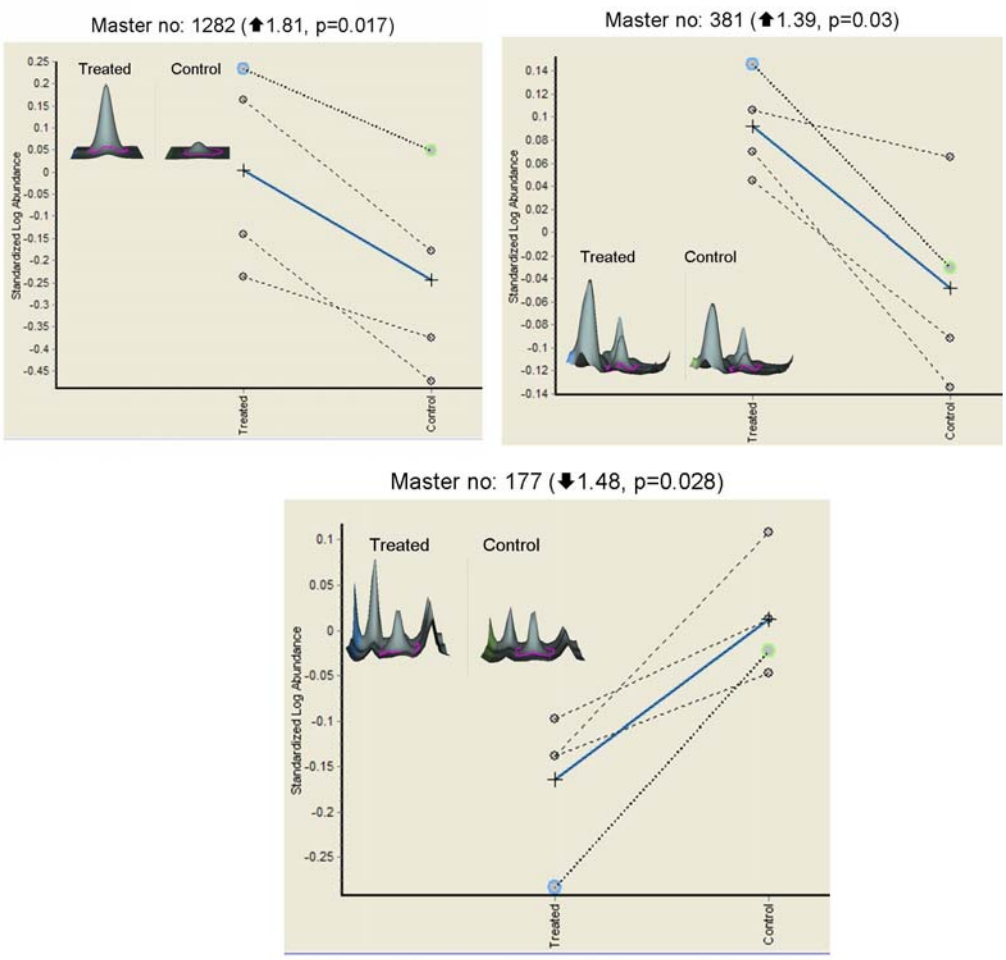

Fig.2.16 Differential protein expressions of individual spots found by DeCyder Differential Analysis Software.
Fold-changes and paired t-test values are shown. The graph shows the standardized log abundance of spot volume of each protein spot (y-axis) against the treated and control groups. The treated eyes were under 3 days of myopia induced by occluders. A 3-D view is also shown for each individual spot.

Table 2.5. Differentially expressed proteins after 3 days of myopia induced by occluder.

DIGE spot no.	NCBI GI no. [a]	Mascot protein name	Mowse Score [b]	Sequence coverage	Mascot pI [c]	Mascot Mw /kDa [d]	No. of peptides [e]	Organism [f]
1282	45382979	Destrin	84	16%	7.52	18.9	3	Gallus gallus

a. A GI number (GenInfo Identifier) was assigned to each nucleotide and protein sequence accessible through The National Center for Biotechnology Information (NCBI)
b. Score was calculated by Mowse scoring algorithm in the Mascot system
c,d. The theoretical isoelectric point and molecular weight calculated using the databases in Mascot system
e. Number of peptides used for sequencing
f. Species of the identified protein

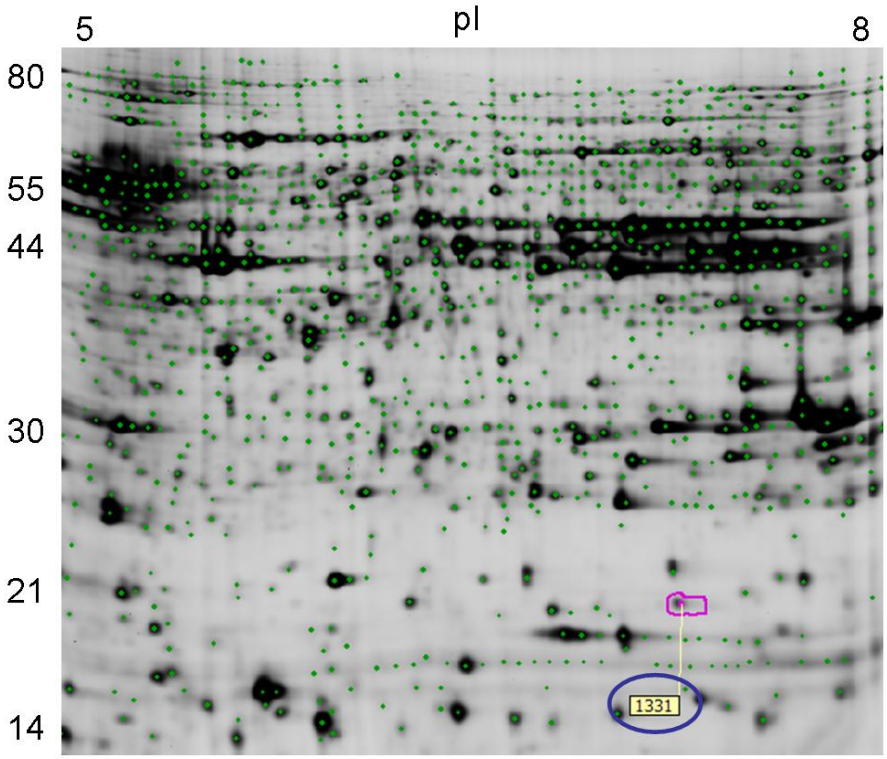

Fig.2.17 Identification of differential protein expressions after 7 days of myopia induced by occluders.
The gel image is a representative DIGE gel. Approximate molecular weights and isoelectric points are indicated. Protein spots in red circle indicate down-regulated proteins while the blue circle is a up-regulated protein in myopic retinas.

There was one protein spot showed up regulation in expression after myopia induced by occluders for 7 days (Fig.2.17 and Fig.2.18). It was found to be destrin which showed an increase in expression of 2.41 folds (Table 2.6).

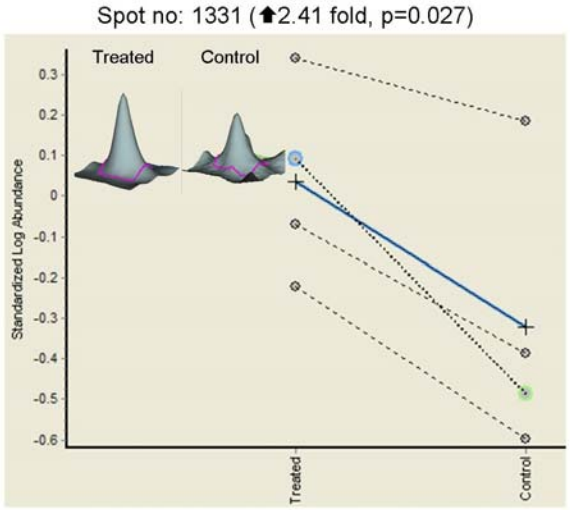

Fig.2.18 Differential protein expressions of individual spots found by DeCyder Differential Analysis Software.
Fold-changes and paired t-test values are shown. The graph shows the standardized log abundance of spot volume of each protein spot (y-axis) against the treated and control groups. The treated eyes were under 7 days of myopia induced by occluders. A 3-D view is also shown for each individual spot.

Table 2.6. Differentially expressed proteins after 7 days of myopia induced by occluders.

DIGE spot no.	NCBI GI no. [a]	Mascot protein name	Mowse Score [b]	Sequence coverage	Mascot pI [c]	Mascot Mw /kDa [d]	No. of peptides [e]	Organism [f]
1331	45382979	Destrin	84	16%	7.52	18.9	3	Gallus gallus

a. A GI number (GenInfo Identifier) was assigned to each nucleotide and protein sequence accessible through The National Center for Biotechnology Information (NCBI)
b. Score was calculated by Mowse scoring algorithm in the Mascot system
c,d. The theoretical isoelectric point and molecular weight calculated using the databases in Mascot system
e. Number of peptides used for sequencing
f. Species of the identified protein

2.5 Discussion

The differentially expressed proteins after 3 and 7 days of induced myopia were summarized in the Table 2.7 below.

Table 2.7 Summary of differential protein expressions after 3 and 7 days of induced myopia.

	3 days wear	**7 days wear**
Lens induced myopia	ApoA1[a] ⬇[c] 1.47 fold PGAM[b] ⬆ 1.24 fold	Destrin ⬆[d] 2.07 fold
Form deprived myopia by diffusers	ApoA1 ⬇1.98 fold Destrin ⬆1.63 fold	PGAM ⬆1.31 fold
Myopia induced by occluders	Destrin ⬆1.81 fold	Destrin ⬆2.41 fold

a. Apolipoprotein A1
b. Phosphoglycerate mutase 1 (brain)
c. ⬇ indicates down regulation of protein
d. ⬆ indicates up regulation of protein

The numbers of differential protein expressions found in myopic retinas were less than expected. This could be related to the stringent criteria in selecting differentially expressed proteins (Chapter 2.4.1). However, it is important to maintain stringent criteria so as to ascertain as much as possible that those proteins are involved in the process of myopic growth. Furthermore, these candidate proteins will be the important starting points for further experimentation exploring the exact biochemical network that orchestrates myopic growth. Another possible reason for the small amount of candidate proteins may be due to the limitation of 2D-DIGE itself. Typically, the membrane bound proteins and low abundance proteins are not easily detected using 2D-DIGE. Therefore, differential changes in these groups of proteins may not have been captured by the present investigation.

It is also possible that most of the differential protein expressions occur after a shorter period of deprivation than the time frame of this experiment. Although the current experimental design on time points has made reference to the rate of myopic growth in terms of refractive errors and axial length, it is unknown whether proteins expressions will mirror the same rate of growth. It is plausible that more differentially expressed proteins may be found in shorter period of deprivation such as a few hours, since there is evidence that the eye is able to respond to even a few minutes of defocus (Zhu et al. 2005; Zhu and Wallman 2009). Therefore, further work will be needed to study changes in protein expressions after a shorter period of deprivation.

It is also interesting to note that more proteins showed different expressions after 3 days of both LIM and FDM than 7-day deprivation (Table 2.7). On one hand, this may suggest more significant changes in retinal proteome have occurred during the earlier phase of myopia development. On the other hand, as the eyes approach fully emmetropization after 7 days, the biochemical and proteins changes may begin to subside. Therefore, the retinal proteome may not be necessary to change as much and "stabilized" in the later stage of myopia development.

Among the differential proteins found in LIM and FDM for 3 days, apolipoprotein A1 (ApoA1) was the common protein that was down regulated in all myopic retinas (Table 2.8).

Table 2.8 Summary of protein expression of apolipoprotein A1 and mean refractive errors (spherical equivalent ± SEM) after 3 days of lens-induced and form deprivation myopia. *Asterisk* indicates $p<0.05$, paired Student's t-test.

	Protein expression	**Mean refractive errors**
Lens-induced myopia	⬇ 1.47 fold *	-4.63D ± 0.48 *
Form deprivation myopia by diffusers	⬇ 1.98 fold *	-6.31D ± 0.76 *
Myopia induced by occluders	⬇ 1.91 fold	-5.58D ± 0.94 *

Although the change in ApoA1 under myopia induced by occluders was marginally not significant ($p=0.071$), it did show the same down regulation as found in LIM and FDM by diffusers. It is also noted that there was a larger variation in refractive errors in the occluder wearing group (Table 2.8). This large variation may also have rendered the differential protein expression of ApoA1 marginally insignificant.

Greater reduction of retinal ApoA1 expression was observed in the FDM. Apparently, there was more reduction in the retinal ApoA1 expressions with the greater amount of myopia as in the diffuser group (Table 2.8).

The changes in retinal ApoA1 expressions in the 7 days of LIM and FDM were not significantly different from the control. This indicates that ApoA1 may play a role in the early stages of biochemical changes that ultimately lead to myopia.

2.4.4 The functions and role of differential protein expressions in myopia

2.4.4.1 Apolipoprotein A1

Apolipoprotein A1 (ApoA1) is the major component in high density lipoprotein (HDL). It is involved in the reverse cholesterol transport which moves cholesterol from peripheral tissues to the liver for excretion (Zannis et al. 2006).

There is few published information relating ApoA1 to eye growth. Since there was down regulation of retinal ApoA1 expression in early myopic growth in chicks, it arouses speculation on the possible relationship between HDL and myopia.

Previous study has shown that children received breast feeding had more hyperopic refractive errors than those did not receive breast feeding (Sham et al. 2009). Breast milk is known to consist of high amounts of HDL (Schweigert et al. 2004) and high amounts of HDL in breast milk could have contributed to more hyperopic errors. Further investigation is required to explore the relationship of intake of HDL and myopia development.

Besides, ApoA1 was found to be able to increase transforming growth factor beta 2 (TGF-β2) (Norata et al. 2005). The role of TGF-β isoforms in the development of myopia have been proposed previously (Honda et al. 1996; Jobling et al. 2004). Down regulation of TGF-β isoforms has been shown in mammalian sclera during FDM (Jobling et al. 2004). Therefore, it is plausible that the reduction in retinal ApoA1 expression in myopic retina may lead to a decrease in TGF-β isoforms which modulates myopic eye growth.

2.4.4.2 Destrin

Destrin is also named as actin depolymerizing factor (ADF). It plays an important role in actin cytoskeleton of cells by increasing the actin filaments turnover. It acts by severing the actin filaments and increasing the rate of actin monomers leaving the pointed end of actin filaments (Maciver and Hussey 2002). Destrin is able to

increase the depolymerization of F-actin which is involved in cytokinesis, cell locomotion and plant cell elongation (Chen et al. 2001). Besides the role in remodeling the actin cytoskeleton, it has been suggested that destrin may inhibit actin denaturation during heat shock and chemical stress (Maciver and Hussey 2002).

In the eyes, destrin was found to be involved in structural homeostasis of cornea. Knockout of destrin in mice caused epithelial hyperplasia in cornea. This could be due to the increased content of actin filaments in corneal epithelial cells as the lack of actin depolymerizing factor (Ikeda et al. 2003; Zhang et al. 2008).

The mechanism of regulation of destrin is complicated. LIM kinase is one of the regulators of destrin while phosphorylation by LIM kinase causes inactivation of destrin. This induces accumulation of actin filaments (Arber et al. 1998; Bernard 2007). Interestingly, previous study has shown that transforming growth factor beta 1 (TGF-β1) could increase LIM kinase phosphorylation (Lee et al. 2008). Therefore, changes in the TGF-β1 level may affect the activity of destrin via LIM kinase.

TGF-β isoforms have been investigated in the development of myopia previously (Honda et al. 1996; Jobling et al. 2009). TGF-β isoforms were found to be down regulated in mammalian sclera during FDM (Jobling et al. 2004) and this led a reduction of collagen synthesis in scleral fibroblasts. Down regulation TGF-β isoform could further decrease LIM kinase phosphorylation (Lee et al. 2008) which would ameliorate the inactivation of destrin. Therefore, the expression of destrin would be increased in myopic eye.

In the current study, the expression of destrin was found to be increased during myopia development. This may increase the actin depolymerization in cells. As a consequence, there will be decrease in actin filaments due to the enhanced destrin activity. This reduction of actin filaments may have accounted for the increased scleral elasticity found during myopia development (McBrien et al. 2009).

However, the proposed interplay between TGF beta isoform and destrin in myopia development remains speculative. There is current controversy over the involvement of TGF-β in myopia development (Wang et al. 2009; Zha et al. 2009) since it is recently shown that there was no genetic association between high myopia and TGF-β (Wang et al. 2009). Therefore, the involvement of destrin in myopia development will require further characterization in animal and human myopia.

2.4.4.3 Phosphoglycerate mutase 1 (brain)

Phosphoglycerate mutase 1 (PGAM) is an enzyme involved in glycolysis. Glycolysis is the major metabolic pathway which generates a form of cellular energy - adenosine triphosphate (ATP). Since the expression of PGAM was found to be increased during myopia development, it indicates that the rate of glycolysis may be increased during myopia.

It was found that the glycolytic rate is higher than normal in a malignant tumor during its rapid cellular growth (Yalcin et al. 2009). In myopia, the eyeball elongates excessively which signifies accelerated eye growth. Therefore, it is not surprising to observe higher expression of PGAM in myopic eye which implicates high glycolytic rate and accelerated cellular growth.

Besides, there was a reduction, rather than an increase, in choroidal blood flow in myopic chicks (Fitzgerald et al. 2002). Theoretically, this will lead to a reduction of oxygen supply to the retina. Intuitively, increased in expression of PGAM may be useful because it can compensate the reduced supply of oxygen by increasing the rate of glycolysis.

2.4.5 ApoA1 as a candidate protein for further characterization

In order to further characterize the biochemical pathways that drive eye growth, it was attempted to investigate the role of one of the differentially expressed proteins. In the current results, destrin was changed more significantly in the later stage of myopia development. Therefore, its effect is suspected to be more downstream and it is likely to be involved in actin cytoskeletal changes during cellular growth. Whereas PGAM is a ubiquitous enzyme involved in metabolism and is expected to change according to the metabolic needs during growth. ApoA1 appeared to be an attractive candidate and its change was observed in both the LIM and FDM paradigms in the present study. Previous study on myopic retinas has demonstrated that ApoA1 may act as a "STOP" signal to inhibit myopic eye growth (Bertrand et al. 2006). In the current study, a decrease in retinal ApoA1 expression under LIM and FDM was demonstrated, which was not found in the previous study using conventional 2-DE (Bertrand et al. 2006). Overall, there is literature evidence as well as results from the current study to support an important role of ApoA1 in myopia development. Furthermore, when compared with other differentially expressed proteins, ApoA1 appeared as an early signal in myopia development.

Therefore, ApoA1 is chosen as the candidate protein to be further investigated in the later experiments.

2.5 Conclusions

In the current study, the retinal proteomes of growing myopic chicks were profiled and identified. The use of 2-D DIGE has enabled accurate detection of differential protein expressions as it eliminates the gel-to-gel variation which is frequently present in conventional 2-DE.

There were altogether thirteen differentially expressed spots found after 3 days of LIM and FDM. Among these spots, six of them were identified which gave the identities of three proteins, namely ApoA1, destrin and PGAM. Destrin and PGAM showed an increase in expression during myopia whereas ApoA1 showed a down regulation in myopic eye. ApoA1 was the common protein spot that was down-regulated in both LIM and FDM. ApoA1 was therefore selected to be further characterized for its relationship in myopia development.

Chapter 3: Effect of intravitreal injection of nicotinic acid and bezafibrate in development of myopia

3.1 Introduction

In Chapter 2, a number of candidate proteins were found to be differentially expressed in myopic retinas using negative lenses or form deprivation. Apolipoprotein A1 (ApoA1) was one of these differentially expressed proteins present in both lens-induced myopia (LIM) and form deprivation myopia (FDM). Therefore, ApoA1 was selected to be further investigated in this study. The aim was to explore the relationship between high density lipoprotein (HDL) and myopia development.

ApoA1 was found to be decreased in expression after 3 days of LIM or FDM. In order to investigate the role of ApoA1 in the development of myopia, physiological experiments were performed in chicks by raising the level of ApoA1 pharmacologically. ApoA1 is the major component in HDL. The level of HDL is found to be closely related in cardiovascular diseases (Barter et al. 2007). High level of HDL showed a protective effect in cardiovascular diseases. Nicotinic acid and fibrates are one of the drugs used to raise the HDL level in human.

Nicotinic acid is also known as niacin or vitamin B_3. It was first discovered to be effective in lowering the plasma cholesterol level in rabbits in the middle of the 20^{th} century (Altschul and Herman 1954). It was further found that nicotinic acid can

decrease the free fatty acid of the plasma lipids (Carlson 2005). A number of clinical studies also showed that the intake of nicotinic acid caused a significant increase in HDL level in plasma. One of the studies found 50% increase in HDL level in hyperlipidaemic patients after treatment of nicotinic acid (Birjmohun et al. 2004). The increase in HDL level was achieved by decreasing hepatic removal of ApoA1 (Parsons and Flinn 1959) while the synthesis of ApoA1 remained unchanged (Jin et al. 1997). Nicotinic acid was also effective in lowering the triglyceride synthesis in the liver by inhibition of diacylglycerol acyltransferase 2. Diacylglycerol acyltransferase 2 is the key enzyme in esterification of fatty acid to form triglycerides. Nicotinic acid has also been reported to decrease the very low-density lipoprotein in plasma (Siripurkpong and Na-Bangchang 2009). Nicotinic acid is a potent lipid-modifying drug and available in the market as Niaspan (KOS pharmaceuticals, Miami, FL, USA).

Fibrates can increase the HDL level in human and it acts as peroxisome proliferator-activated receptor (PPAR)-α agonist. PPAR-α is the first identified member of PPAR. PPAR takes part in lipid and glucose metabolisms, cellular differentiation and inflammation. Activation of PPAR-α increases HDL level via the induction of hepatic ApoA1 and A2 expression in human (Gervois et al. 2000). Fibrates were found to increase HDL level significantly in mice and human (Fruchart and Duriez 2006; Inaba et al. 2008). Moreover, a large scale randomized trial of the effect of bezafibrate, a member of fibrate, on myocardial infarction has shown that bezafibrate can reduce the risk of myocardial infarction (Tenenbaum et al. 2005).

ApoA1 could be increased by using nicotinic acid or fibrates (Parsons and Flinn 1959; Nagai et al. 2000; Sharma et al. 2006). As the protein expression of ApoA1 was decreased in the myopic chicks, it was intuitive to explore the effects of ApoA1 enhancing drugs on the development of myopia in chicks.

3.2 Objectives

The aim of this study was to investigate the effect of intravitreal injection of nicotinic acid and bezafibrate in myopia development. The protein expressions of ApoA1 in the retinas were examined after the intravitreal injection.

3.3 Materials and methods

White leghorn chicks (Gallus gallus domesticus) were bred from Specific Pathogen Free (SPF) eggs (SPFEGG, Jinan, China). The environment, care and use of the animals in these experiments were same as those in Chapter 2.

Four groups of chicks, 2 days old, were used in the experiment. Each group contained 6-8 chicks. On the day before intravitreal injections and 4 days post-injection, refractive errors and ocular parameters were measured. Ocular parameters were examined by high-frequency A-scan ultrasound system with a 30-MHz transducer sampled at a rate of 100MHz. Refractive errors were measured by a streak retinoscopy. Refractive errors were presented in terms of spherical equivalent, which was the sum of spherical power and half of cylindrical power.

Chicks were anaesthetized with 2% isoflurane in oxygen during intravitreal injection. The doses were administered in 10 µl vehicle solutions into vitreous of right eyes using a 30-gauge needle and a Hamilton syringe. Vehicle solution (10 µl) was injected into the contralateral eye as control (Table 3.1). The injections were made through the conjunctiva at approximately 3 mm above the corneal limbus. The site of injection was kept away from blood vessels on the conjunctiva. The needle was pointed towards the vitreous chamber in order to avoid damage to the crystalline lens. The injections were carried out daily at 11am-1pm for 4 days. Immediately after intravitreal injection in both eyes, negative (-10D) lenses were applied to both eyes of chicks with Velcro.

Table 3.1 Dosage and volume used in intravitreal injection.

Drugs	Dosage	Volume	Control
Nicotinic acid (Sigma-Alrich, St. Louis, MO, USA)	120mM and 60mM in PBS	10 µl	PBS
Bezafibrate (Sigma-Alrich, St. Louis, MO, USA)	50mM and 25mM in DMSO:PBS, 7:3 v/v	10 µl	DMSO:PBS, 7:3 v/v

3.3.1 Sample preparation

After the measurement of refractive errors and ocular parameters, the chicks were sacrificed by an overdose of carbon dioxide and the eyes were enucleated. Extraocular muscles were removed and eye was hemisected near the equator using a razor blade. The vitreous was removed carefully. The retina was then separated as

described in Chapter 2.3.1. The separated retina was immediately frozen in liquid nitrogen and kept under -80 ℃ for further use.

A frozen retinal sample with 300 µl lysis buffer was homogenized in a liquid nitrogen-cooled Teflon freezer mill (Mikrodismembrator Braun Biotech, Germany) for a total of 6 minutes at 1600 revolutions per minute. Lysis buffer contained 7 M urea, 2 M thiourea, 40 mM Tris, 0.2% (w/v) Biolytes, 1% (w/v) DTT, 2% (w/v) CHAPS, 1% (w/v) ASB14 (Calbiochem, San Diego, CA, USA) and 1 tablet of Complete, Mini protease inhibitor cocktail (Roche Applied Science, Switzerland) in 10ml buffer. The sample was collected and incubated at room temperature for 20 minutes, and then centrifuged at 16100 g for 20 minutes at 4 ℃. The supernatant was collected while the pellet was discarded. Three microlitres of supernatant was used to measure the protein concentration.

3.3.2 Protein quantification

The amount of protein in supernatant collected was measured by 2D Quant Kit (GE Healthcare Life Science, Sweden), as described in Chapter 2.3.3.

3.3.3 Gel electrophoresis

The sample were mixed with loading buffer (0.3M Tris, 10% SDS, 50% v/v glycerol, 3.6M beta-mercaptoethanol and 0.5% bromophenol blue) and heated at 95℃ for 5 minutes. The samples and protein markers were loaded into separate wells and electrophoresed in a 10% sodium dodecyl sulfate (SDS) polyacrylamide gel. Prestain protein marker (Fermentas PageRuler Protein Ladder Plus, Canada) was

also used so as to visualize the process of separation during gel electrophoresis. Constant voltage (80mV) for 140 minutes was applied and the proteins were separated according to its molecular weight.

3.3.4 Transfer of protein to PVDF membrane

After gel electrophoresis, the proteins were then transferred to the polyvinylidene difluoride (PVDF) membrane by electroblotting in a Mini Trans-Blot® Electrophoretic Transfer Cell (BioRad, San Diego, CA, USA). The gel and PVDF membrane (Immuno-Blot PVDF membrane, BioRad, San Diego, CA, USA) were placed together with filter pad and paper in a cassette. Constant voltage (57mV) was applied to the cell for 90 minutes at 4℃ in the transfer buffer (25mM Tris, 192mM glycine, 20%v/v methanol, pH 8.3).

3.3.5 Blocking

The non-specific binding sites of PVDF membrane were blocked by 5% non fat dry milk (Carnation non fat dry milk, Nestle, Switzerland) in Tris-buffered solutions (0.1M Tris-HCL, pH8.0, 0.5M NaCl) with 0.05% Tween-20 (TBST). The membrane was blocked overnight at 4℃ with shaking.

3.3.6 Antibodies incubation

The membranes were then incubated with primary antibodies in 0.3% non fat dry milk TBST for 1.5 hours at room temperature. TBST was used for washing the membranes for 6 times, 10 minutes each.

HRP-conjugated secondary antibodies in 0.3% non fat dry milk TBST were applied to the membrane for 1.5 hours at room temperature. The membranes were washed by TBST for 6 times, 10 minutes each (Table 3.2).

Table 3.2 Sources and concentrations of antibodies used in Western blotting.

Protein of Interest	Primary Antibody	Dilution	Secondary Antibody	Dilution	Positive Control	Sources
Apolipoprotein A1 (Apo A1)	Rabbit anti-chick Apo A1 polyclonal antibody	1:1000 in 0.3% non fat dry milk TBST	HRP-Goat anti-Rabbit IgG (H+L) Conjugate (Zymed Laboratories, CA, USA)	1:2000 in 0.3% non fat dry milk TBST	Chick Liver	Donated from Prof. Tarugi, Department of Biomedical Sciences, University of Modena and Reggio Emilia, Italy
Tubulin (loading control)	α Tubulin (DM1A) mouse monoclonal antibody	1:2000 in 0.3% non fat dry milk TBST	HRP-Goat anti-Mouse IgG (H+L) Conjugate (Zymed Laboratories, CA, USA)	1:2000 in 0.3% non fat dry milk TBST	N/A	Santa Cruz Biotechnology, Inc., CA, USA

3.3.7 Detection of signals

The signals were detected by enhanced chemiluminescent substrates. In the presence of HRP and a peroxide buffer, luminol is oxidized and forms an excited state product that emitted light. The intensity of light emission depends on the amount of reaction from HRP and substrate. Pierce SuperSignal® West Pico Chemiluminescent substrate (ThermoFisher Scientific, Waltham, MA, USA) was used in this study. Equal amount of peroxide buffer and luminol solution was

prepared, about 0.1ml/ cm^2. The membranes were incubated with the mixture for 5 minutes at room temperature.

After incubation, the membranes were placed in a plastic bag. Air bubbles in between membrane and bag were removed gently.

Signals were captured by a CCD camera called Lumi-Imager (Roche Applied Science, Switzerland). The intensities of the signals were calculated with the LumiAnalyst Software. The exposure time of the membrane varied from 10 seconds to 5 minutes depending on the strength of signals.

3.3.8 Positive and negative controls in Western blotting

Positive control was prepared from appropriate sources. They underwent the same incubation condition as listed in the Table 3.2. Negative control was performed by incubating with secondary antibodies only.

3.4 Results

With bezafibrate injection, the changes in vitreous chamber depth of the treated eye (25mM or 50mM bezafibrate injected) were similar to that of the control eye (Fig.3.1). The axial length of the treated eye (25mM or 50mM bezafibrate injected) was not significant different from the control eye (Fig.3.2).

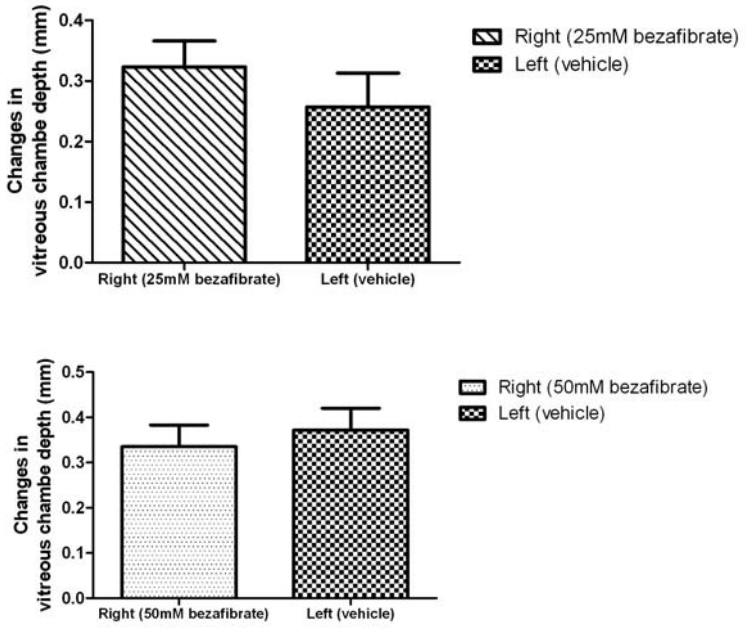

Fig.3.1 The effects of 25mM and 50mM bezafibrate on the vitreous chamber depth after four daily consecutive intravitreal injections.
Both eyes were wearing -10D lenses. Each data point represents mean value ± SEM, n=6.

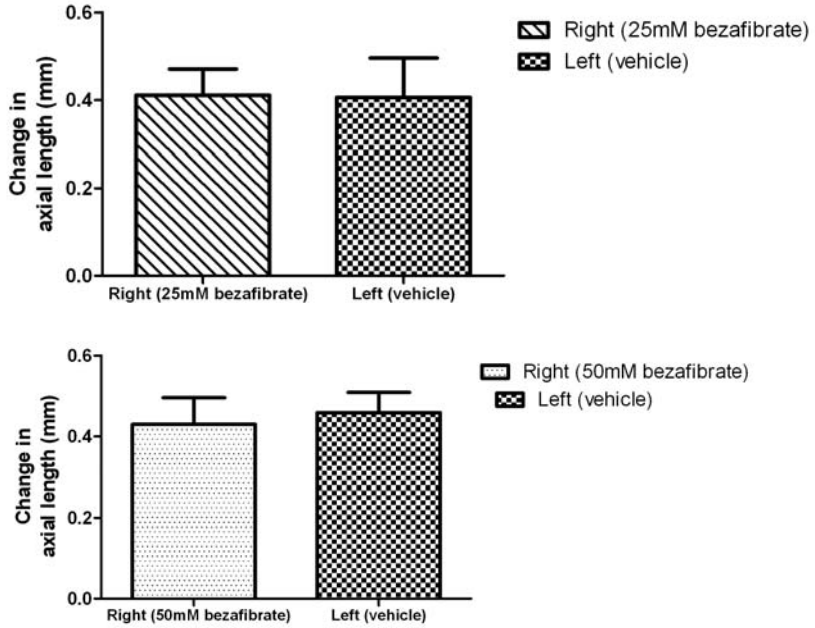

Fig.3.2 The effects of 25mM and 50mM bezafibrate on the axial length after four daily consecutive intravitreal injections.
Both eyes were wearing -10D lenses. Each data point represents mean value ± SEM, n=6.

Bezafibrate, either 25mM or 50mM, had no effect on refractive errors, anterior chamber depth, lens, retinal, choroidal and scleral thickness. Changes in these parameters over the course of experiment were summarized in the Table 3.3 and 3.4. These results showed that 25mM or 50mM bezafibrate did not affect the development of LIM in chicks. The eyes still compensated for the -10D lenses even with intravitreal injection of 25mM or 50mM bezafibrate.

Table 3.3 The effects of 25mM and 50mM bezafibrate injections (Mean ± SEM, n=6).
Drugs were injected into right eye (R) while PBS was injected into left eye (L) as control. Abbreviations are as follows: ACD is anterior chamber depth. Lens denotes lens thickness. Retina denotes retinal thickness.

		Δ ACD (mm)		**Δ Lens (mm)**		**Δ Retina (mm)**	
Group	**Dose**	**R**	**L**	**R**	**L**	**R**	**L**
Bezafibrate	**25mM**	-0.042±0.015	-0.034±0.018	0.222±0.021	0.251±0.019	-0.007±0.003	-0.005±0.005
	50mM	-0.057±0.037	-0.101±0.031	0.222±0.021	0.269±0.019	0.008±0.004	0.005±0.005

Table 3.4 The effects of 25mM and 50mM bezafibrate injections (Mean ± SEM, n=6).
Drugs were injected into right eye (R) while PBS was injected into left eye (L) as control. Abbreviations are as follows: Choroid is choroidal thickness. Sclera denotes scleral thickness. Rx denotes refractive errors.

		Δ Choroid (mm)		**Δ Sclera (mm)**		**Δ Rx (D)**	
Group	**Dose**	**R**	**L**	**R**	**L**	**R**	**L**
Bezafibrate	**25mM**	-0.096±0.012	-0.076±0.019	0.011±0.006	0.013±0.016	-3.139±1.097	-2.861±0.983
	50mM	-0.084±0.015	-0.090±0.022	0.006±0.008	0.005±0.005	-3.667±0.612	-5.583±0.708

Before measuring the protein expression of ApoA1 after intravitreal injection, positive control of the antibody was performed. Liver is the organ that synthesized ApoA1 and therefore positive control was performed using the chick liver (Tarugi et al. 1996). A clear, single band around 28kDa was shown in the positive control (Fig.3.3). This band matched the expected molecular weight of chick's ApoA1 and indicated that the antibody was effective in probing ApoA1 of chicks.

Negative control was performed with the incubation of secondary antibodies only. No signal was detected.

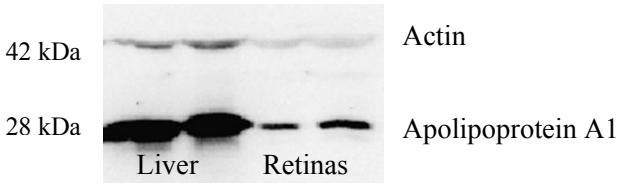

Fig.3.3 Western blot analyses of apolipoprotein A1 in liver and retinas.
A single band with 28 kDa is shown in both liver and retinas of chicks. Actin was used as a loading control.

The protein expressions of ApoA1 after intravitreal injection of 25mM or 50mM bezafibrate were examined using Western blotting. The expression of ApoA1 was higher in the retinas with 50mM bezafibrate when compared to those with 25mM bezafibrate. However, both of them did not show any significant increase in expression of ApoA1 when compared to the control eye (Fig.3.4).

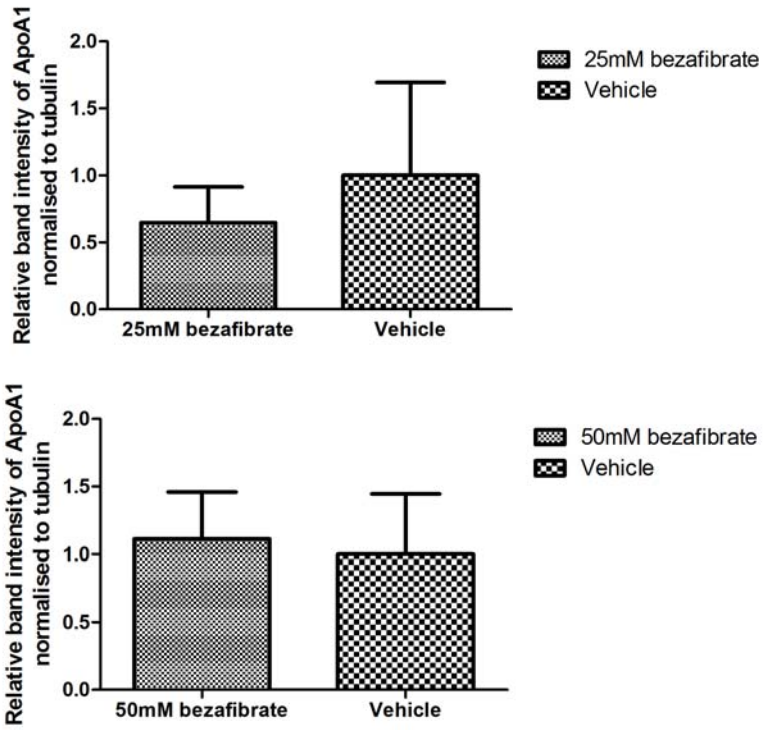

Fig. 3.4 The effects of four consecutive day of intravitreal injection of 25mM and 50mM bezafibrate on protein expressions of apolipoprotein A1 in the retina. Bezafibrate was dissolved in vehicle solution of DMSO:PBS, 7:3, v/v. Both eyes received -10D lenses, n=6.

In terms of nicotinic acid injections, two concentrations, 60mM and 122mM, were used in this study. 60mM nicotinic acid was effective in retarding the LIM as it induced less elongation of vitreous chamber depth than those from control eye ($P<0.05$) (Fig.3.5).

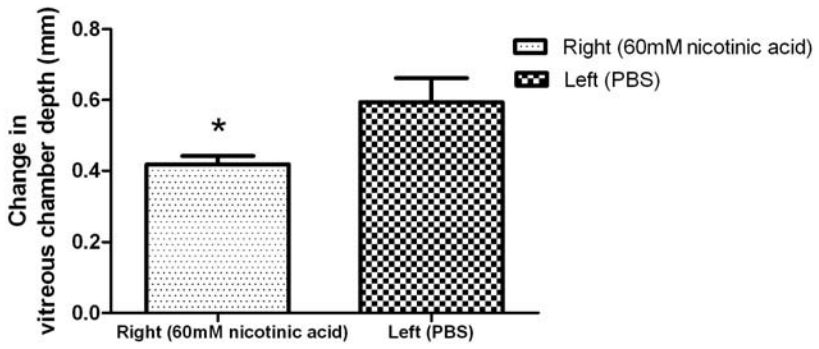

Fig.3.5 The effect of four consecutive day of intravitreal injection of 60mM nicotinic acid on change in vitreous chamber depth.
Both eyes received -10D lenses. *Asterisks* over bars indicate paired, two-tailed Student's *t*-tests comparing data from right and left eye. * P<0.05, ** P<0.01, *** P<0.001, n=8.

Both eyes demonstrated an increase in axial length. The axial length of 60mM nicotinic acid intravitreal injected eye was apparently shorter than that of the control eye but they were not statistically significant (p=0.078) (Fig.3.6).

As far as refractive errors were concerned, both eyes were myopic eventually. The nicotinic acid (60mM) intravitreal injected eye was apparently smaller than the control eyes. The mean change in refractive error of the nicotinic acid injected eye was -5.83D while the control eye was -7.83D. However, the difference was not statistically significant (Fig.3.6).

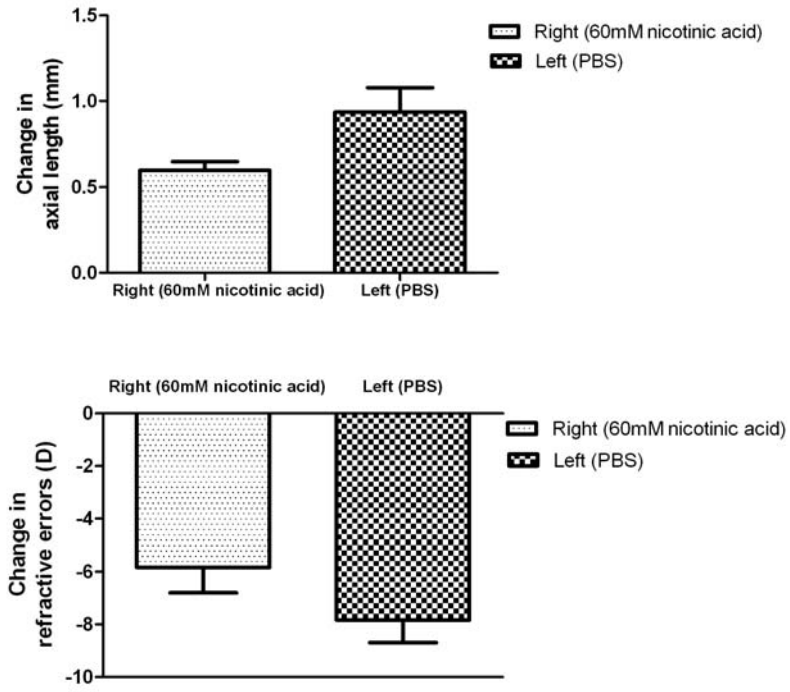

Fig.3.6 The effects of four consecutive day of intravitreal injection of 60mM nicotinic acid on axial length and refractive errors. Both eyes received -10D lenses, n=8.

The retinas were extracted to assess the effect of nicotinic acid on the protein expressions of ApoA1. A significant increase of about 50% in the expression of ApoA1 was observed in the nicotinic acid (60mM) injected eye when compared to the control eye ($P<0.05$) (Fig.3.7).

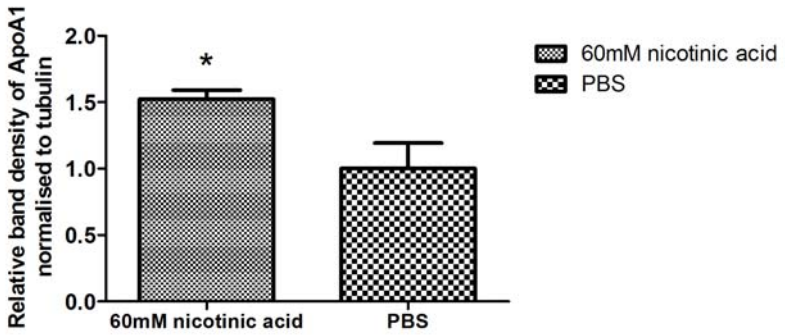

Fig.3.7 The effect of four consecutive days of intravitreal injection of 60mM nicotinic acid on protein expressions of apolipoprotein A1 in retinas.
Both eyes received -10D lenses. *Asterisks* over bars indicate paired, two-tailed Student's *t*-tests comparing data from right and left eye. * P<0.05, ** P<0.01, *** P<0.001, n=8.

Because only a marginal effect in vitreous chamber depth and axial length was observed with 60mM nicotinic acid, a higher concentration of 122mM was tried (which was the maximum concentration of nicotinic acid dissolvable in PBS). Although the axial lengths of both eyes were increased, the nicotinic acid injected eye were significantly shorter than that of the control eye (0.649mm vs. 0.878mm; injected vs. control; P<0.05) (Fig.3.8).

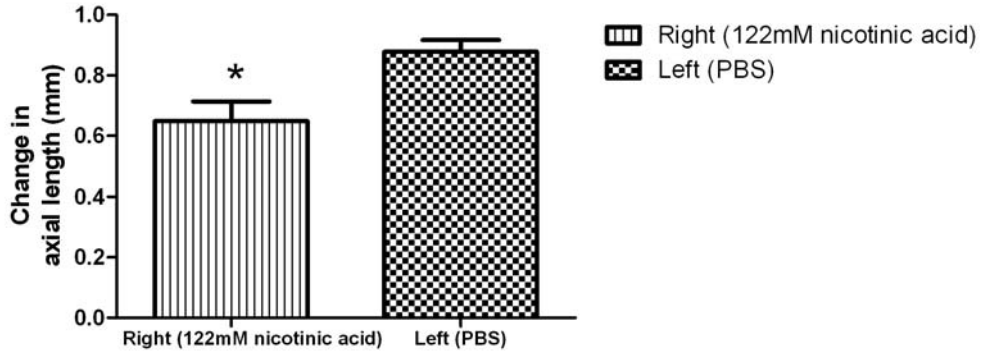

Fig.3.8 The effects of 4 consecutive day of intravitreal injection of 122mM nicotinic acid on axial length.
Both eyes received -10D lenses. *Asterisks* over bars indicate paired, two-tailed Student's *t*-tests comparing data from right and left eye. * P<0.05, ** P<0.01, *** P<0.001, n=8.

The vitreous chamber depth of the nicotinic acid injected eyes was smaller than that of the control eye (0.441mm vs. 0.581mm). However, the difference was not statistically significant (Fig.3.9).

In terms of refractive errors, the nicotinic acid injected eye was less myopic as compared to the control eye (mean change, -6.21D vs. -7.96D) although both eyes became myopic in the course of experiment (Fig.3.9). However, the difference was not statistically significant.

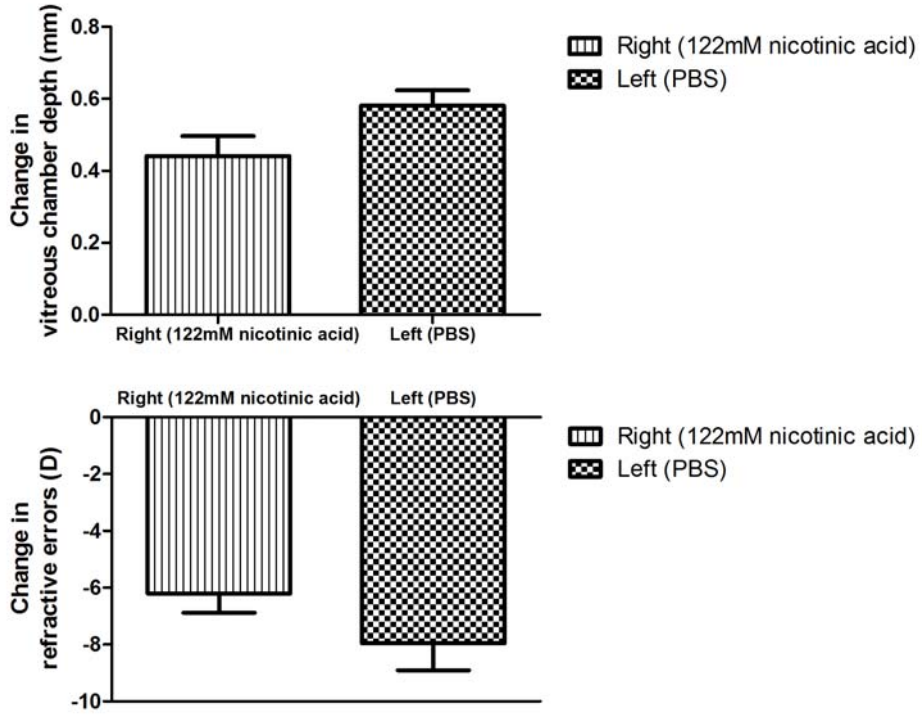

Fig.3.9 The effect of four consecutive day of intravitreal injection of 122mM nicotinic acid on change in vitreous chamber depth and refractive errors. Both eyes received -10D lenses, n=8.

The higher dosage (122mM) of nicotinic acid injection apparently did not increase the protein expressions of ApoA1 in the retina as its expression was not significantly different from the control. It was also noted that the variations in expression among individuals were large (Fig.3.10). Interestingly, among the two doses tested, the lower dosage (60mM nicotinic acid) seemed more effective in increasing the retinal ApoA1 level than the higher dosage (122mM nicotinic acid).

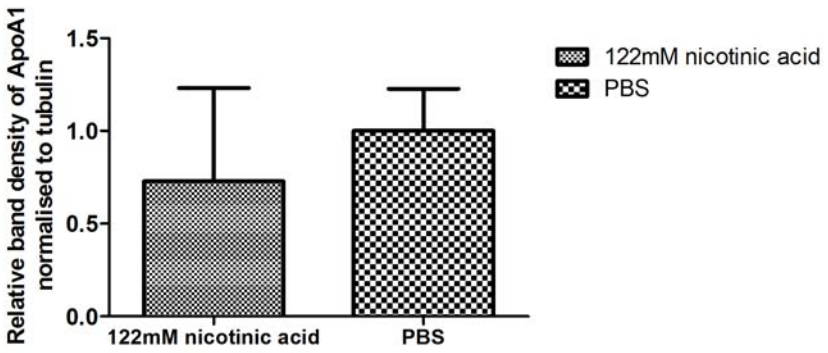

Fig.3.10 The effect of four consecutive days of intravitreal injection of 122mM nicotinic acid on protein expressions of apolipoprotein A1 in retinas. Both eyes received -10D lenses, n=8.

3.5 Discussion

Intravitreal injection of 25mM or 50mM bezafibrate did not affect the ocular growth induced by LIM in chicks. According to the results from Western blotting, intravitreal injection of 25mM or 50mM bezafibrate for four days failed to increase the protein expressions of ApoA1 in the retinas significantly. This may be why bezafibrate did not affect the development of LIM in chicks. Although the exact reason for its failure to increase ApoA1 is unclear, the poor solubility of bezafibrate may be a possible one since bezafibrate was only sparingly soluble in aqueous buffer. It was barely soluble in the vehicle solution of DMSO:PBS in 7:3 volume ratio. Therefore it is difficult to load higher concentration of bezafibrate. Given the large volume of liquid in the vitreous chamber which occupies at least 60% of chamber (Balazs et al. 1965), the dilution effect is crucial to the action of intravitreal injected drugs. Higher concentration of bezafibrate was tried with vehicle solution but failed and precipitates were observed in the solution. In addition, it caused the formation of opacity in vitreous which was evident by dissection of the eye after experiments.

Therefore, 50mM bezafibrate was the maximum concentration that can be applied to the vitreous. This directly affected and limited the final concentration of bezafibrate and its effects on the retina. It is plausible that insignificant amount of retinal ApoA1 was stimulated by the current dose of intravitreal injection of bezafibrate. This in turn, failed to prevent myopia development by bezafibrate. In other words, the low loading concentration may have affected its effect in raising retinal ApoA1 expressions.

In term of nicotinic acid, only the lower dose (60mM) was able to reduce the growth of vitreous chamber depth in LIM with a significant increase in retinal ApoA1 expressions, but the higher dosage (122mM) of nicotinic acid failed to do so. There was no significant dose-dependent increase in retinal ApoA1 when higher dosage of nicotinic acid was injected. Although it appeared puzzling, the insignificant increase in ApoA1 by higher dose of nicotinic acid was not unprecedented. Similar phenomenon has been also observed with other members of fibrates tested in rodents (Bachmann et al. 2004). Gemfibrozil is one of the members in fibrate, which acts as a PPAR-α agonist. When high ($100 mgkg^{-1}$) and low ($20 mgkg^{-1}$) dosages of gemfibrozil were administrated to rats by gavage daily, the lower dosage elicited a greater increase in ApoA1 level (Bachmann et al. 2004). Apparently, if the dosage used is higher than the optimal concentration, the level of ApoA1 increase may be less as in the case of 122mM nicotinic acid injection. The exact dose relationship between nicotinic acid and ApoA1 expression awaits further experimentation and exploration.

3.6 Conclusions

Although, both bezafibrate and nicotinic acid were tested, only the lower dosage of nicotinic acid (60mM) was effective in reducing the growth of vitreous chamber depth and increasing the protein expressions of retinal ApoA1 in LIM. The efficacy of reducing growth by nicotinic acid was apparently associated with its ability in increasing retinal ApoA1. The observation was consistent with the notion that ApoA1 expression is important in myopia development.

Chapter 4: Localization of apolipoprotein A1 in chick retina using immunohistochemistry

4.1 Introduction

The role of apolipoprotein A1 (ApoA1) in myopia development was investigated in Chapter 3. Increasing the retinal ApoA1 expression was able to reduce the growth of vitreous chamber depth in lens-induced myopia (LIM). ApoA1 is present in the normal human retina. Its distribution has been reported previously and ApoA1 was found in all layers in the retina and RPE (Simo et al. 2009).

The immunoreactivity of retinal ApoA1 was recently reported in chick eyes having different refractive errors (Bertrand et al. 2006). The retinal ApoA1 expression was increased in lens-induced hyperopia (LIH) while there was less immunoreactivities of ApoA1 in normal chick retina (Bertrand et al. 2006). Surprisingly, they did not find significant difference in protein expressions of retinal ApoA1 between LIM and normal eyes. In the present study and in contrast to Bertrand's study, significant down regulation of retinal ApoA1 expression was found in both LIM and form deprivation myopia (FDM) using two-dimensional fluorescence difference gel electrophoresis (2-D DIGE) (Chapter 2). It is important to locate the change of ApoA1 to particular retinal cell types during refractive development. Therefore the distributions and localization of ApoA1 expressions in LIM and LIH were investigated in this chapter.

4.2 Objectives

The aim of this study was to localize ApoA1 in chick retina of different refractive status using immunofluorescence staining.

4.3 Materials and methods

The method of immunohistochemistry (IHC) involved a number of steps as described below.

4.3.1 Tissue harvesting

White leghorn chicks (Gallus gallus domesticus) were bred from Specific Pathogen Free (SPF) eggs from Jinan in China. The environment for rearing the chicks, care and use of the animals were the same as in the Chapter 2.

The experiments were performed in four chicks when they were two days old. Negative (-10D) and positive (+10D) lenses were applied on the right and left eyes respectively. The chicks wore lenses binocularly for three days. Before and after the treatment, high-frequency A-scan ultrasound system with a 30-MHz transducer sampled at a rate of 100 MHz was used for measuring the ocular parameters. Refractive errors were also examined with a streak retinoscope. Refractive errors are presented in terms of spherical equivalent, which is the sum of spherical power and half of cylindrical power.

After three days of treatment, the chicks were sacrificed by an overdose of carbon dioxide. The eyes were enucleated and its extraocular muscles were removed. Several small incisions on equator were made by a 30-gauge needle to facilitate the

tissue fixation. Four chicks without treatment aged 5 days were also killed in order to locate the ApoA1 in the normal retina.

4.3.2 Fixating and embedding the eyes

The eyes were fixed in 4% paraformaldehyde (PFA) for a week. The eyes were placed in embedding cassette for paraffin embedding in Shandon Pathcentre Tissue Processor (ThermoFisher Scientific, Waltham, MA, USA). The detailed procedure was as follow. The eyes were first soaked in 70% ethanol for four hours. After four hours, 70% ethanol was replaced with 80% ethanol for four hours and followed by incubation of 90% ethanol for another four hours. The eyes were rinsed with 100% ethanol for three times, one hour each. Xylene was then substituted for two times, one hour each. Finally, the eyes were incubated with paraffin wax for one hour at 60℃. The processed eyes were finally embedded in paraffin wax to form eye blocks for sectioning.

4.3.3 Cutting and mounting the sections

The eye blocks were cut with a Leica RM2125 rotary microtome (Leica Microsystems, Wetzlar, Germany) into tissue sections of 5μm thick. The paraffin ribbons were placed in water bath at 37℃ and mounted onto the positively charged and coated slides (Superfrost Plus, Adhesion microscopic slides, ThermoFisher Scientific, Waltham, MA, USA). The slides were then air-dried under room temperature overnight.

4.3.4 Deparaffinizing and rehydrating the section

The sections were first deparaffinized with two changes of xylene for five minutes each. The sections were then rehydrated from 100% to 70% ethanol for three minutes each and rinsed under water for one minute.

4.3.5 Immunohistochemical staining by 3,3'-Diaminobenzidine (DAB)

The immunoreactivities of ApoA1 in normal chick retina were stained by DAB. Several steps were done to optimize the results before incubating with primary antibodies. The rehydrated sections were first permeabilized in phosphate buffered saline, pH 7.4 (PBS) plus 0.1% Triton X-100 for ten minutes. This can reduce the surface tension of the slides helping reagents to spread over with ease. The sections were then washed with PBS three times, five minutes each and soaked in 3% hydrogen peroxide (H_2O_2) in methanol for 30 minutes. H_2O_2 is used as blocking agent in IHC as it blocks the endogenous peroxidase activity causing high non-specific background. The sections were then blocked with 3% bovine serum albumin (BSA) in PBS for one hour at room temperature. Primary antibodies to ApoA1 (1:500 dilution) were applied onto the slides for overnight at 4℃ (Table 4.1). After washing with PBS plus 0.05% Tween 20 for four times, ten minutes each, horseradish peroxidase (HRP)-conjugated secondary antibodies (1:100 dilution) were incubated onto the section for one hour at room temperature. The slides were washed again with PBS plus 0.05% Tween 20 for four times, ten minutes each. The signals from immunoreactivites of ApoA1 were developed using DAB Tetrahydrochloride-Plus kit substrate for HRP (Zymed Laboratories, CA, USA). The

reagent mixture was prepared and kept at dark before use. The sections were incubated with reagent mixture for four minutes at room temperature. Colour development was monitored under microscope and stopped by rinsing in distilled water (dH_2O).

4.3.6 Counterstaining

The stained sections were subsequently counterstained with hematoxylin and washed in dH_2O two times for five minutes each.

4.3.7 Dehydrating and stabilizing with mounting medium

The stained sections were dehydrated from 70% to 100% ethanol for three minutes each and soaked in two changes of xylene for five minutes each. After dehydration, the sections were mounted with coverslips and observed under microscope.

4.3.8 Positive and negative controls

Positive control was prepared from appropriate sources. They underwent the same incubation condition as listed in the Table 4.1. Negative control was performed by incubating with secondary antibodies only.

Table 4.1 Conditions and sources of antibodies used in immunohistochemistry.

Protein of Interest	Primary Antibody	Dilution	Secondary Antibody	Dilution	Positive Control	Sources
Apolipoprotein A1 (Apo A1)	Rabbit anti-chick Apo A1 polyclonal antibody	1:500 in PBS	HRP-Goat anto-Rabbit IgG (H+L) Conjugate (Zymed Laboratories, CA, USA)	1:100 in PBS	Chick Liver	Donated from Prof. Tarugi, Department of Biomedical Sciences, University of Modena and Reggio Emilia, Italy

4.3.9 Immunofluorescence staining

Those sections from eyes which had worn -10D and +10D for three days were undergone immunofluorescence staining. Unlike the previous staining using DAB, immunofluorescence does not require the incubation with H_2O_2. Blocking solution (5% normal goat serum in PBS plus 0.3% Triton X-100) was applied onto the rehydrated sections for one hour at room temperature.

Primary antibodies, same as those used in DAB staining were applied onto the slides for overnight at 4℃. The slides were washed with PBS for three times, five minutes each.

Fluorochrome-conjugated secondary antibodies were incubated onto the section for two hours at room temperature in the dark. The slides were washed with PBS for four times, five minutes each (Table 4.2).

The sections were coverslipped with a drop of 4',6-diamidino-2-phenylindole(DAPI)/Antifade solution (Chemicon, Millipore, Billerica, MA, USA)

for visualization of cell nuclei. The immunoreactivities of ApoA1 were then examined under appropriate wavelength with fluorescence microscope (Nikon Eclipse Ti-S microscope, Japan).

Table 4.2 Conditions and sources of antibodies used in immunofluorescence staining

Protein of Interest	Primary Antibody	Dilution	Secondary Antibody	Dilution	Wavelength	Sources
Apolipoprotein A1 (Apo A1)	Rabbit anti-chick Apo A1 polyclonal antibody	1:500 in PBS plus 0.3% Triton X-100	Alexa Fluor® 568 goat anti-rabbit IgG (H+L) (Invitrogen, CA USA)	1:100 in PBS plus 0.3% Triton X-100	Excitation: 578nm Emission: 603nm	Donated from Prof. Tarugi, Department of Biomedical Sciences, University of Modena and Reggio Emilia, Italy

4.4 Results

An overview of localization of ApoA1 in normal chick retina was first assessed by immunohistochemical staining by DAB. The immunoreactivity from ApoA1 was shown in brown color with blue-purple cell nuclei as counterstain. This helps to illustrate different layers in retina using IHC.

Positive and negative controls were examined to validate the results. Chick liver was chosen as positive control of ApoA1 because it is the major site of ApoA1 synthesis and secretion (Tarugi et al. 1996). A strong immunoreactivity of ApoA1 was present

in the chick liver (Fig.4.1B). Negative control was also carried out to investigate non-specific staining by secondary antibodies. There was no staining (brown colour) when only secondary antibodies were incubated (Fig. 4.1A).

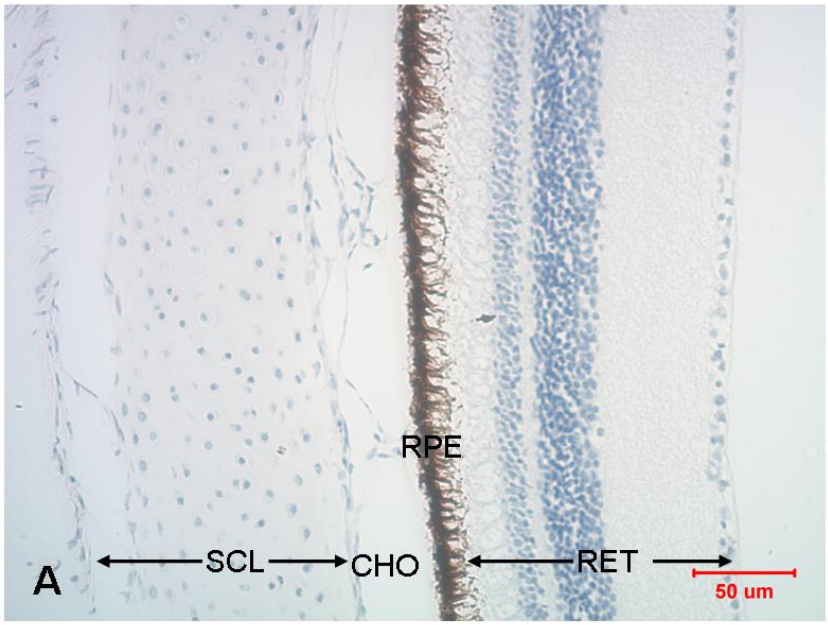

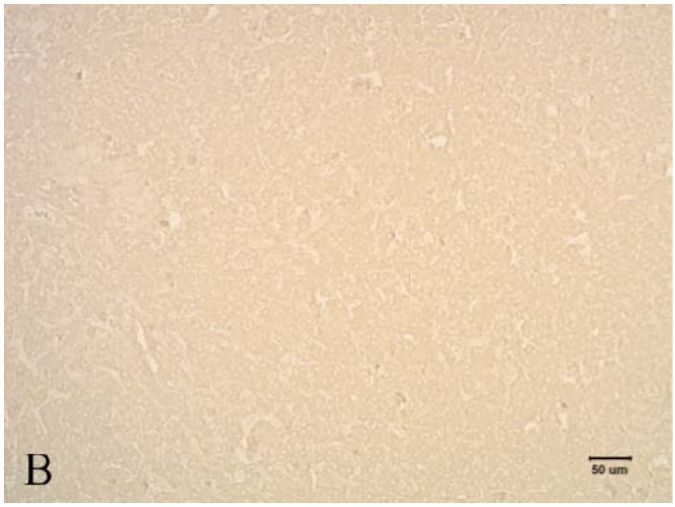

Fig.4.1 A: Negative control of apolipoprotein A1 in normal chick retina. B: Positive control of apolipoprotein A1 in chick liver.
Abbreviations are as follow: SCL: sclera, CHO: choroid, RPE: retinal pigmented epithelium, RET: retina.

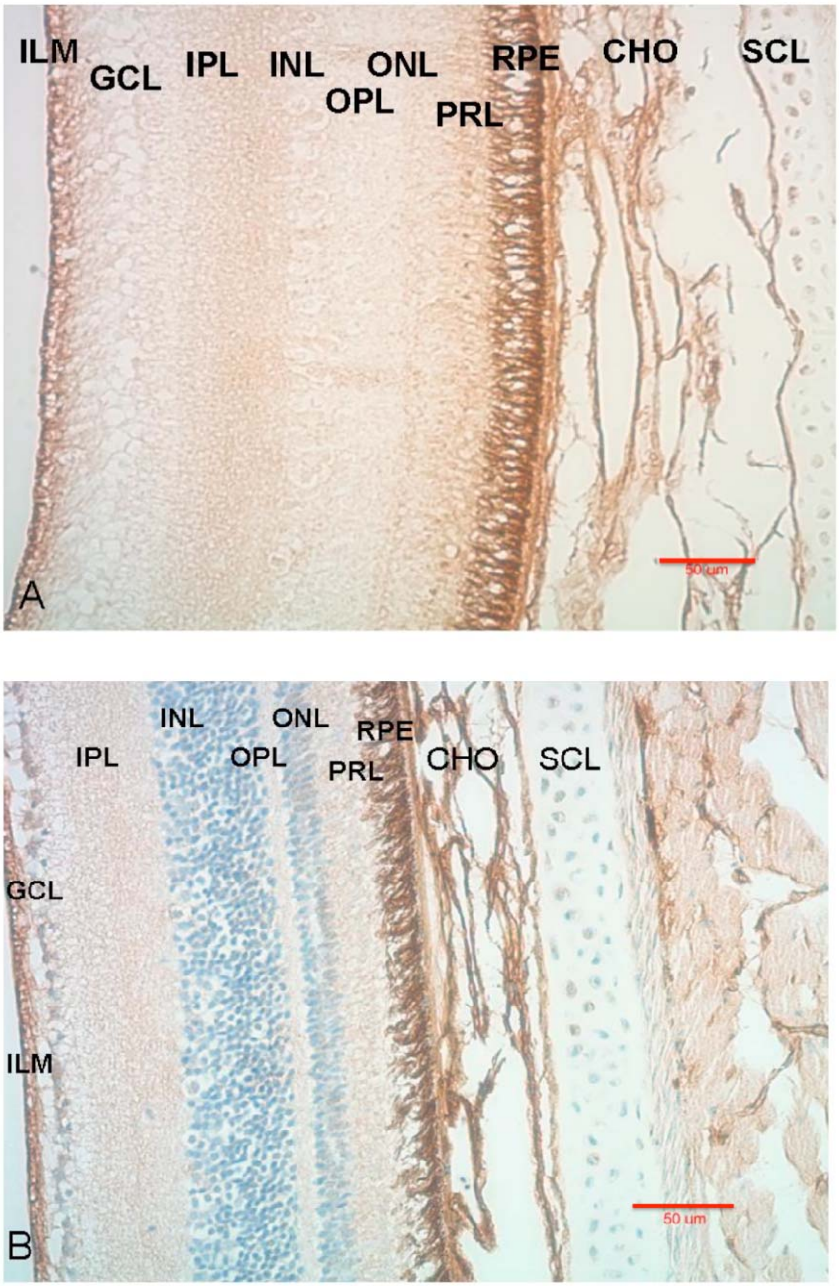

Fig.4.2 The immunoreactivity from apolipoprotein A1 in normal chick retina. Brown colour indicates the location of apolipoprotein A1. A: without counterstain. B: with counterstain.
Abbreviations are as follows: ILM: inner limiting membrane, GCL: ganglion cell layer, OPL; outer plexiform layer. ONL: inner nuclear layer; IPL: inner plexiform layer, INL: inner nuclear layer, PRL: photoreceptor layer, RPE: retinal pigmented epithelium. CHO: choroid, SCL: sclera.

ApoA1, stained as brown colour, was located in all areas across chick retina. Darker colour indicated heavier staining or higher immunoreactivity of ApoA1. Heavier staining was observed in the inner limiting membrane (Fig. 4.2). ApoA1 was also present in the choroid. This was likely due to the chick serum having abundant amount of ApoA1 (Tserentsoodol et al. 2006). Using DAB as immunostaining substrate had limitation in observing immunoreactivity from the RPE and choroid because they are also in brown colour which might have obstructed the staining from DAB substrate. Therefore, immunofluorescence staining was introduced to observe the immunoreactivity of ApoA1 under LIM or LIH.

The right eyes with negative lenses became myopic (-2.75D ± 0.44, mean ± SEM) after three days of treatment. The left eyes developed significant amount of hyperopia (+12.75D ± 0.24, mean ± SEM) after wearing +10D lenses for three days (paired Student's t-tests, $p<0.05$) (Fig. 4.3).

Elongation of vitreous chamber depth and axial length in the right (myopic) eyes were observed. Concurrently, there were a decrease in vitreous chamber depth and axial length in left (hyperopic) eyes (Fig. 4.4).

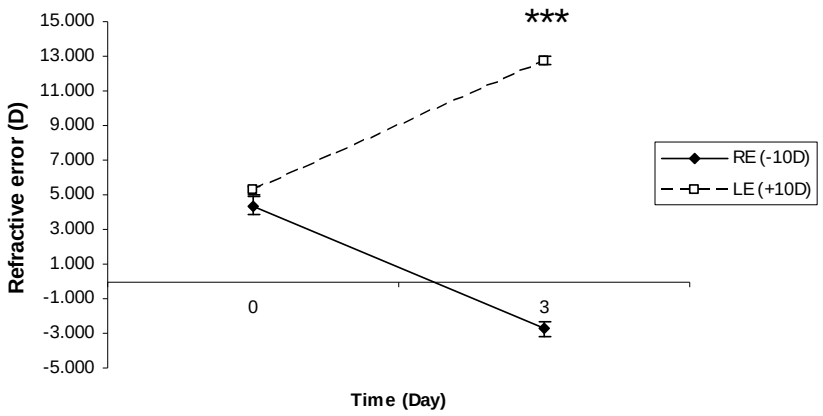

Fig.4.3 The development of refractive error (spherical equivalent) under 3-day lens-induced deprivation.
Right and left eyes wore negative (-10D) and positive (+10D) lenses respectively for 3 days. Each data point represents mean refractive error ± SEM (n=4), *asterisks* over bars indicate paired, two-tailed Student's *t*-tests comparing data from right and left eye. * P<0.05, ** P<0.01, *** P<0.001.

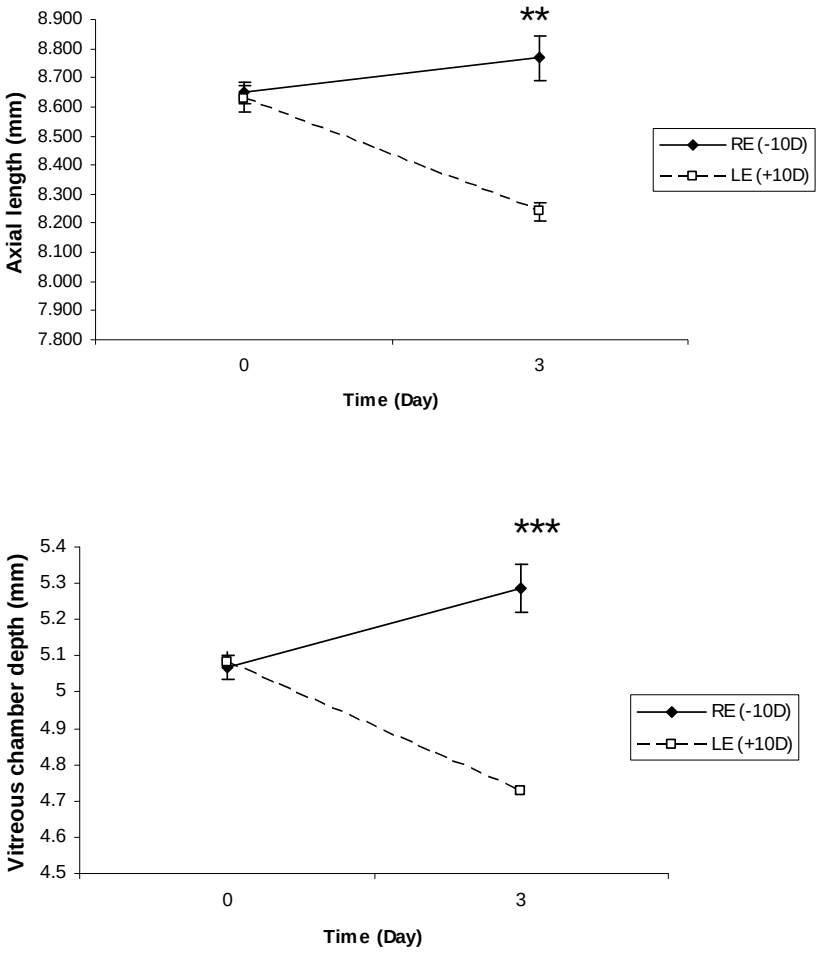

Fig.4.4 The vitreous chamber depth and axial length under 3-day lens-induced deprivation.
Each point represents mean measurement ± SEM (n=4), *asterisks* over bars indicate paired, two-tailed Student's *t*-tests comparing data from right and left eye. * P<0.05, ** P<0.01, *** P<0.001.

Since significant amount of myopia and hyperopia were induced to right and left eyes respectively after 3 days of lens wear, they were used for investigating the localization of ApoA1 in the myopic and hyperopic retinas.

Two images were generated from immunofluorescence staining. Red images from Alexa Fluor 568 were produced from immunoreactivity of ApoA1 while blue images from DAPI were generated from nuclei presented in the retina. The blue images were acted as a counterstain helping to identify the layers in the retina. In normal retina, ApoA1 were present in all layers using immunofluorescence staining (Fig. 4.5).

The thickness of inner nuclear layer from myopic retina was different from that of the hyperopic retina when comparing the DAPI images between myopic and hyperopic retina. The inner nuclear layer was approximately 6-8 cells thick in myopic retina but was around 11-12 cells thick in hyperopic retina (Fig. 4.6B and 4.6D).

Immunoreactivities of ApoA1 in red colour were found in all layers in the retinas under different visual manipulations. There were different distributions in immunoreactivities of ApoA1 in myopic and hyperopic retinas. Stronger immunoreactivity of ApoA1 in myopic eye was found in outer segment of photoreceptor layer (Fig. 4.6A and 4.7A). Concurrently, RPE and inner limiting membrane were strongly labeled in the hyperopic retina (Fig. 4.6C and 4.7B).

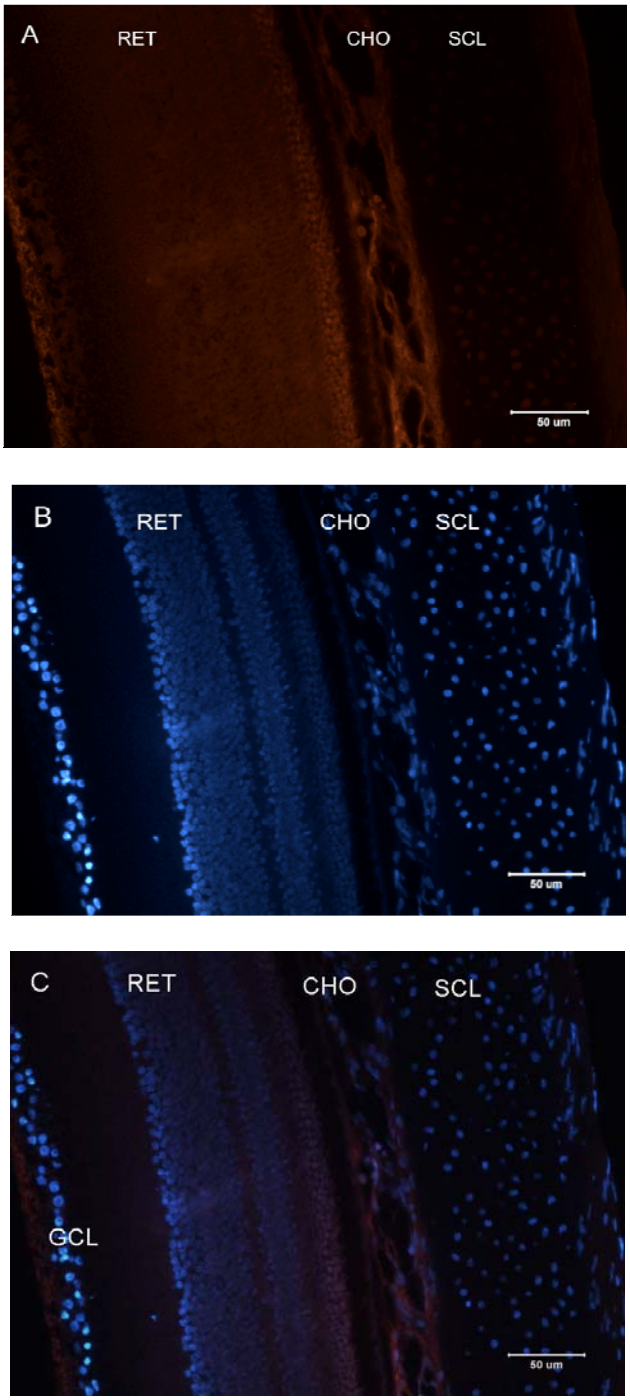

Fig 4.5 The immunoreactivites of ApoA1 in normal retina using fluorescence staining.
A. Immunoreactivity of apolipoprotein A1 by Alexa Fluor® 568 secondary antibodies (red). B. Nuclei stained with DAPI (blue). C. Merged image of Fig. 4.5A and Fig 4.5B.
Abbreviations are as follows: RET: retina, CHO: choroid, SCL: sclera, GCL: ganglion cell layer.

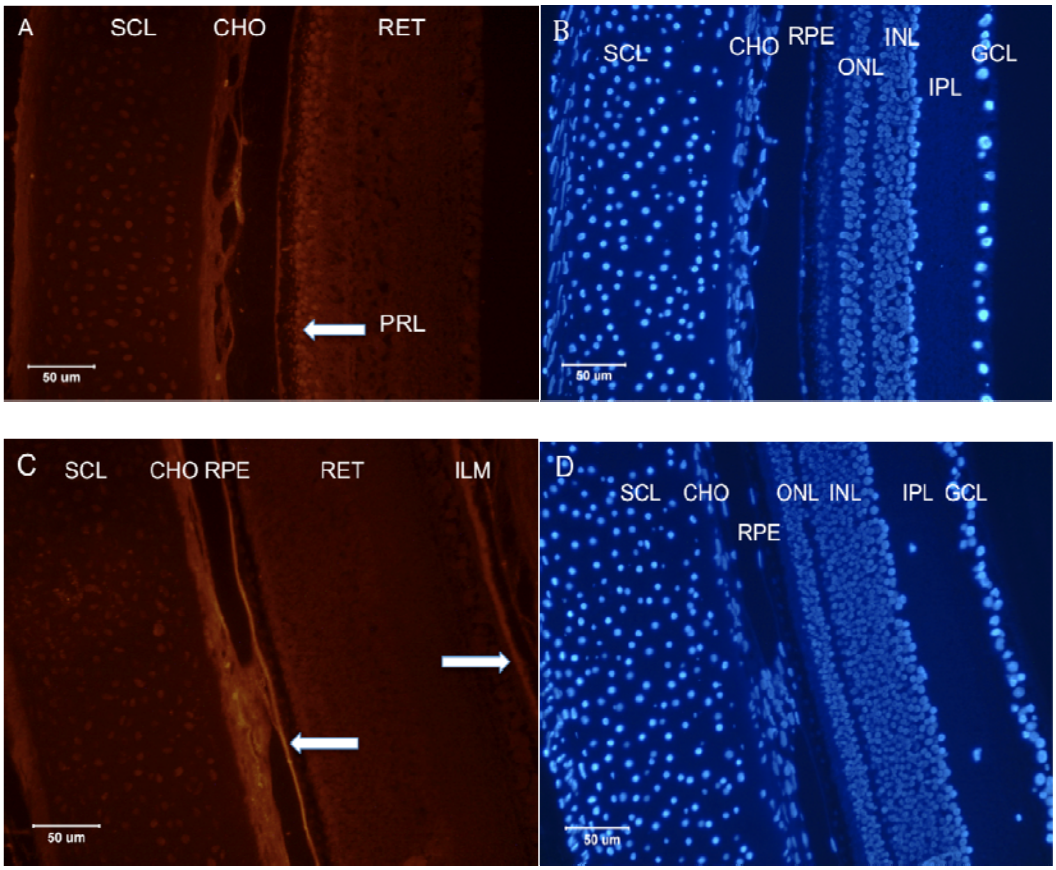

Fig.4.6 Immunohistochemical localization of apolipoprotein A1 in myopic (A and B) and hyperopic (C and D) chick retina.
A, C. Immunoreactivity of apolipoprotein A1 by Alexa Fluor® 568 secondary antibodies (red)
B, D. Nuclei stained with DAPI (blue)

Arrows indicate the strong immunoreactivity of ApoA1 in the photoreceptor layer in myopic retina, RPE and inner limiting membrane in hyperopic retina.
Abbreviations are as follows: ILM: inner limiting membrane, GCL: ganglion cell layer, OPL; outer plexiform layer. ONL: inner nuclear layer; IPL: inner plexiform layer, INL: inner nuclear layer, PRL: photoreceptor layer, RPE: retinal pigmented epithelium. CHO: choroid, SCL: sclera.

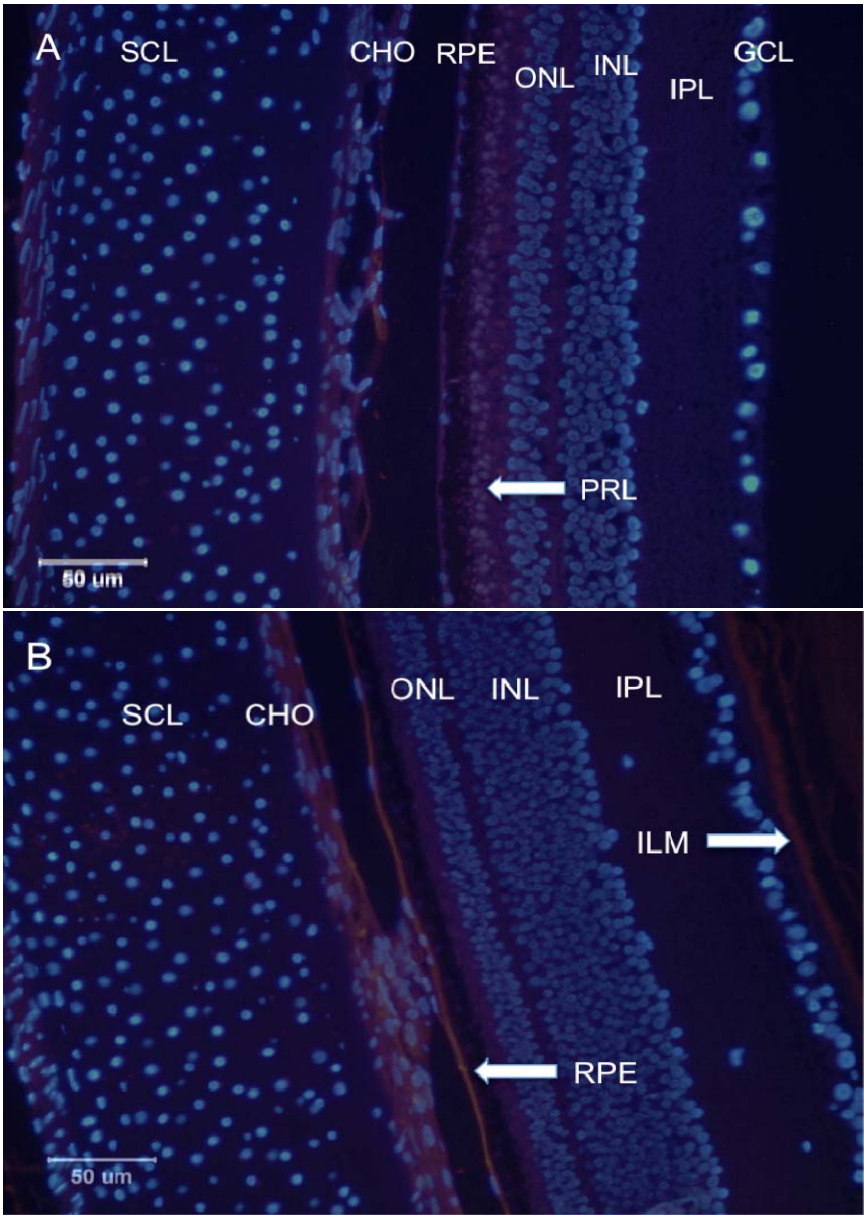

Fig.4.7 Immunohistochemical localization of apolipoprotein A1 in myopic and hyperopic chick retina.
A. Merged image of Fig.4.5A and Fig.4.5B from myopic retina.
B. Merged image of Fig.4.5C and Fig.4.5D from hyperopic retina.
Immunoreactivity of apolipoprotein A1 by Alexa Fluor® 568 secondary antibodies was stained in red. Nuclei were stained with DAPI (blue) Arrow indicates the strong immunoreactivity of ApoA1.

Abbreviations are as follows: ILM: inner limiting membrane, GCL: ganglion cell layer, OPL; outer plexiform layer. ONL: inner nuclear layer; IPL: inner plexiform layer, INL: inner nuclear layer, PRL: photoreceptor layer, RPE: retinal pigmented epithelium. CHO: choroid, SCL: sclera.

4.5 Discussion

The inner nuclear layer in normal retina was 11-12 cells thick, but it reduced to 6-8 cells thick in myopic retina. This phenomenon was also demonstrated in other study with the similar thinning of inner nuclear layer in myopic retina (Liang et al. 2004). The reduction may be due to an increase of apoptosis of inner nuclear layer found in myopic chick retina (Mao et al. 2006). The significance of inner nuclear layer in ocular development has been shown in the study by Bitzer and Schaeffel. Damage in inner nuclear layer was found to alter the compensation of LIM and LIH. This can be induced by intravitreal injection of quisqualic acid, a glutamatergic excitotoxin. The quisqualic acid injected eye showed an increase in axial length and became myopic, regardless of positive or negative lens wear (Bitzer and Schaeffel 2004). This suggested that damage in inner nuclear layer could result in myopic growth in either LIM or LIH. In other words, the integrity of inner nuclear layer is crucial in guiding normal eye growth.

In addition, the immunoreactivities of ApoA1 were stronger in outer segment of photoreceptors than that in hyperopic retinas which indicated that more ApoA1 were accumulated in outer segment of photoreceptors during myopia development. An increase in ApoA1 in the outer segment was shown to stimulate the lipid efflux from the photoreceptors to RPE cells in culture (Ishida et al. 2006). The lipid efflux across the retina to RPE may be increased during myopia development, but the role of lipid transport in eye growth has not been described previously.

Moreover, an increase in ApoA1 in photoreceptors may relate to an increase in oxidative stress in retinas during myopia. Since ApoA1 is a potent scavenger of reactive oxygen species (Mackness and Durrington 1995; Robbesyn et al. 2005), increased ApoA1 may be required to combat an increase in oxidative stress in retinas during myopia. Oxidative stress was found to be associated with many diseases such as age-related macular degeneration (Ding et al. 2009), cataract (Berthoud and Beyer 2009) and diabetics retinopathy (Simo et al. 2009). However, it is unclear how myopia and oxidative stress are related and further studies are needed to clarify the relationship.

The fact that there was increased expression of ApoA1 in photoreceptors is interesting and it has highlighted the importance of photoreceptors in ocular growth as well as being the receptors of light. In fact, a number of structural changes in photoreceptors under LIM have been depicted in previous studies (Liang et al. 1995; Crewther 2000; Chui et al. 2008). In FDM chicks, the rod outer segments of chicks became elongated so its distal tips were closely apposed to basal lamina of RPE or indented to cell nuclei of RPE (Liang et al. 1995). Cone inner segments were thicker while its outer segment lamellae appeared damaged (Crewther 2000). The cone photoreceptor packing density in human myopic eyes was found to be lower than that of the control eye (Chui et al. 2008).

A number of studies have investigated the role of photoreceptors in myopia. Tunicamycin, which was thought to be specific in suppressing the normal function

of photoreceptors, inhibited the FDM significantly. However, gross damage of other cell types in the retinas were found after intravireal injection of tunicamycin (Ehrlich et al. 1990). Since the toxic effect of tunicamycin is general, its effect on preventing myopia cannot be solely attributed to its inhibition on photoreceptor function.

Another chemical, formoguanamine (FG), was used in studying the role of photoreceptors in myopia development. FG, acting specifically on the mitochondrial enzymes in RPE and photoreceptors, was able to inhibit FDM in chicks (Oishi and Lauber 1988; Westbrook et al. 1995). FG was found to decrease the activity of mitochondrial enzymes in RPE and photoreceptors and therefore abolished the functional and physiological activities of the photoreceptors and RPE (Obara et al. 1985; Liang et al. 1995). This indicated that photoreceptors, likely together with the RPE, are required in the myopia development. There is growing evidence indicating a potential role of RPE in myopia development. One of the important functions of RPE is to regulate chemical compositions in extracellular environment around RPE. Changes in this composition may alter the fluid transport across RPE and change choroidal thickness consequently. A numbers of transporters and channels such as potassium channel and sodium-potassium-chloride cotransporter were found in chick RPE (Rymer and Wildsoet 2005). Recent study showed that intravitreal injections of inhibitors of potassium channel and sodium-potassium-chloride cotransporter affected compensation for positive and negative lens defocus in chicks (Crewther et al. 2008). This further suggests that fluid transport mediated by RPE may play a role in regulating ocular growth.

According to the present results, RPE has strong ApoA1 expression in hyperopic retinas (Fig. 4.6). Similar ApoA1 expressions, together with other lipid related receptors and proteins were identified in the monkey retinas (Tserentsoodol et al. 2006). These machineries are thought to be important in facilitating lipid transport and metabolism of the retina in monkey. The current finding showed different distributions of ApoA1 in myopic and hyperopic retinas. This may suggest differential transport of ApoA1 during myopia and hyperopia and implies intraretinal lipid transport may be perturbed during different visual manipulations.

4.6 Conclusions

Localization of ApoA1 was found in multiple areas in normal retina. Intense staining of ApoA1 was found in the inner limiting membrane. The immunoreactivity of ApoA1 varied under different visual manipulations. It was more evident in photoreceptor layer in LIM eye. In LIH eye, ApoA1 was mainly found in the RPE and inner limiting membrane. These differential distributions of ApoA1 in the retina of different refractive status may indicate the altered transport of ApoA1 across the different retinal layers which is important in eye growth. The exact relationship between the lipid transport of ApoA1 and refractive errors is an important direction for further exploration.

Chapter 5: Effect of intravitreal injection of 8-Br-cAMP on myopia development in chicks

5.1 Introduction

Cyclic adenosine monophosphate (cAMP) is an important second messenger involved in signaling pathway. It is synthesized from adenosine triphosphate (ATP) by adenylyl cyclase. Cyclic adenosine monophosphate plays a key role in modulating a numbers of hormones, neurotransmittors and growth hormones (Kopperud et al. 2003). The major effect of cAMP is frequently mediated intracellularly by protein kinase A (PKA), also known as cAMP-dependent protein kinase (cAPK). Besides, there is a cAMP sensor protein called exchange protein directly activated by cAMP (Epac) which is another effector of cAMP (de Rooij et al. 1998).

In Chapter 2, apolipoprotein A1 (ApoA1) was shown to be differentially expressed in both lens-induced myopia (LIM) and form deprivation myopia (FDM). ApoA1 has been extensively investigated in cellular cholesterol transport physiology (Zannis et al. 2006; Zhu et al. 2007).

Cyclic adenosine monophosphate was found to be able to affect cholesterol transport by changing the activities of ApoA1. Previous study showed that cAMP promoted cholesterol efflux by increasing the ApoA1 binding activity to ATP binding cassette transporter A1 (ABCA1) in macrophages (Oram et al. 2000). ABCA1 acts as a

transporter of phospholipids and cholesterol to ApoA1 which causes time dependent cellular cholesterol efflux (Zhu et al. 2007). On the other hand, incubation of ApoA1 can increase the intracellular cAMP level in fibroblasts in concentration dependent manner. It activates the phosphorylation of ABCA1 which promotes the cholesterol efflux (Haidar et al. 2002; Haidar et al. 2004). It seems that cAMP and ApoA1 are closely related in a signaling cascade, however the causative effect of cAMP and ApoA1 is unclear. Therefore, it is attempted to explore the effect of cAMP on the protein expression of retinal ApoA1 and also on the myopia development by intravitreal injection of a cAMP analog.

5.2 Objectives

The aim of this study was to investigate the effect of 1mM 8-Br-cAMP on myopia development by intravitreal injection. The protein expression of ApoA1 in the retina after intravitreal injection of 8-Br-cAMP was also studied.

5.3 Materials and methods

White leghorn chicks (Gallus gallus domesticus) were bred from Specific Pathogen Free (SPF) eggs (SPFEGG, Jinan, China). The environment, care and use of the animals in these experiments were same as that in Chapter 2.

The intravitreal injections were carried on the 9 chicks at the age of 8 days after hatchling. Refractive errors and ocular parameters were measured before and after fours days of intravitreal injections. High-frequency A-scan ultrasound system with

a 30-MHz transducer sampled at a rate of 100 MHz was used for measuring ocular parameters while refractive errors were measured by a streak retinoscope. Refractive errors were presented in terms of spherical equivalent, which was the sum of spherical power and half of cylindrical power.

Chicks were anaesthetized with 2% isoflurane in oxygen during intravitreal injection. The doses were administered in 10 µl vehicle solutions into the vitreous of right eyes using a 30-gauge needle and Hamilton syringe. Vehicle solutions (10 µl) were injected into the contralateral eye as control (Table 5.1). The injections were made as in Chapter 3.3. It was carried out daily at 11am-1pm for four days. Immediately after the injections in both eyes, -10D lenses were applied to the both eyes of chicks via a Velcro ring.

Table.5.1 Dosage and volume used in intravitreal injection.

Drugs	Dosage	Volume	Control
8-Br-cAMP (Sigma-Alrich, St. Louis, MO, USA)	1mM in PBS	10 µl	PBS

5.3.1 Western blotting

After measuring the refractive errors and ocular parameters, the chicks were sacrificed by carbon dioxide overdose. The eyes were enucleated and hemisected to harvest the retinas. The retinas were subjected to the Western blotting procedures as described in Chapter 3. The amount of antibodies used for probing ApoA1 and tubulin was listed in Table 5.2 below. The signals were captured by a CCD camera

called Lumi-Imager (Roche Applied Science, Switzerland) as an image. The relative band intensity of ApoA1 was normalized to tubulin and compared between eyes.

Table 5.2 Sources and concentrations of antibodies used in Western blotting.

Protein of Interest	Primary Antibody	Dilution	Secondary Antibody	Dilution	Positive Control	Sources
Apolipoprotein A1 (Apo A1)	Rabbit anti-chick Apo A1 polyclonal antibody	1:1000 in 0.3% non fat dry milk TBST	HRP-Goat anti-Rabbit IgG (H+L) Conjugate (Zymed Laboratories, CA, USA)	1:2000 in 0.3% non fat dry milk TBST	Chick Liver	Donated from Prof. Tarugi, Department of Biomedical Sciences, University of Modena and Reggio Emilia, Italy
Tubulin (loading control)	α Tubulin (DM1A) mouse monoclonal antibody	1:2000 in 0.3% non fat dry milk TBST	HRP-Goat anti-Mouse IgG (H+L) Conjugate (Zymed Laboratories, CA, USA)	1:2000 in 0.3% non fat dry milk TBST	N/A	Santa Cruz Biotechnology, Inc., CA, USA

5.4 Results

The estimated volume of vitreous chamber was around 200µl (Zhu and Wallman 2009). The resultant concentration in the vitreous chamber was estimated to be 0.5mM.

After four days of consecutive daily intravitreal injection of 1mM 8-Br-cAMP, the refractive errors were significantly different from the fellow control eye which received PBS only. The control eye became myopic after four days of LIM. For

those eyes wearing negative lenses and receiving 1mM 8-Br-cAMP, the refractive errors remained hyperopic (1.56D ± 1.07, mean spherical equivalent ± SEM, n=9). It was significantly different from the control eye (Student's *t*-test, p<0.001) (Fig.5.1).

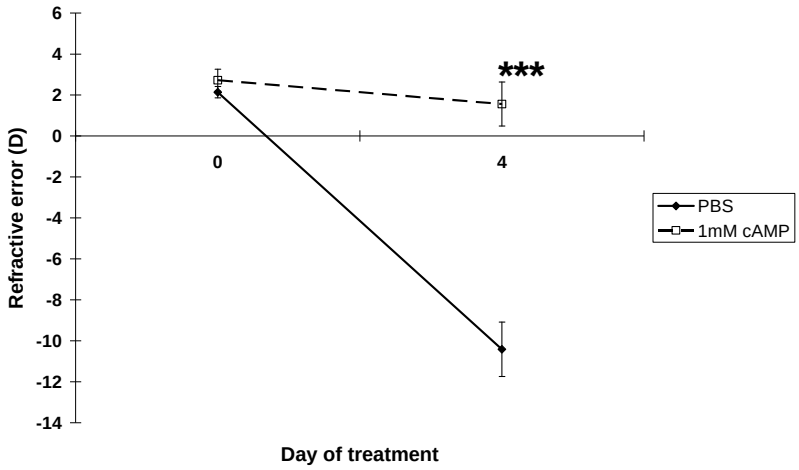

Fig.5.1 The effect of intravitreal injection of 1mM 8-Br-cAMP on refractive errors. Both eyes were wearing -10D lenses for four days. Intravitreal injection of 1mM 8-Br-cAMP significantly inhibited the lens-induced myopia. . Each data point represents mean refractive error ± SEM (n=9), *asterisks* over bars indicate paired, two-tailed Student's *t*-tests comparing data from right and left eye. * P<0.05, ** P<0.01, *** P<0.001.

Although both the injected and control eyes elongated after four days of LIM, the increase in axial length in the injected eye was less than that in the control eye (0.408 mm vs. 0.784 mm, injected eye vs. control eye, Student's t-test, P<0.01) (Fig. 5.2).

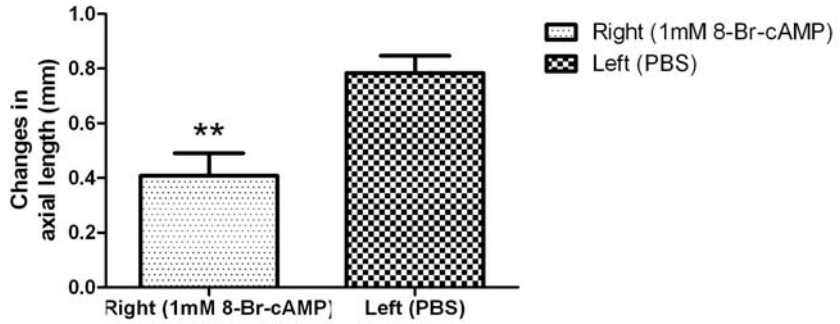

Fig.5.2 The effect of intravitreal injection of 1mM 8-Br-cAMP on changes in axial length.
Both eyes were wearing -10D lenses for 4 days. Intrvitreal in jection of 1mM 8-Br-cAMP significantly inhibited the lens-induced myopia. Each data point represents mean change ± SEM (n=9), *asterisks* over bars indicate paired, two-tailed Student's *t*-tests comparing data from right and left eye. * P<0.05, ** P<0.01, *** P<0.001.

The vitreous chamber depth of the injected eye correlated well with its refractive error and it did not show significant changes. Its refractive error was also hyperopic. The vitreous chamber depth of control eye increased after LIM as expected. The vitreous chamber depth of the control eye increased for 0.385mm after LIM, which was significant different from the 1mM 8-Br-cAMP injected eye (Student's t-test, P<0.01) (Fig.5.3).

As far as choroidal thickness is concerned, choroid became thinner (-0.114 mm ± 0.007, mean change ± SEM) in the control eyes as expected in LIM. Although the choroidal thickness also decreased in the injected eye, it was to a lesser extent (-0.047 mm ± 0.025, mean change ± SEM) and was significant different from the control eye (Student's t-test, P<0.01) (Fig.5.3). The changes in the vitreous chamber

depth and choroidal thickness can account for the changes in refractive errors between the 1mM 8-Br-cAMP injected eyes and the control.

There were significant differences in retinal thinkness between injected and control eye (Student's t-test, $P<0.01$) (Fig. 5.3). Thinner retinas were observed in the control eye which was expected in LIM.

Intravitreal injection of 1mM 8-Br-cAMP did not cause any significant change in the anterior chamber depth, lens and scleral thickness when compared to the control eye (Fig.5.4). Therefore, cAMP seemed to have specific effects on vitreous chamber depth, retinal and choroidal thicknesses of chick eye only.

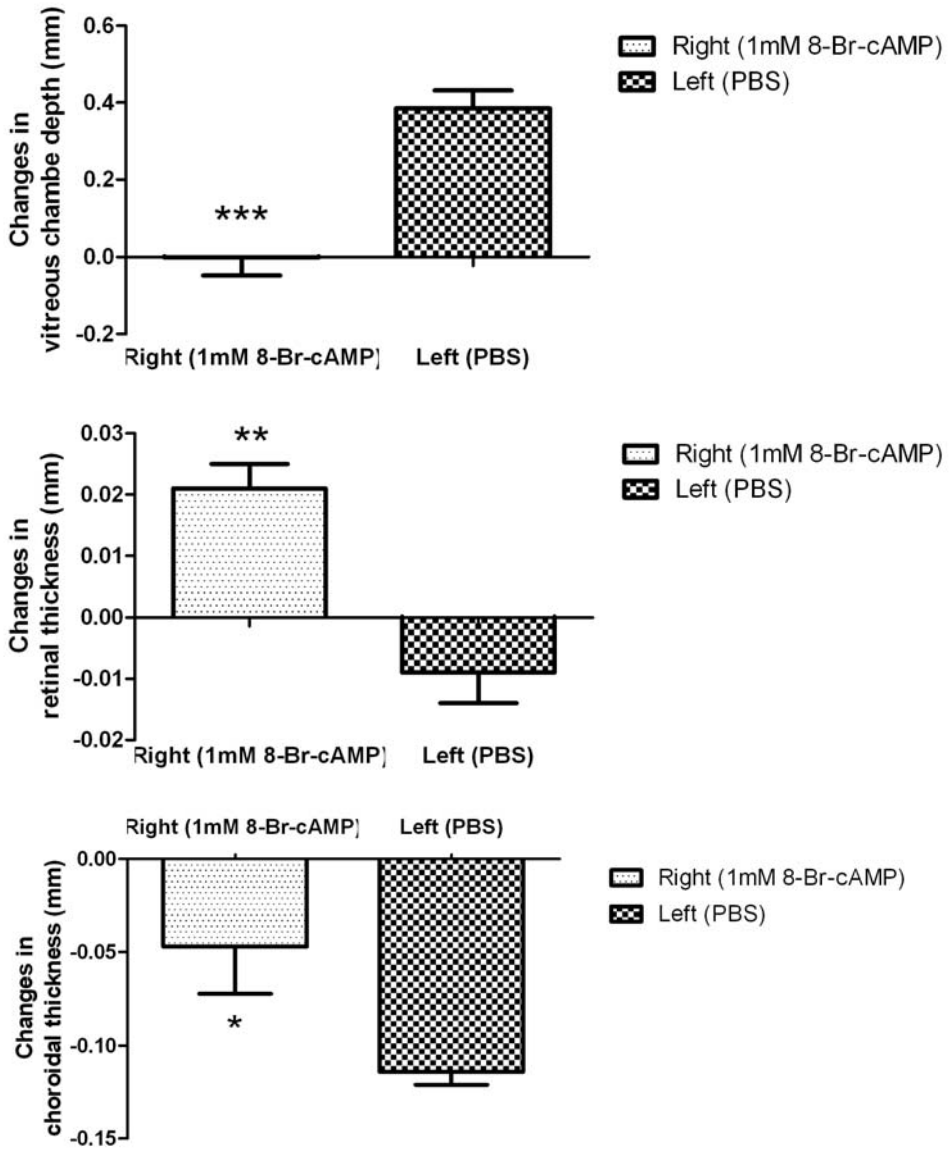

Fig.5.3 The effect of intravitreal injection of 1mM 8-Br-cAMP on changes in vitreous chamber depth, retinal and choroidal thickness.
Both eyes were wearing -10D lenses. Each data point represents mean change ± SEM (n=9), *asterisks* over bars indicate paired, two-tailed Student's *t*-tests comparing data from right and left eye. * P<0.05, ** P<0.01, *** P<0.001.

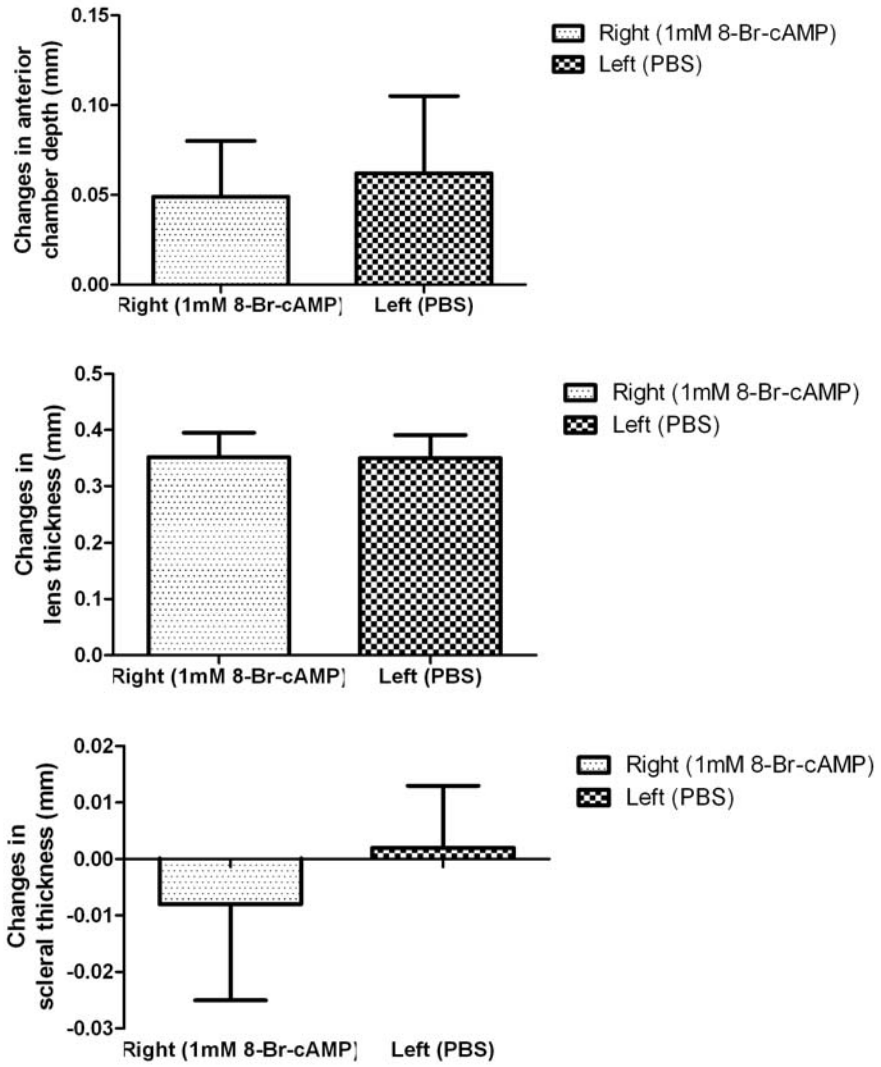

Fig.5.4 The effect of intravitreal injection of 1mM 8-Br-cAMP on changes in anterior chamber depth, lens and scleral thickness.
Both eyes were wearing -10D lenses. Each data point represents mean change ± SEM (n=9). No significant differences were found in these three ocular parameters.

After measuring the refractive errors and ocular parameters, the eyes were dissected and the retinas were sampled. The expressions of retinal ApoA1 in the 1mM 8-Br-cAMP injected eyes and control eyes were assessed using Western blotting. The expressions of ApoA1 were found to be increased by more than two folds when

compared to the control eye (P<0.01). Tubulin was used for loading control in the Western blotting (Fig. 5.5).

A.

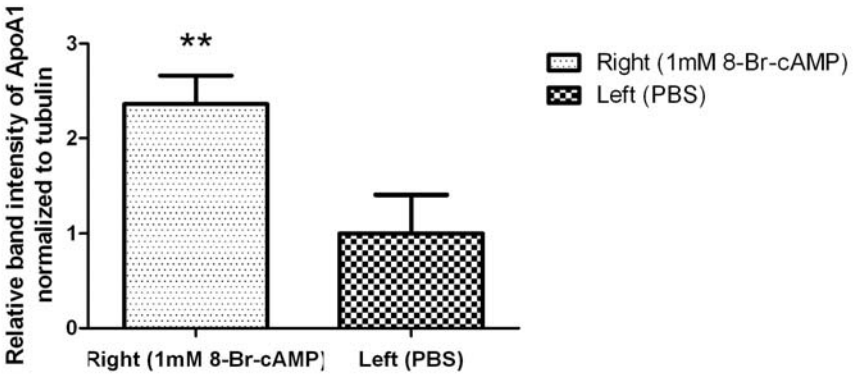

B.

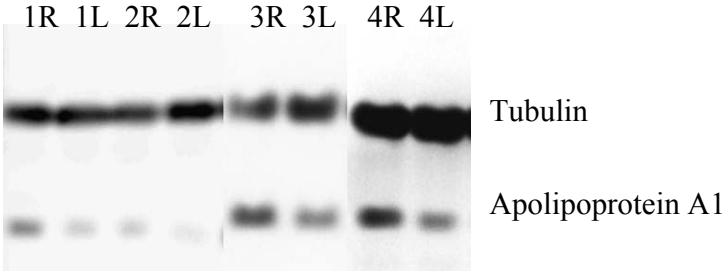

Fig.5.5 A. The effects of four consecutive days of intravitreal injection of 1mM 8-Br-cAMP on protein expressions of apolipoprotein A1 in the retinas.
B. Representative images of 4 pairs of samples from Western blotting. Right eye (R) received 10µl of 1mM 8-Br-cAMP while left eye (L) received 10µl of PBS as control. Both eyes received -10D lenses.
Asterisks over bars indicate paired, two-tailed Student's *t*-tests comparing data from right and left eye. * P<0.05, ** P<0.01, *** P<0.001, n=9.

5.5 Discussion

The intravitreal injection of 1mM 8-Br-cAMP was effective in inhibiting the myopia development induced by -10D lens. It acted through the inhibition of elongation of vitreous chamber depth. It also slowed down the thinning of the choroid under LIM.

Biochemically, intravitreal injection of 8-Br-cAMP increased the retinal ApoA1 expression significantly. Interestingly, this result appeared similar to the effect of 60mM nicotinic acid in reducing the ocular growth by -10D lens in Chapter 3. The protein expression of ApoA1 was also increased by around 50% after intravitreal injection of nicotinic acid whereas the 8-Br-cAMP can increase the retinal ApoA1 expression by two folds. Thus, the effect against LIM by 1mM 8-Br-cAMP was apparently stronger than that by 60mM nicotinic acid; and that the effect correlates well with the level of expressions of ApoA1 in the retinas. Furthermore, intravitreal injection of 1mM 8-Br-cAMP can effectively raise the retinal ApoA1 expression. It suggests a possible signaling role by cAMP on ApoA1 expression in the process of inhibiting LIM.

Cyclic AMP has been studied extensively in signaling pathway of many physiological processes, such as metabolism, cell division and growth (Cheng et al. 2008). Cyclic AMP was found to decrease the RNA and DNA synthesis and inhibit the cell proliferation in rat retinoblastoma-like tumor cells (Nishida et al. 1982). Besides, cAMP inhibited vascular smooth muscle cell growth by metabolizing adenosine (Dubey et al. 1996). These findings suggested that cAMP plays an important role in cell growth and differentiation. Cyclic AMP was found to be effective in inhibiting cell growth. Therefore, it may not be surprising that cAMP is effective in inhibiting LIM, as myopia is also described as excessive eye growth.

In the eye, cAMP was able to inhibit the transforming growth factor beta 1 (TGF-β1) induced corneal myofibroblast transformation and alpha-smooth muscle actin (SMA) expression (Xing and Bonanno 2009). Indeed, myofibroblasts are also present in sclera and these are highly contractile cells in sclera that expressed alpha-SMA. In mammalian myopic eye, sclera showed an increase in alpha-SMA which may allow the sclera to expand during myopia development (Jobling et al. 2009). Intravitreal injection of cAMP may act through the inhibition of alpha SMA expression in scleral myofibroblasts to retard LIM in the current study. However, myofibroblasts are only present in mammalian sclera but not in chick sclera (Phillips and McBrien 2004). Therefore, it is unsure whether cAMP works through other kinds of fibroblasts expressing alpha SMA in chicks.

Dopamine, a neurotransmitter, has been studied extensively in myopia and it is also thought to be closely associated with cAMP. The effect of dopamine is mediated by G protein coupled receptors in which D1 and D2 dopamine receptors exhibit opposite effects on adenylyl cyclase (Reis et al. 2007). D1 dopamine receptor activates adenylyl cyclase while D2 dopamine receptor inhibits it. Thus, binding on the D1 dopamine receptor will induce an increase in cAMP by activating adenylyl cyclase while binding on the D2 dopamine receptor will decrease cAMP production. Dopamine release is decreased in the FDM (Stone et al. 1989; Megaw et al. 1997) and both dopamine and apomorphine could prevent FDM (Schmid and Wildsoet 2004; Gao et al. 2006). Apomorphine is a non-specific D1 and D2 dopamine receptor agonist (Li et al. 2006) and previous study has shown that its inhibition on

FDM may be through action on D2 dopamine receptors (Rohrer et al. 1993). Therefore, based on the literatures, the prevention of FDM with dopamine agonist may be due to the action on D2 dopamine receptors which decrease cAMP release.

However in the current study, intravitreal injection of cAMP analog significantly inhibited LIM. Since an increase rather than a decrease of cAMP inhibited myopia growth, it is unlikely that D2 dopamine receptors play a role in the cAMP effect observed here. Conversely, it indicates that dopamine agonist may act on other pathways, in addition to D2 receptors, to prevent myopia.

5.5 Conclusions

The present study has established that a cAMP analog, 8-Br-cAMP, could inhibit myopia development in chick model, although the exact biochemical pathway by which cAMP regulates eye growth or myopia development is still unclear. Furthermore, cAMP was shown to modulate retinal ApoA1 expression and this signaling pathway may play a role in inhibiting LIM in chicks.

Further investigations can aim at the interplay among different biochemical pathways involving cAMP and ApoA1 that regulate eye growth as observed in LIM.

Chapter 6: Retinal cyclic adenosine monophosphate (cAMP) and lens-induced deprivation

6.1 Introduction

In Chapter 5, four consecutive daily intravitreal injections of 1mM 8-Br-cAMP were able to retard myopia development induced by negative lens significantly. It suggested a possible role of cAMP in the development of lens-induced myopia (LIM). Although cAMP is known for its secondary messenger function in lots of physiological processes (Cheng et al. 2008), there was few literature exploring the role of cAMP in myopia development. Since the current study showed that cAMP may be related to eye growth, it is of interest to explore the changes in retinal cAMP level during different refractive status.

6.2 Objectives

The aim of this study was to measure the retinal cAMP levels in eyes with different durations of lens-induced deprivation using enzyme immunoassay (EIA). Protein expressions of apolipoprotein A1 (ApoA1) in the retinas were also examined using Western blotting.

6.3 Materials and methods

White leghorn chicks (Gallus gallus domesticus) were breed from Specific Pathogen Free (SPF) eggs from Jinan in China. The environment, care and use of the animals in these experiments were same as that in Chapter 2.

The levels of cAMP in chick retina were measured by using competitive EIA.

6.3.1 Sample preparation

Three groups of 2-day-old chicks, each containing 6-8 animals were used for experiments. Refractive errors and ocular parameters were measured before and after the experiments. The ocular parameters were examined by high-frequency A-scan ultrasound system with a 30-MHz transducer sampled at a rate of 100 MHz. Refractive errors were measured by a streak retinoscope. They were presented in terms of spherical equivalent, which was the sum of spherical power and half of cylindrical power.

Chicks from group 1 received -10D and +10D on right and left eyes respectively. A -10D lens was applied onto the right eye of group 2 while a plano lens was worn by the left eye. The right and left eyes of group 3 worn +10D and plano lens respectively. All the lenses were worn for 3 days.

After three days of lens deprivation, the chicks were killed by carbon dioxide overdose. The eyes were then enucleated. Retinas were collected as in Chapter 2.3.1.

The retinas were collected and immediately frozen in liquid nitrogen and kept under -80 ℃ for future use.

6.3.2 Extraction of cAMP

The frozen retinas were homogenized with 200µl 5% trichoroacetic acid (TCA) in water using a Polytron-type homogenizer for 30 seconds. The homogenized samples were then centrifuged at 1500g for 10 minutes at 4℃. The supernatant (extract of cAMP) was collected while the precipitate was kept and measured for its protein concentration.

The supernatant was purified using water-saturated ether. One milliliter of water-saturated ether was mixed with the supernatant for 10 seconds. The mixture was allowed to set until the organic and aqueous phrases separate from each other. Once separated, the top ether layer was carefully removed and discarded. The purification step was repeated for two more times. The extract of cAMP was then heated at 70℃ for 5 minutes so as to remove the residue ether from aqueous phrase.

The precipitate (protein pellet) was mixed and washed with 300µl ice-cold acetone. The mixture was further centrifuged at 16000g for 15 minutes at 4℃. The supernatant was removed and 250 µl lysis buffer containing 7 M urea, 2 M thiourea, 40 mM Tris, 0.2% (w/v) Biolytes, 1% (w/v) DTT, 2% (w/v) CHAPS, 1% (w/v) ASB14 (Calbiochem, San Diego, CA, USA) and 1 tablet of Complete, Mini protease inhibitor cocktail (Roche Applied Science, Switzerland) in 10ml buffer was added.

The protein pellet was ground directly in the microcentrifuge tube using sterilized Kontes pellet pestle (Fisher Scienitific, Waltham, MA USA). Grinding was continued until there was no visible pellet left behind. The mixture was centrifuged at 16100 g for 20 minutes at 4 ℃. The supernatant was collected while the pellet was discarded. Three microlitres of supernatant was used to measure the protein concentration. Protein concentration was measured by 2D Quant Kit (GE Healthcare Life Science, Sweden) as described in Chapter 2.3.3.

6.3.3 Preparation of standard curve

The standard curve of cAMP level was produced according to the Cyclic AMP EIA Kit (Cayman Chemical, Michigan, USA). The stock solution of cAMP EIA standard was reconstituted with 1 ml of ether-extracted 5% TCA. A total of eight concentrations of cAMP standard were prepared by sequential dilution from the stock solution. The concentrations of cAMP in standard curve ranged from 0.3 pmol/ml to 750 pmol/ml. The standard curve was preformed freshly when performing assay in new set of data.

6.3.4 Incubation of reagents in the plate

The 96-well plate was used for incubation of reagents. In order to facilitate the accurate and reproducible results, two blanks, two non-specific binding (NSB) wells and two maximum binding (B_0) wells were required for each measurement of cAMP. NSB and B_0 wells were prepared with appropriate amount of EIA buffer in Cyclic AMP EIA Kit (Cayman Chemical, Michigan, USA). Fifty microlitres of eight

standard concentrations and samples was added in the separated wells. Each standard and sample was run in duplicate. Equal amount (50µl) of cAMP AChE tracer and cAMP antiserum were added to wells with standards and samples. The plate was covered with plastic film and incubated for 18 hours at 4℃.

6.3.5 Development of the plate

Ellman's Reagent was reconstituted with water before use. The reagents incubated in the wells were removed. All the wells were then washed five times with wash buffer provided. Two hundred microlitres of Ellman's Reagent was added into each well and the plate was covered with plastic film and incubated in dark at room temperature for 120 minutes with gentle shaking. After incubation, the bottom of the plate was wiped with a clean tissue. The plate was read at 410 nm wavelength by BioRad Microplate Reader Model 680 (San Diego, CA, USA). Absorbance readings in all wells were recorded. The readings in all wells were subtracted from readings of non specific binding wells. The ratio of sample bound to maximum bound (B/B_0) was calculated for each well. The cAMP concentrations of each sample were determined from the standard curve.

6.3.6 Western blotting

The proteins extracted from the pellet were studied by Western blotting procedures as described in Chapter 3. The signals were captured by a CCD camera called Lumi-Imager (Roche Applied Science, Switzerland) as an image file. The relative band intensity of ApoA1 was normalized against tubulin and was compared between eyes.

6.4 Results

In group 1, the chicks were undergone different lens-induced deprivations in two eyes. The right eye received -10D lens while the left eye worn a +10D lens. After three days of lens deprivation, there was a significant difference in refractive errors (spherical equivalent) between two eyes, using paired Student's t-test ($p<0.05$). Myopia (-3.68D ± 0.6, mean ± SEM) was developed in right eye while hyperopia (+11.50D ± 0.86, mean ± SEM) was found in the left eye after 3 days of lens wear (Fig.6.1). The vitreous chamber depth of right eye was found to be increased. Concurrently, there was a decrease in vitreous chamber depth in left eyes. Elongation of axial length was also detected in the right eye in response to the LIM by -10D lens (Fig.6.2).

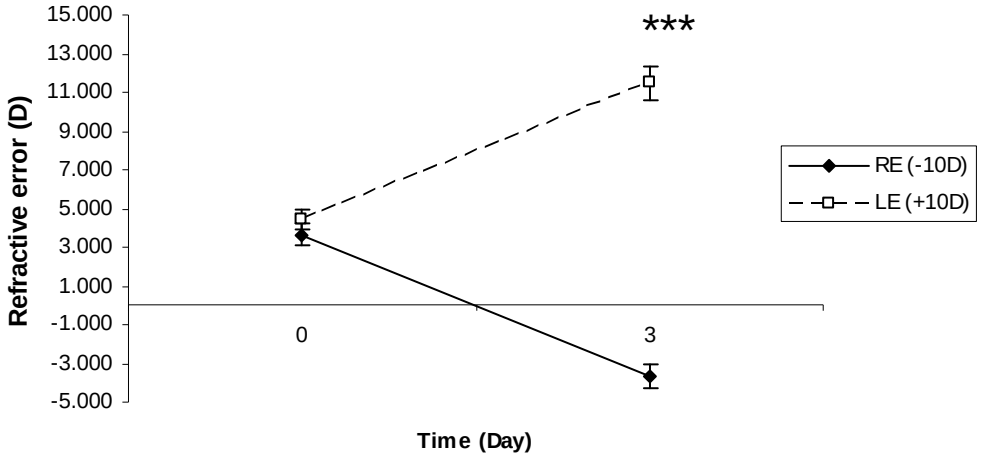

Fig.6.1 The development of refractive error (spherical equivalent) under 3-day lens-induced deprivation.
Negative (-10D) and positive (+10D) lenses were applied on the right and left eyes respectively for 3 days. Each data point represents mean refractive error ± SEM (n=8), *asterisks* over bars indicate paired, two-tailed Student's *t*-tests comparing data from right and left eye. * P<0.05, ** P<0.01, *** P<0.001.

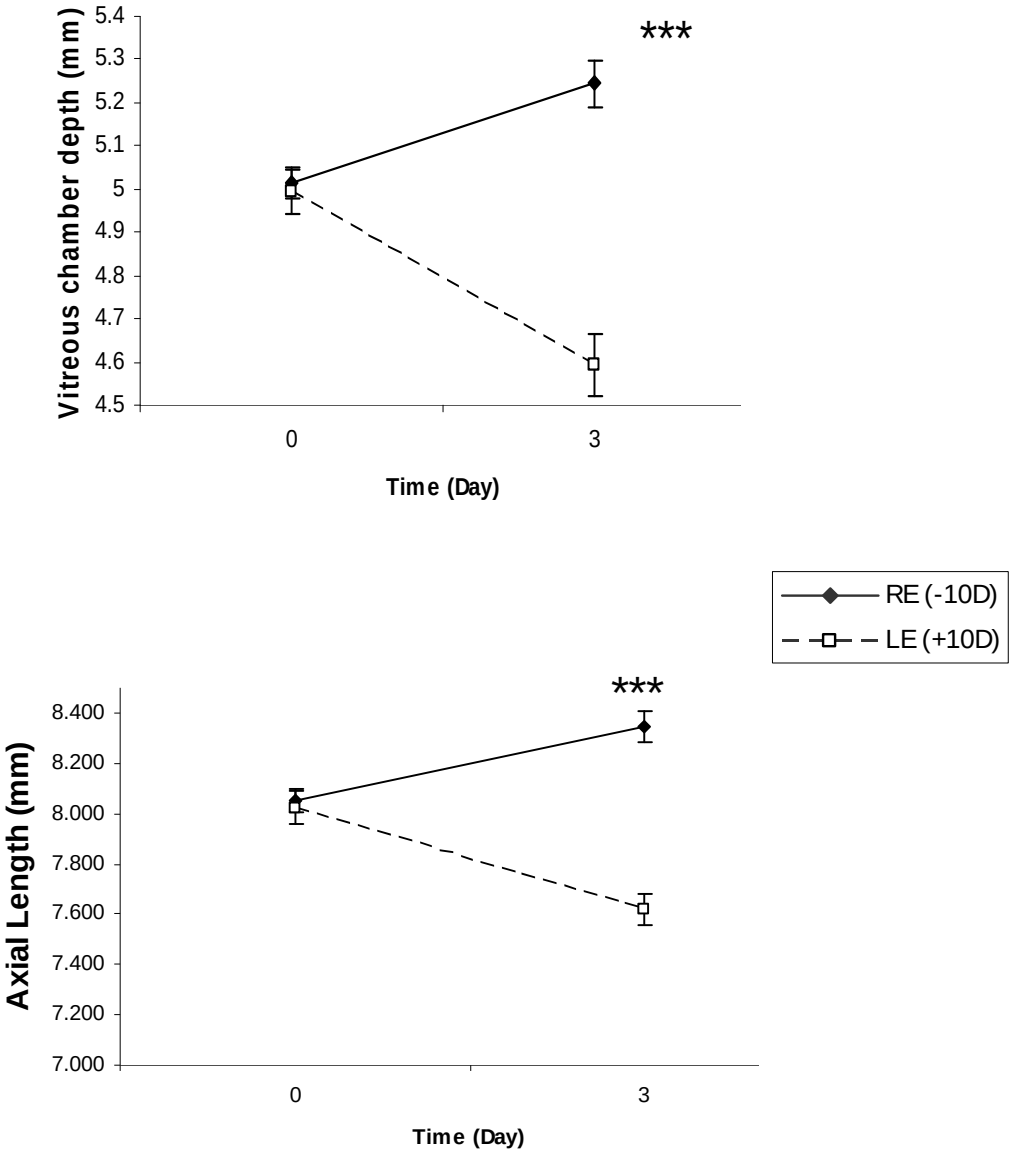

Fig.6.2 The vitreous chamber depth and axial length under 3-day lens-induced deprivation.
Negative (-10D) and positive (+10D) lenses were applied on the right and left eyes respectively for 3 days. Each data point represents mean change ± SEM (n=8), *asterisks* over bars indicate paired, two-tailed Student's *t*-tests comparing data from right and left eye. * P<0.05, ** P<0.01, *** P<0.001.

The retinal cAMP was extracted and measured by enzyme immunoassay. Figure 6.3 showed a significant difference in retinal cAMP level between the right and left eyes in group 1 ($p<0.001$). Retinal cAMP level of the hyperopic eye was 32% more than that of the myopic eye. This difference could be resulted from a decrease in cAMP level in the myopic retina or an increase in cAMP level in the hyperopic retina. Therefore, it was necessary to investigate the retinal cAMP under different refractive status individually.

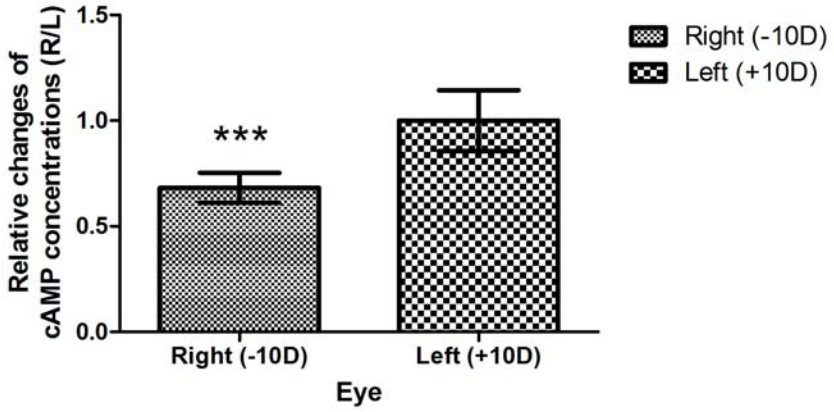

Fig.6.3 Retinal cAMP concentrations in 3-day -10D and +10D lens wear.
The ratio of retinal cAMP concentrations of right eye (R) to left eye (L) is plotted (mean ± SEM). A significant difference in retinal cAMP was shown between two eyes. *Asterisks* over bars indicate paired, two-tailed Student's *t*-tests comparing data from right and left eye. * $P<0.05$, ** $P<0.01$, *** $P<0.001$, n=8.

Protein expressions of retinal ApoA1 in 3-day -10D and +10D lens wear were also measured using Western blotting. Similar to the results of retinal cAMP level, protein expressions of retinal ApoA1 differed significantly between the myopic and

hyperopic eyes ($p<0.01$). When compared to the hyperopic eye, its expression in myopic eye was decreased by about 50% (Fig.6.4).

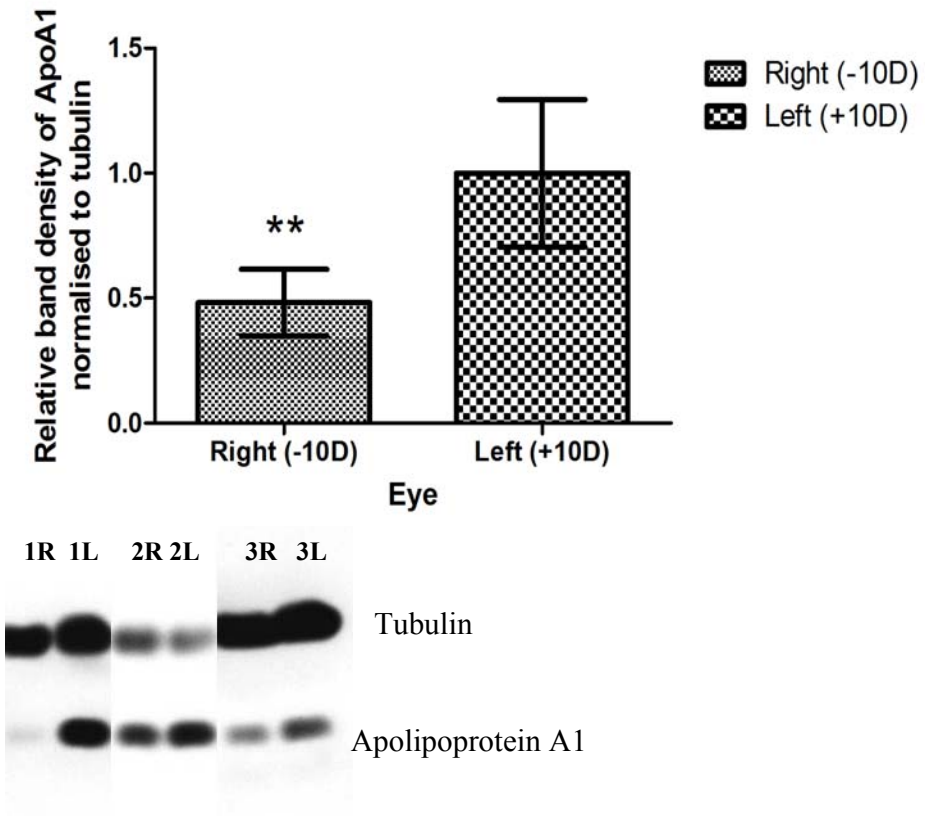

Fig.6.4 Protein expressions of apolipoprotein A1 under different lens wear using Western blotting.
Representative images of 3 pairs of samples by Western blotting are shown. Negative (-10D) and positive (+10D) lenses were applied to the right and left eyes for 3 days respectively (n=8). *Asterisks* over bars indicate paired, two-tailed Student's *t*-tests comparing data from right and left eye. * $P<0.05$, ** $P<0.01$, *** $P<0.001$.

In group 2, myopia was induced by -10D lens wearing on the right eye for 3 days. Plano lenses were applied to the other eye as control. In terms of refractive errors, myopia (-4.07D ± 0.72) was induced in the right eye. The left eye remained slightly hyperopic (+3.50D ± 1.13) after 3 days of plano lens wear (Fig.6.5). In addition, the

right eye had a longer axial length and longer vitreous chamber when compared with the left eye (Fig.6.6).

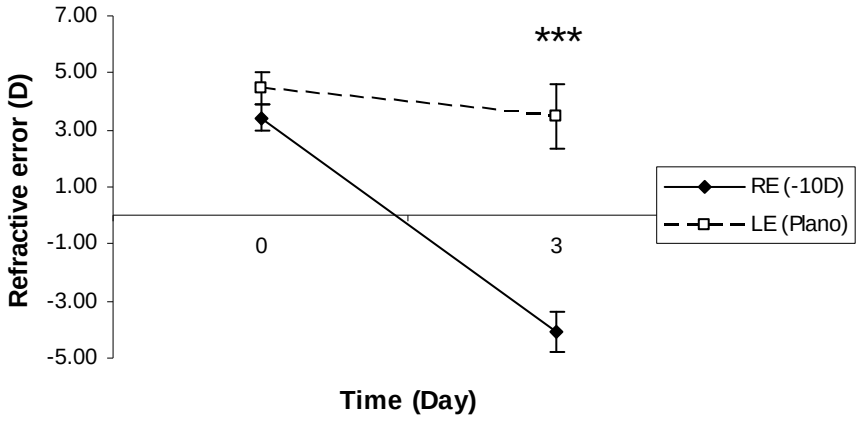

Fig.6.5 The development of refractive error (spherical equivalent) under 3-day lens-induced deprivation.
Negative (-10D) and plano lenses were applied on the right and left eyes respectively for 3 days. Each data point represents mean refractive error ± SEM (n=6), *asterisks* over bars indicate paired, two-tailed Student's *t*-tests comparing data from right and left eye. * P<0.05, ** P<0.01, *** P<0.001.

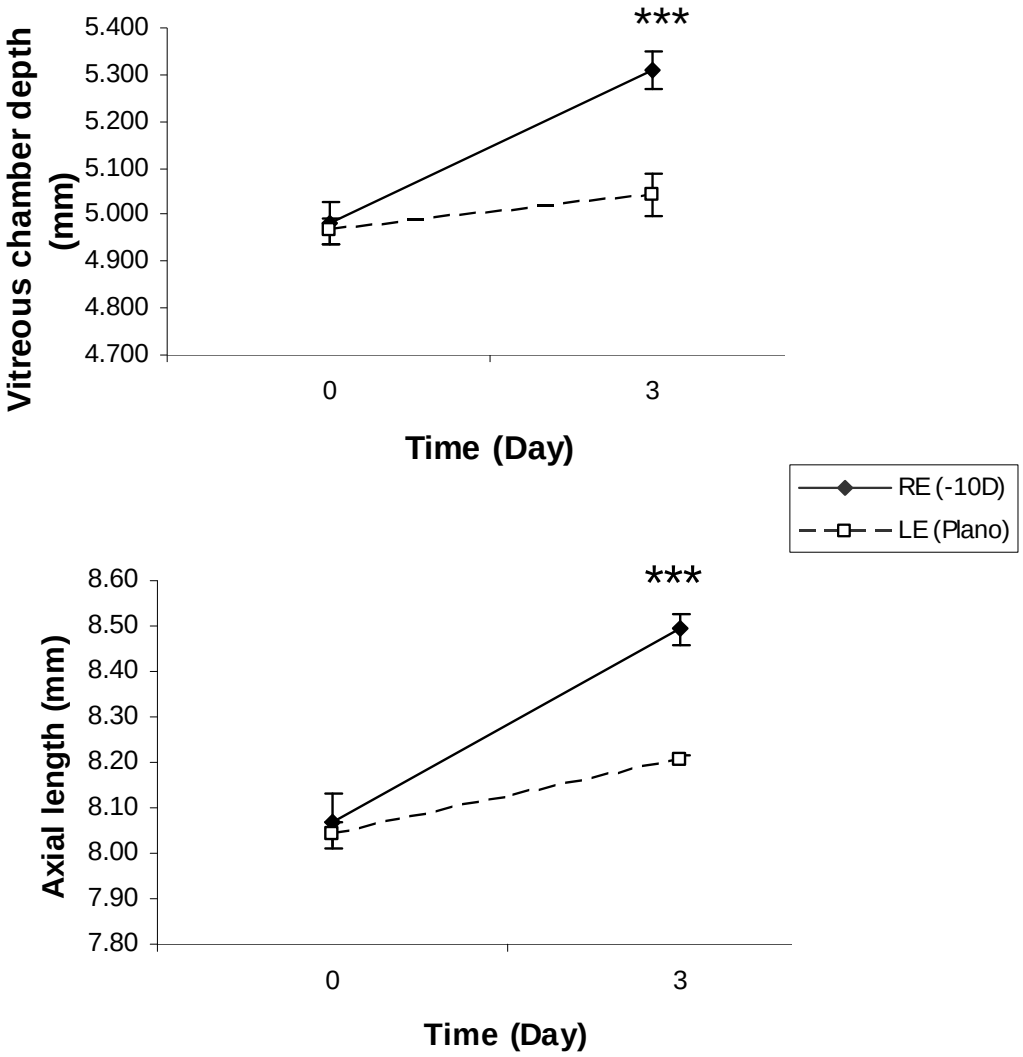

Fig.6.6 The vitreous chamber depth and axial length under 3-day lens-induced deprivation.
Negative (-10D) and plano lenses were applied on the right and left eyes respectively for 3 days. Each data point represents mean change ± SEM (n=6), *asterisks* over bars indicate paired, two-tailed Student's *t*-tests comparing data from right and left eye. * P<0.05, ** P<0.01, *** P<0.001.

Although significant amount of myopia was introduced in right eye after 3 days of lens wear, there was no difference in the retinal cAMP level in group 2 (Fig.6.7).

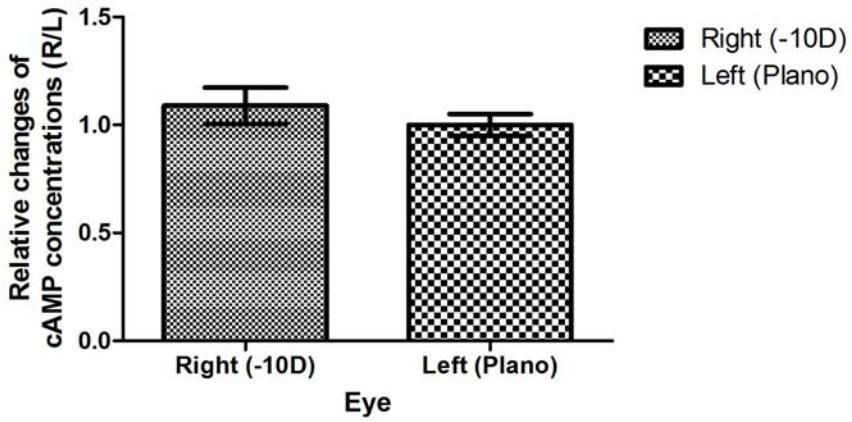

Fig.6.7 Retinal cAMP concentration in 3-day -10D and plano lens wear.
The ratio of retinal cAMP concentration of right eye (R) to left eye (L) is plotted (mean ± SEM, n=6). The graph shows no significant difference in retinal cAMP between two eyes.

In terms of the protein expression of ApoA1, its expression in myopic eye was slightly lower than the control eye although it was not statistically significant (Fig.6.8).

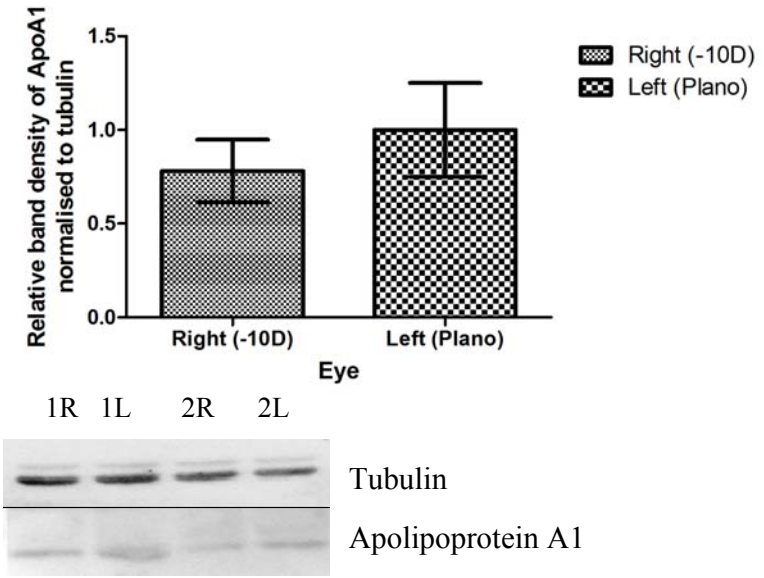

Fig.6.8 Protein expressions of apolipoprotein A1 under different lens wear using Western blotting.
Representative images of 2 pairs of samples by Western blotting are shown. Negative (-10D) and plano lenses were applied to the right and left eyes for 3 days respectively (n=6).

In group 3, a +10D lens was attached to the right eye of chicks for 3 days with plano lens on the other eye as control. Significant hyperopia (+11.38D±0.44) was induced in the right eye in 3-day lens wear (Fig.6.9). Expectedly, both the vitreous chamber depth and the axial length of the right eye were shorter than those of left eye (Fig.

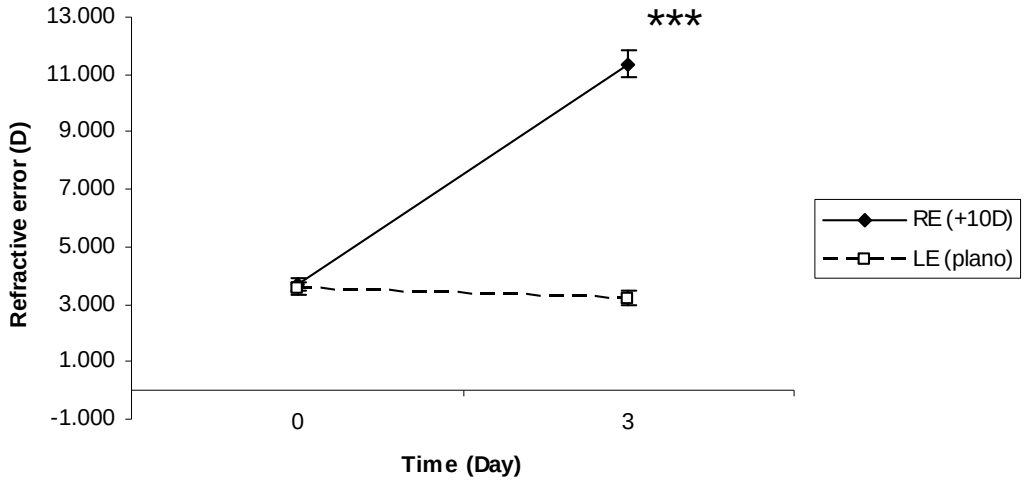

Fig.6.9 The development of refractive error (spherical equivalent) under 3-day lens-induced deprivation.
Positive (+10D) and plano lenses were applied on the right and left eyes respectively for 3 days. Each data point represents mean refractive error±SEM (n=8), *asterisks* over bars indicated paired, two-tailed Student's *t*-tests comparing data from right and left eye. * P<0.05, ** P<0.01, *** P<0.001.

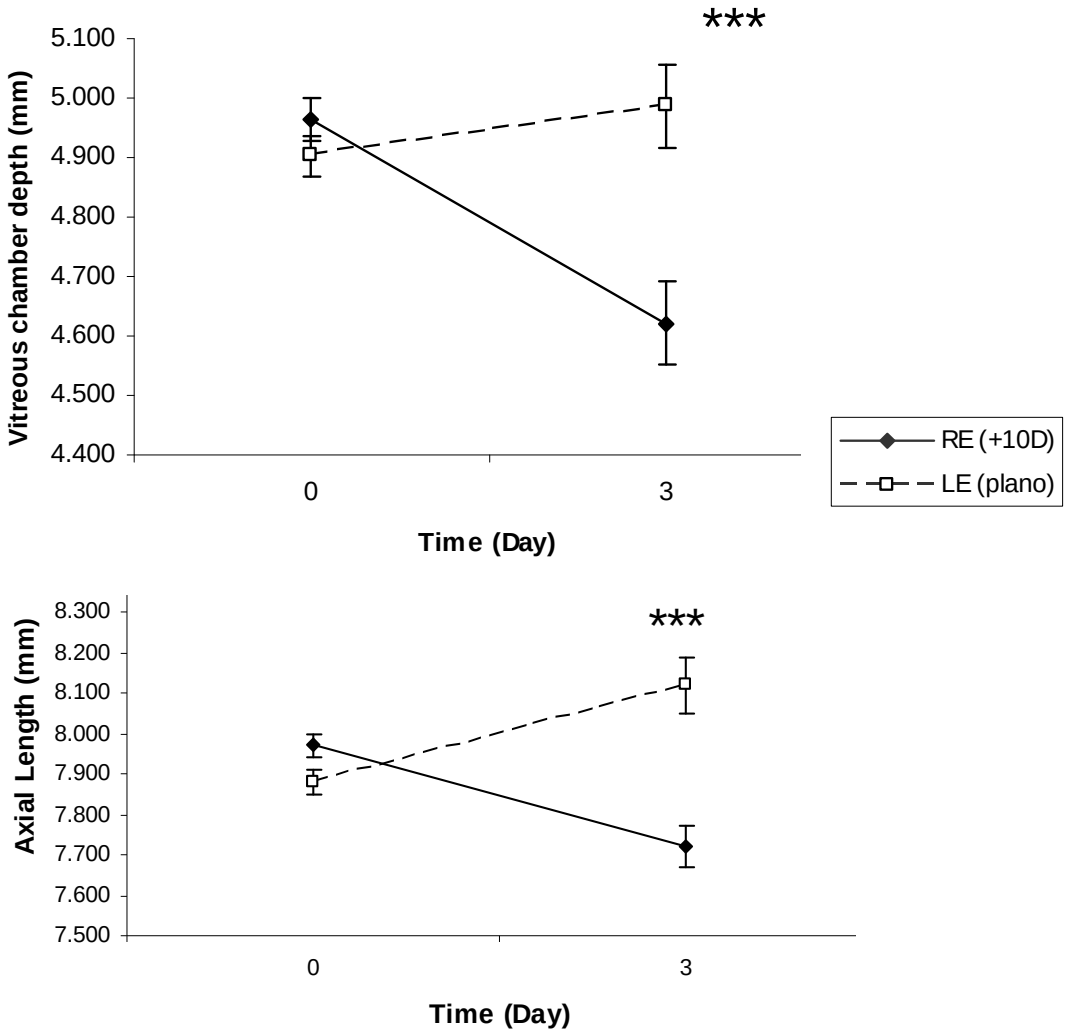

Fig.6.10 The vitreous chamber depth and axial length under 3-day lens-induced deprivation.
Positive (+10D) and plano lenses were applied on the right and left eyes respectively for 3 days. Each data point represents mean change ± SEM (n=8), *asterisks* over bars indicate paired, two-tailed Student's *t*-tests comparing data from right and left eye. * P<0.05, ** P<0.01, *** P<0.001.

In group 3, higher abundance of retinal cAMP was found in right eye when compared to those in the left eye ($P<0.05$). The retinal cAMP in hyperopic eye was about 30% higher than those in the myopic eye (Fig.6.11).

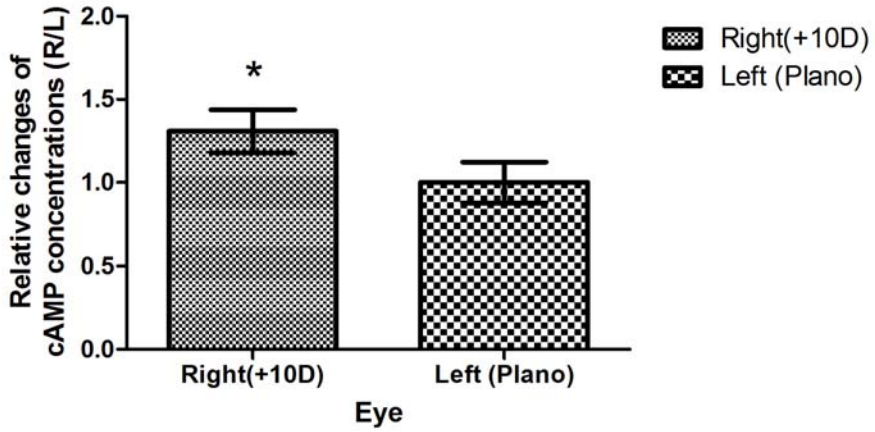

Fig.6.11 Retinal cAMP concentration in 3-day +10D and plano lens wear.
The ratio of retinal cAMP concentration of right eye (R) to left eye (L) is plotted (mean ± SEM, n=8). The graph shows a significant increase in retinal cAMP in right eye. *Asterisks* over bars indicate paired, two-tailed Student's *t*-tests comparing data from right and left eye. * $P<0.05$, ** $P<0.01$, *** $P<0.001$.

Interestingly, the protein expressions of retinal ApoA1 in the hyperopic eye were significantly increase by more than twofold when compared to the control eye ($P<0.01$) (Fig.6.12).

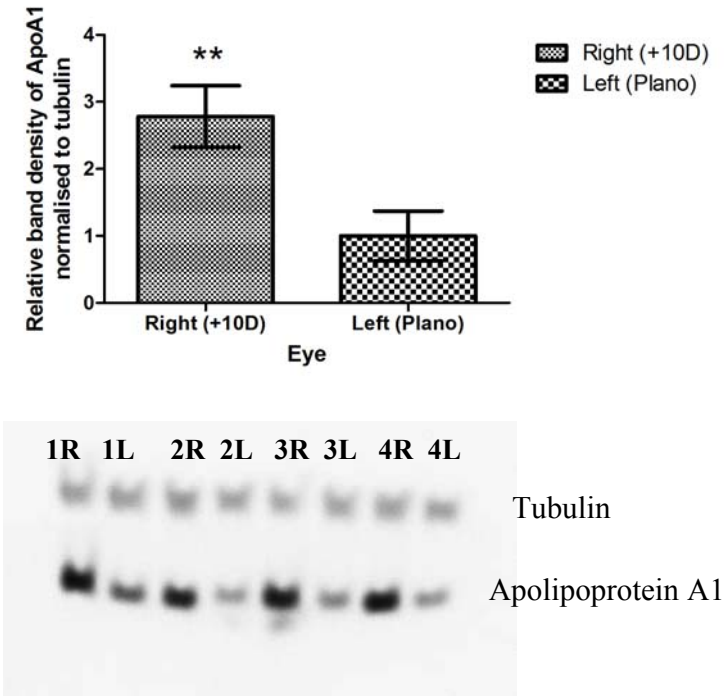

Fig.6.12 Protein expressions of apolipoprotein A1 under different lens wear using Western blotting.
Representative images of 4 pairs of samples by Western blotting are shown. Positive (+10D) and plano lenses were applied to the right and left eyes for 3 days respectively (n=8). *Asterisks* over bars indicate paired, two-tailed Student's *t*-tests comparing data from right and left eye. * P<0.05, ** P<0.01, *** P<0.001.

6.5 Discussion

The levels of retinal cAMP changed in different refractive errors. It increased by about 30% in lens-induced hyperopia (LIH), but remained unchanged in LIM. This was an unexpected result. Since intravitreal injection of 1mM 8-Br-cAMP inhibited the LIM in Chapter 5, it was anticipated that there should have been a decrease in the retinal cAMP level in LIM. However, no significant change in the retinal cAMP level was found. Although the retinal cAMP level did not change in myopic eye, judging from increase of cAMP in LIH, it could arguably still play a role as a "STOP" biochemical signals in eye growth, since "STOP" signals are those that can

retard the growth of eye which would result in hyperopia. The fact that the retinal cAMP increased significantly in LIH may indicate its important role in the retardation of eye growth in hyperopia.

Protein expression of ApoA1 also changed under different refractive errors. In the case of LIH, it caused an increase in the retinal cAMP and ApoA1. In LIM, the protein expression of ApoA1 decreased with no change in retinal cAMP level. In Chapter 5, intravitreal injection of 1mM 8-Br-cAMP induced an increase in retinal ApoA1 significantly. Intuitively, a similar decrease in the retinal cAMP level may also induce a decrease in retinal ApoA1 in LIM. Apparently, the retinal ApoA1 level was not solely controlled by cAMP level alone, since the retinal ApoA1 expression was decreased when there was no significant change in the retinal cAMP level as observed in the LIM. This indicated that changes in ApoA1 protein expression in the myopic retinas did not follow the changes in the retinal cAMP level. It is plausible that cAMP may be one of the components that could inhibit ocular growth, rather than stimulate growth as in the LIM.

Together with the experiments in Chapter 5, the results suggested that both the cAMP and ApoA1 may play an important role in controlling myopia development. Intravitreal injection of 1mM 8-Br-cAMP induced an increase in retinal ApoA1 expression which could significantly prevented LIM. It could be inferred that the prevention of LIM by cAMP may be through the regulation of retinal ApoA1 expression. Increase in retinal ApoA1 expression was unlikely to be incidental and

unrelated event in the prevention of myopia, since intravitreal injection of nicotinic acid targeted to increase the retinal ApoA1 expression (in Chapter 3) could inhibit the elongation of vitreous chamber depth in LIM. Therefore the data suggested that prevention of LIM may depend on the retinal ApoA1 expression. However, the effect of cAMP is likely to be more complex and it may not simply and solely act on retinal ApoA1 expression.

The magnitude of inhibiting LIM by 60mM nicotinic acid and 1mM 8-Br-cAMP was different. Intravitreal injection of 8-Br-cAMP was more effective in preventing LIM than nicotinic acid. Cyclic AMP (1mM) was able to abolish all the myopia induced by -10D lenses. However, 60mM nicotinic acid only prevented 1-2D myopia induced by -10D lenses. This could be due to their different abilities in inducing increase in retinal ApoA1 expression. Nicotinic acid (60mM) increased 50% of retinal ApoA1 expression while 8-Br-cAMP (1mM) led to twofold increase in expression.

As cAMP is involved in many signaling pathways that regulated a variety of biological processes, there may be other proteins or pathways modulated by cAMP in the process of eye growth.

Nitric oxide

Nitric oxide (NO) is one of the molecules that can be influenced by both cAMP and ApoA1. Cyclic AMP was found to increase NO production in the endothelial cells (Gonzalez-Flores et al. 2009). It facilitates the NO pathway involved in estrous

behavior in rats (Grossini et al. 2009). ApoA1 is also able to increase NO production by enhancing the endothelial NO synthase activity (Drew et al. 2004). Both the cAMP and ApoA1 have the ability in increasing NO production.

The roles of NO in myopia development have been investigated previously. Findings showed that intravitreal injection of L-NAME inhibited choroidal thickening induced by recovery from myopia and LIH (Nickla and Wildsoet 2004). L-NAME is a non specific NO synthase inhibitor. It also prevented the inhibition of axial length produced in recovery from myopia and LIH (Nickla et al. 2009). It was suggested that depletion of NO by NO synthase inhibitor prohibited the thickening of choroid under recovery from myopia (Nickla et al. 2009). In addition, the choroid was thinner even during the recovery from myopia (Nickla and Wildsoet 2004). Therefore, NO could play a role in initiating choroidal thickening during recovery from myopia.

It is possible that while intravitreal injection of 8-Br-cAMP enhanced the retinal ApoA1 expression, it may also stimulate NO production. NO may further initiate the choroidal thickening which prevented LIM.

Early growth response 1

Early growth response 1(Egr-1) is also known as ZENK which is a transcription factor present in retinal glucagon amarcine cells. Both the protein and mRNA of ZENK were found to be differentially expressed under different refractive errors (Fischer et al. 1999; Bitzer and Schaeffel 2002). Retinal ZENK mRNA decreased after 1 hour of FDM (Schippert et al. 2007). It increased when negative lens was

removed from LIM for 1 hour (Ashby et al. 2007). In ZENK knockout mice, it was found that their eyes had longer axial length and myopia (Schippert et al. 2007). ZENK showed an early and transient response to myopic and hyperopic defocus as its mRNA level could be changed after a short exposure of defocus (Ashby et al. 2007). Therefore, ZENK has been proposed as one of the early signals modulating eye growth.

It has been found that 8-Br-cAMP increased ZENK mRNA expression in rats (Yoshino et al. 2002). Previous studies have also shown that ZENK could modulate the ApoA1 gene transcription (Kilbourne et al. 1995; Zaiou et al. 1998).

The present data showed that intravireal injection of 1mM 8-Br-cAMP increased retinal ApoA1 expression. It is plausible that 8-Br-cAMP may act through the activation of ZENK mRNA and result in up-regulation of retinal ApoA1 expression and inhibition of LIM. In addition, an increase in retinal cAMP level was also observed in LIH, in which the ocular growth was retarded. All these effects potentially may be accomplished by modulating the ZENK expression.

Insulin

Cyclic AMP is a key component in regulating the insulin secretion (Seino et al. 2009) and it exerts a potent effect in stimulating insulin in pancreatic cells (Kang et al. 2003). Insulin could further stimulate myopia development induced by negative lenses (Feldkaemper et al. 2009; Zhu and Wallman 2009). Higher myopic refractive errors were resulted after intravitreal injection of insulin in LIM. In general, it appears that insulin acts as a stimulator in ocular growth.

In theory, if insulin production was increased after intravireal injection of cAMP analog, eye growth should have been stimulated rather than inhibited. However, the present results showed that cAMP prevented rather than promoting eye growth in LIM. This discrepancy could be due to the multiple effects of insulin in stimulating the ocular growth in LIM. Although insulin induced higher myopia than with negative lens alone, it mostly increased the anterior chamber depth and lens thickness (Feldkaemper et al. 2009). This is different from the typical changes produced by negative lenses, which mainly increases the vitreous chamber depth. Interestingly, these insulin injected retinas demonstrated higher retinal ZENK mRNA level (Feldkaemper et al. 2009), whereas the retinal ZENK mRNA was decreased in FDM. Therefore, the ocular growth promoting effect of insulin is probably due to pathways other than ZENK pathways.

There is published evidence on the interactions between the ApoA1 and insulin as insulin was found to able to induce ApoA1 and its gene expression (Zheng et al. 2001). ApoA1 is a major component of high density lipoprotein (HDL) and the intake of reconstituted HDL in diabetes patients can improve their blood glucose level via an increase in insulin (Drew et al. 2009). A close relationship between ApoA1 and insulin was also indicated in experimentation with ApoA1 knockout mice. There was an increase in fat mass and impaired glucose tolerance in these knockout mice (Han et al. 2007). This suggested that ApoA1 is one of the important components in regulating blood glucose metabolism together with insulin.

Increase in the retinal ApoA1 expression was found in LIH and 1mM 8-Br-cAMP injected eyes. Both manipulations resulted in a retardation of ocular growth.

According to the literatures, an increase in the HDL (including ApoA1) level may increase the insulin level which should stimulate ocular growth and cause more myopia. This was not the case in the present study as cAMP was shown to prevent rather than promote LIM. The discrepancy is unclear and given that cAMP takes part in many signaling pathways, its effect on eye growth may not be solely mediated through insulin.

Retinoic acid receptor

Retinoic acid receptor (RAR) alpha is another possible target involved in the cAMP mediated inhibition on LIM. Cyclic AMP affects RAR in a indirect way by phosphorylating protein kinase A (PKA) which in turn induces an increase in phosphorylation of RAR alpha (Rochette-Egly et al. 1995; Zhao et al. 2004). The mRNA of RAR alpha was found to be increased during recovery from FDM (Morgan et al. 2004). During the recovery from FDM, the ocular growth is retarded as dictated by the presence of myopic defocus. Intravitreal injection of cAMP analog may have activated RAR alpha mRNA which resulted in retardation of ocular growth and prevention of LIM.

RAR alpha has been shown to involve in the synthesis of ApoA1 in hepatocytes. The addition of retinoic acid caused a decrease in the synthesis and mRNA expression of ApoA1 in these cells and the effect was achieved through RAR alpha (Neele et al. 1999). It implied that RAR alpha was able to regulate the synthesis of ApoA1. Previous study has also found that retinoic acid can activate RAR (Idres et

al. 2002). The decrease in ApoA1 synthesis may be induced by the activation of RAR alpha.

However, it was unclear whether RAR alpha is a key player in the cAMP effect which ultimately leads to the prevention of LIM. Since cAMP analog causes the activation of RAR alpha which should induce a decrease in ApoA1 expression, instead of an increase as found in the previous chapter (Chapter 5). Apparently, RAR alpha action is not consistent with the current effect of cAMP and findings of an increase in retinal ApoA1 expressions from Western blotting in Chapter 5.

The exact mechanism of inhibiting LIM by cAMP is yet to be understood. Based on the current results, the interplay between cAMP and ApoA1 to effect prevention of myopia requires further investigations. For example, proteome analysis could be performed on the extracted retinas after intravitreal injection of 1mM 8-Br-cAMP. Differential protein expressions between intravitreal injected retinas and control retinas could be studied using two dimensional fluorescence differential gel electrophoresis (2-D DIGE). The differential proteins could shed important light in mapping the inhibitory mechanism of cAMP on LIM.

6.6 Conclusions

In the current study, different levels of retinal cAMP were demonstrated in LIM and LIH. Together with the results in Chapter 5, the possible role of cAMP in inhibition of myopia development was suggested. An increase in retinal cAMP level may be crucial in inhibiting the ocular growth during myopia. ApoA1, which was

differentially expressed in myopic retinas found by 2-D DIGE (Chapter 2), and cAMP play an important role in myopia development. Since cAMP is a ubiquitous second messenger involved in many physiological processes, there could be a numbers of proteins or pathways in modulating eye growth through cAMP and ApoA1 (Fig. 6.13). In Chapter 5, inhibition of myopia by cAMP was more effective and potent than that by nicotinic acid, an agent increasing ApoA1 expressions (Chapter 2). It indicated that cAMP may trigger more than one possible factor rather than ApoA1 only to regulate the eye growth. In order to understand the underlying mechanism of myopia development, the interaction between ApoA1 and cAMP in eye growth needs further investigations.

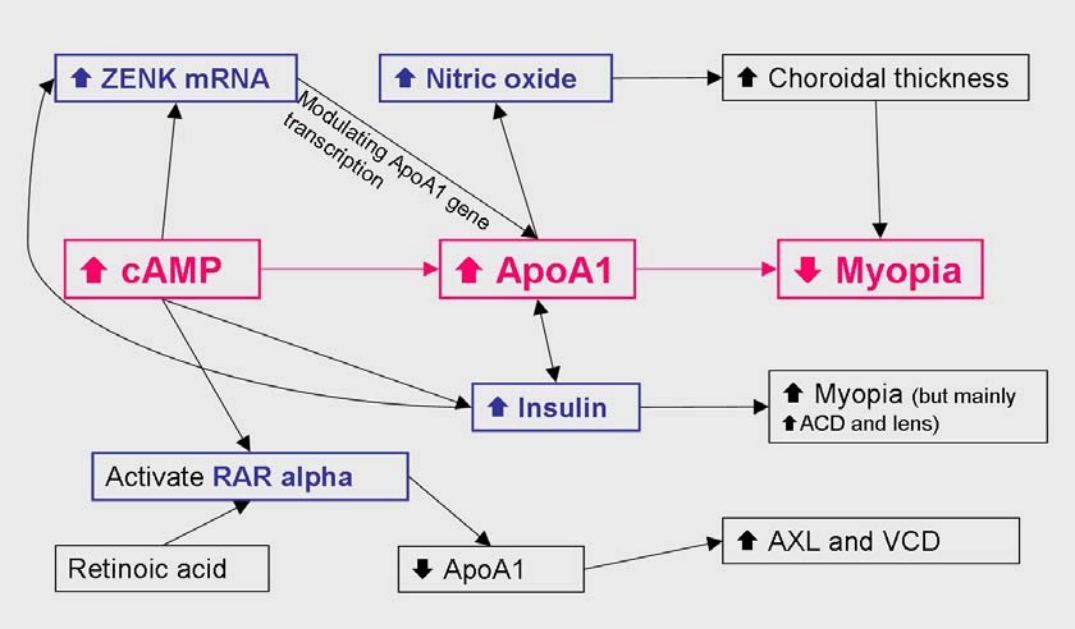

Fig.6.13. Summary of possible factors linking between cAMP and apolipoprotein A1 in modulating ocular growth.
Red colour indicates the current findings; blue colour indicates the possible factors. Abbreviations are as follow, ACD: anterior chamber depth; ApoA1: apolipoprotein A1; AXL: axial length; cAMP: cyclic adenosine monophosphate; RAR: retinoic acid receptor; VCD: vitreous chamber depth.

Chapter 7: Summary and conclusions

One of the aims of this study is to analyze the retinal proteome in myopic chick using two-dimensional fluorescence difference gel electrophoresis (2-D DIGE). Myopia was introduced by negative lenses (-10D), diffusers and occluders for three and seven days. Differential protein expressions in myopic chick retinas induced by lens-induced myopia (LIM) or form deprivation myopia (FDM) were found. There were total thirteen protein spots that were differentially expressed in myopic retinas after three days of experimental myopia. Six of them were successfully identified by nano-liquid chromatography with tandem mass spectrometry (LC-MS/MS) and they belonged to three proteins. Destrin was up-regulated in both three-day FDM by diffusers and occluders. The expression of phosphoglycerate mutase 1 (brain) (PGAM) was increased after three days of LIM. Apolipoprotein A1 (ApoA1) was shown to be decreased after three days of LIM and FDM by diffusers. After seven days of LIM and FDM, less differential protein spots were found in myopic retinas. Only up regulation of destrin was seen in LIM and myopia induced by occluders. PGAM was increased in FDM by diffusers.

The involvement of ApoA1 was further studied as its expression was consistently decreased in both the LIM and FDM after three days. Nicotinic acid and bezafibrate are agents that can increase ApoA1 level clinically. They were injected intravitreally into the chick eyes and their effects on eye growth were studied. It was found that nicotinic acid (60mM) reduced the growth of vitreous chamber depth in LIM effectively.

Localizations of ApoA1 were examined in the retinas during myopia and hyperopia. The presence of ApoA1 was more evident in photoreceptor layer of myopic chick retina using immunohistochemistry. However, ApoA1 was located more intensively at the inner limiting membrane and RPE in hyperopic retina. The present data showed differential distributions of ApoA1 in the retinas of LIM and lens-induced hyperopia (LIH) for the first time. The data suggest that lipid transport and metabolism of ApoA1 may differ in different refractive errors.

Since cyclic adenosine monophosphate (cAMP) is known to affect ApoA1 expression in cholesterol transport, their relationship in myopia development was studied. Intravitreal injection of cAMP analog was effective in inhibiting the axial length elongation induced by negative lenses with an increase in retinal ApoA1 expressions. These results strongly indicated an important inhibitory role of cAMP in myopia development.

In the last part of the current study, enzyme immunoassay was employed to measure the retinal cAMP levels during myopia and hyperopia. There was no significant change in cAMP level in myopic retinas, but the retinal cAMP level showed an increase in hyperopic eye. An increase in retinal ApoA1 expression was also found in hyperopic eye. Together with the results from the intravitreal injection of cAMP analog, an increase of retinal cAMP level may induce an increase in retinal ApoA1 expressions. Cyclic AMP and ApoA1 may act as “STOP” signals in eye growth.

In conclusion, the analysis of retinal proteome of myopic chicks using 2-D DIGE has revealed a number of differential protein expressions in related to myopic growth. ApoA1 was the only common protein spot down-regulated in both LIM and FDM retinas. Increasing the retinal ApoA1 through intravitreal injection could inhibit vitreous elongation in LIM. The significance of ApoA1 in ocular growth as a "STOP" signal has been shown in our study. Moreover, ApoA1 and cAMP are possibly linked biochemically in complex signaling pathways to regulate ocular development, which was discussed in Section 5.5 (p.130) of Chapter 5 and section 6.5 (p.150) of Chapter 6. However, the exact mechanism of modulating eye growth by cAMP and ApoA1 remains uncertain. Based on the literature, cAMP may increase ApoA1 through increasing ZENK mRNA expressions. An increase in ZENK mRNA also occurred in the early stage of recovery from myopia (Bitzer and Schaeffel 2002) which suggested ZENK may play a role in inhibiting eye growth. In addition to ZENK, NO could be another important candidate modulated by cAMP during myopia development, since both cAMP and ApoA1 could increase NO, which initiates choroidal thickening (Nickla and Wildsoet 2004; Nickla et al. 2009). This process of choroidal thickening may contribute to the inhibition of eye growth induced by negative lenses after intravitreal injection of cAMP. Although there are close relationships between cAMP, insulin and retinoic acid receptor (RAR) alpha, the interactions among them are complex. Cyclic AMP was found to stimulate insulin in pancreatic cell (Kang et. al. 2003). However, insulin was shown to enhance myopic growth induced by negative lenses (Feldkaemper et al. 2009; Zhu and Wallman 2009). Therefore, if cAMP would stimulate insulin secretion, it

should have produced more accelerated eye growth. However the current results showed that cAMP inhibited rather than stimulated LIM.

As far as RAR alpha is concerned, cAMP could activate RAR alpha and subsequently down-regulate ApoA1 expressions (Neele et al. 1999; Rochette-Egly et al. 1995; Zhao et al. 2004). However, the current data showed an up-regulation of ApoA1 after intravitreal injection of cAMP. Therefore, there is no clear indication from the literature on the involvement or interaction of insulin, RAR alpha with cAMP. For insulin and RAR alpha to be involved in the cAMP and ApoA1 signaling pathway, they have to act through very different mechanisms as reported in the literature and future work will be needed to clarify their relationship. Nevertheless, the current findings provided a new direction towards understanding the mechanism of myopia through ApoA1 and cAMP pathway.

Appendices

Raw data of ocular parameters in 3 days of lens-induced myopia (LIM) (Chapter 2)

Vitreous chamber depth / mm	Day 0	Day3	Day 0	Day3
	RE	RE	LE	LE
R21_1	4.885	5.285	4.856	4.887
R21_2	4.958	5.377	4.941	5.017
R21_3	4.974	5.494	4.96	4.955
R21_4	5.225	5.395	5.157	5.213

Axial length/ mm	Day 0	Day3	Day 0	Day3
	RE	RE	LE	LE
R21_1	8.484	9.004	8.492	8.681
R21_2	8.525	9.229	8.471	8.851
R21_3	8.418	9.201	8.421	8.706
R21_4	8.778	9.011	8.734	9.026

Refractive errors/ D	Day 0	Day3	Day 0	Day3
	RE	RE	LE	LE
R21_1	6	-5	4	5
R21_2	5.5	-6	6	5.5
R21_3	5.5	-7.5	3.5	4
R21_4	4.75	0	4.5	2.75

Raw data of ocular parameters in 3 days of form deprived myopia (FDM) by diffuser (Chapter 2)

Vitreous chamber depth / mm	Day 0	Day3	Day 0	Day3
	RE	RE	LE	LE
R21_7	5.095	5.424	5.053	5.1
R21_8	5.032	5.361	5.251	5.016
R22_5	5.016	5.349	5.052	5.032
R22_6	5.228	5.575	5.052	4.972

Axial length/ mm	Day 0	Day3	Day 0	Day3
	RE	RE	LE	LE
R21_7	8.714	9.155	8.674	8.918
R21_8	8.629	8.923	8.69	8.817
R22_5	8.487	8.928	8.446	8.679
R22_6	8.73	9.171	8.593	8.716

Refractive errors/ D	Day 0	Day3	Day 0	Day3
	RE	RE	LE	LE
R21_7	4	-6	4.75	4.5
R21_8	6	-5.75	4	2.5
R22_5	3	-5	2.5	4
R22_6	1.5	-8.5	3	5

Raw data of ocular parameters in 3 days of form deprived myopia (FDM) by diffuser (Chapter 2)

Vitreous chamber depth / mm	Day 0	Day3	Day 0	Day3
	RE	RE	LE	LE
R21_9	4.723	5.121	4.776	4.737
R21_10	5.086	5.438	4.998	4.948
R21_11	5.017	5.075	5.047	4.659
R22_7	5.014	5.349	5.031	5.09

Axial length/ mm	Day 0	Day3	Day 0	Day3
	RE	RE	LE	LE
R21_9	8.384	8.808	8.336	8.517
R21_10	8.645	9.224	8.587	8.92
R21_11	8.595	8.755	8.633	8.439
R22_7	8.526	9.066	8.54	8.942

Refractive errors/ D	Day 0	Day3	Day 0	Day3
	RE	RE	LE	LE
R21_9	5	-5.75	5	4.5
R21_10	5.5	-7	4.5	3.5
R21_11	4	-3.5	4.5	5
R22_7	2.25	-3	3	3

Raw data of ocular parameters from intravitreal injection of 25mM bezafibrate (Chapter 3)

Vitreous chamber depth / mm	Day 0	Day4	Day 0	Day4
	RE	RE	LE	LE
R17_11	5.164	5.525	5.105	5.603
R17_12	5.145	5.59	5.167	5.272
R17_13	5.036	5.306	5.067	5.167
R17_14	4.937	5.218	4.938	5.292
R17_15	5.128	5.618	5.125	5.642
R17_16	5.036	5.326	5.052	5.311

R17_17	5.035	5.094	5.017	5.112
R17_18	4.826	5.112	4.906	5.026
R17_19	5.064	5.488	5.007	5.27

Axial length / mm	Day 0	Day4	Day 0	Day4
	RE	RE	LE	LE
R17_11	8.835	9.413	8.732	9.48
R17_12	8.828	9.418	8.922	9.194
R17_13	8.743	9.057	8.676	8.96
R17_14	8.707	9.098	8.69	9.192
R17_15	8.777	9.358	8.72	9.542
R17_16	8.732	8.921	8.765	8.977
R17_17	8.771	8.919	8.759	9.09
R17_18	8.492	8.807	8.781	8.744
R17_19	8.889	9.486	8.798	9.315

Refractive errors /D	Day 0	Day4	Day 0	Day4
	RE	RE	LE	LE
R17_11	5.25	-1	4	0.5
R17_12	4.5	-3.75	5	1
R17_13	4	1	3.5	4
R17_14	5.75	1.5	4	1.75
R17_15	2.5	0.5	3.5	-5.5
R17_16	2.5	-1	3.25	0.25
R17_17	2	4.5	1.75	2.5
R17_18	2.75	3.5	2.5	1.5
R17_19	2	-2.25	3.5	-0.75

Raw data of ocular parameters from intravitreal injection of 50mM bezafibrate (Chapter 3)

Vitreous chamber depth / mm	Day 0	Day4	Day 0	Day4
	RE	RE	LE	LE
R17_1	5.169	5.399	5.02	5.435
R17_2	5.078	5.303	5.094	5.218
R17_3	4.916	5.409	4.959	5.34
R17_4	5.078	5.298	5.098	5.497
R17_6	4.933	5.45	4.859	5.517
R17_7	5.011	5.545	4.942	5.346
R17_8	4.997	5.344	5.005	5.24
R17_9	5.177	5.463	5.075	5.469
R17_10	4.892	5.057	4.858	5.193

Axial length / mm	Day 0	Day4	Day 0	Day4
	RE	RE	LE	LE
R17_1	8.996	9.075	8.866	9.11
R17_2	8.81	9.196	8.757	9.088
R17_3	8.678	9.199	8.731	9.158
R17_4	8.835	9.206	8.827	9.333
R17_6	8.712	9.337	8.695	9.472
R17_7	8.679	9.382	8.595	9.107
R17_8	8.686	9.221	8.635	9.041
R17_9	8.807	9.256	8.741	9.278
R17_10	8.654	8.853	8.668	9.061

Refractive errors /D	Day 0	Day4	Day 0	Day4
	RE	RE	LE	LE
R17_1	2.5	0.75	2.5	-5
R17_2	3.5	-1	3.25	0.25
R17_3	4	-4	5	-5.5
R17_4	5	-1	5.5	-7
R17_6	4	-1.75	5.75	-7.25
R17_7	3	-3.75	3.5	-3.75
R17_8	3.75	0	3.5	0.25
R17_9	3.5	0.25	5.25	-2.25
R17_10	2.5	0.5	4	-1

Raw data of ocular parameters from intravitreal injection of 60mM nicotinic acid (Chapter 3)

Vitreous chamber depth / mm	Day 0	Day4	Day 0	Day4
	RE	RE	LE	LE
R16_4	4.777	5.303	4.69	5.161
R16_6	4.915	5.267	4.886	5.36
R16_7	4.931	5.491	4.951	5.486
R16_8	4.938	5.435	4.895	5.558
R16_10	5.084	5.46	5.072	5.643
R16_11	4.788	5.233	4.796	5.305
R16_12	4.701	5.168	4.797	5.246

Axial length / mm	Day 0	Day4	Day 0	Day4
	RE	RE	LE	LE
R16_4	8.44	9.176	8.373	9.065
R16_6	8.588	9.137	8.513	9.278
R16_7	8.775	9.564	8.725	9.451

R16_8	8.68	9.444	8.665	9.548
R16_10	8.881	9.308	8.845	9.608
R16_11	8.501	9.13	8.797	9.241
R16_12	8.421	9.014	8.386	9.099

Refractive errors / D	Day 0	Day4	Day 0	Day4
	RE	RE	LE	LE
R16_4	4.75	-4.25	4	-5.75
R16_6	4.5	1.25	3.75	-2.5
R16_7	3	-4.25	4	-4.25
R16_8	3.75	-3.75	4.75	-5.5
R16_10	4	-5.5	4	-4.25
R16_11	3	-2.75	2.5	-7.5
R16_12	3.25	-4	2.75	-6

Raw data of ocular parameters from intravitreal injection of 122mM nicotinic acid (Chapter 3)

Vitreous chamber depth / mm	Day 0	Day4	Day 0	Day4
	RE	RE	LE	LE
R15_5	5.2	5.72	5.103	5.801
R15_7	4.861	5.556	4.902	5.691
R15_8	5.127	5.51	5.155	5.671
R15_9	5.245	5.79	5.149	5.784
R15_10	5.151	5.415	5.098	5.541
R16_2	4.897	5.359	4.855	5.346

Axial length / mm	Day 0	Day4	Day 0	Day4
	RE	RE	LE	LE
R15_5	9.299	9.878	9.264	10.035
R15_7	8.818	9.705	8.818	9.875
R15_8	8.974	9.604	8.966	9.809
R15_9	9.201	9.965	9.057	9.924
R15_10	8.957	9.545	9.088	9.611
R16_2	8.609	9.211	8.547	9.42

Refractive errors / D	Day 0	Day4	Day 0	Day4
	RE	RE	LE	LE
R15_5	4	-1.75	4	-3.75
R15_7	2.5	-6.25	4.5	-5.75
R15_8	4.5	-2	3.5	-6.5
R15_9	3.5	-2	2	-3.5
R15_10	2.5	-1.75	4	-1.5
R16_2	4.5	-2	4	-4.75

Raw data of ocular parameters from 3 days of lens-induced myopia and hyperopia for immunohistochemistry (Chapter 4)

Vitreous chamber depth / mm	Day 0 RE (-10D)	Day 3 RE (-10D)	Day 0 LE (+10D)	Day 3 LE (+10D)
R21_15	4.953	5.089	4.984	4.729
R21_16	5.062	5.42	5.077	4.759
R21_17	5.126	5.452	5.145	4.699
R21_18	5.131	5.185	5.132	4.717

Axial length / mm	Day 0 RE (-10D)	Day 3 RE (-10D)	Day 0 LE (+10D)	Day 3 LE (+10D)
R21_15	8.553	8.537	8.473	8.335
R21_16	8.592	8.906	8.644	8.279
R21_17	8.773	8.963	8.766	8.149
R21_18	8.673	8.663	8.628	8.198

Refractive errors / D	Day 0 RE (-10D)	Day 3 RE (-10D)	Day 0 LE (+10D)	Day 3 LE (+10D)
R21_15	5	-1.5	5.5	12.5
R21_16	2.5	-3.75	4.5	13
R21_17	4.5	-3.75	6	13.5
R21_18	5.5	-2	5	12

Raw data of ocular parameters from intravitreal injection of 1mM 8-Br-cAMP (Chapter 5)

Vitreous chamber depth / mm	Day 0 RE	Day4 RE	Day 0 LE	Day4 LE
S25_4	5.069	5.186	4.926	5.45
S25_5	5.11	5.03	4.906	5.364
S25_6	5.084	4.833	4.967	5.438
S25_7	4.899	4.897	4.951	5.201
S25_8	4.735	5.001	4.776	5.308
S25_9	5.046	4.919	4.819	5.153
S37_12	4.764	4.778	4.779	5.049
S37_14	4.948	4.926	4.856	5.35
S37_16	4.599	4.677	4.698	4.833

Axial length / mm	Day 0 RE	Day4 RE	Day 0 LE	Day4 LE
S25_4	7.925	8.589	7.86	8.799
S25_5	8.019	8.442	7.961	8.755

S25_6	7.881	7.918	7.838	8.724
S25_7	7.88	8.164	7.973	8.513
S25_8	7.661	8.368	7.787	8.644
S25_9	8.012	8.388	7.867	8.491
S37_12	7.852	8.281	7.864	8.502
S37_14	8.085	8.612	7.959	9.088
S37_16	7.5	8.128	7.69	8.339

Refractive errors / D	**Day 0**	**Day4**	**Day 0**	**Day4**
	RE	**RE**	**LE**	**LE**
S25_4	0.5	-4.25	1.5	-13
S25_5	2	-0.5	1.5	-6.25
S25_6	2	3	1.75	-11
S25_7	4.5	5	1.5	-8
S25_8	3	2	2	-13
S25_9	2.5	3	2.5	-8.5
S37_12	2	2.5	2.5	-12
S37_14	4.5	2	3.5	-15.5
S37_16	3.5	1.25	2.5	-6.5

Retinal thickness/ mm	**Day 0**	**Day4**	**Day 0**	**Day4**
	RE	**RE**	**LE**	**LE**
S25_4	0.211	0.227	0.207	0.206
S25_5	0.205	0.24	0.21	0.218
S25_6	0.204	0.228	0.201	0.207
S25_7	0.202	0.235	0.215	0.211
S25_8	0.212	0.236	0.215	0.218
S25_9	0.217	0.234	0.222	0.19
S37_12	0.218	0.234	0.223	0.214
S37_14	0.232	0.269	0.244	0.216
S37_16	0.224	0.231	0.231	0.204

Choroidal thickness/ mm	**Day 0**	**Day4**	**Day 0**	**Day4**
	RE	**RE**	**LE**	**LE**
S25_4	0.241	0.171	0.249	0.143
S25_5	0.299	0.151	0.191	0.108
S25_6	0.263	0.163	0.225	0.113
S25_7	0.218	0.305	0.232	0.101
S25_8	0.157	0.143	0.204	0.09
S25_9	0.134	0.126	0.199	0.092
S37_12	0.244	0.164	0.239	0.107
S37_14	0.203	0.212	0.231	0.14
S37_16	0.304	0.155	0.298	0.151

Scleral thickness/	**Day 0**	**Day4**	**Day 0**	**Day4**

mm	RE	RE	LE	LE
S25_4	0.068	0.077	0.054	0.075
S25_5	0.072	0.067	0.087	0.089
S25_6	0.05	0.081	0.064	0.075
S25_7	0.26	0.111	0.049	0.084
S25_8	0.063	0.081	0.062	0.111
S25_9	0.063	0.092	0.083	0.086
S37_12	0.12	0.124	0.12	0.118
S37_14	0.106	0.085	0.134	0.09
S37_16	0.112	0.114	0.134	0.078

Anterior chamber depth/ mm	Day 0	Day4	Day 0	Day4
	RE	RE	LE	LE
S25_4	1.187	1.352	1.135	1.304
S25_5	1.27	1.34	1.321	1.392
S25_6	1.204	1.112	1.184	1.337
S25_7	1.259	1.224	1.28	1.266
S25_8	1.166	1.198	1.205	1.154
S25_9	1.286	1.326	1.216	1.177
S37_12	1.235	1.285	1.246	1.263
S37_14	1.285	1.422	1.242	1.515
S37_16	1.177	1.37	1.173	1.031

Lens thickness/ mm	Day 0	Day4	Day 0	Day4
	RE	RE	LE	LE
S25_4	1.669	2.051	1.799	2.045
S25_5	1.639	2.072	1.734	1.999
S25_6	1.593	1.973	1.687	1.949
S25_7	1.722	2.043	1.742	2.046
S25_8	1.76	2.169	1.806	2.182
S25_9	1.68	2.143	1.832	2.161
S37_12	1.853	2.218	1.839	2.19
S37_14	1.852	2.264	1.861	2.223
S37_16	1.724	2.081	1.819	2.475

Raw data of ocular parameters from 3-day lens deprivation (Chapter 6)

Vitreous chamber depth / mm	Day 0	Day 3	Day 0	Day 3
	RE (-10D)	RE (-10D)	LE (+10D)	LE (+10D)
R21_15	4.953	5.089	4.984	4.729
R21_17	5.126	5.452	5.145	4.699
R21_18	5.131	5.185	5.132	4.717
R26_8	5.062	5.42	5.077	4.759
R27_9	4.883	5.167	4.879	4.596

R27_7	4.959	5.119	4.941	4.314
R27_12	4.974	5.272	4.784	4.335

Axial length / mm	Day 0 RE (-10D)	Day 3 RE (-10D)	Day 0 LE (+10D)	Day 3 LE (+10D)
R21_15	8.553	8.537	8.473	8.335
R21_17	8.773	8.963	8.766	8.149
R21_18	8.673	8.663	8.628	8.198
R26_8	8.592	8.906	8.644	8.279
R27_9	8.477	8.641	8.386	8.594
R27_7	8.441	8.614	8.8	8.184
R27_12	8.774	8.862	8.643	8.414

Refractive errors / D	Day 0 RE (-10D)	Day 3 RE (-10D)	Day 0 LE (+10D)	Day 3 LE (+10D)
R21_15	5	-1.5	5.5	12.5
R21_17	4.5	-3.75	6	13.5
R21_18	5.5	-2	5	12
R26_8	2.5	-3.75	4.5	13
R27_9	2.5	-5.25	4	13
R27_7	4	-3.5	4	8.5
R27_12	1.5	-6	2	8

Vitreous chamber depth / mm	Day 0 RE (-10D)	Day 3 RE (-10D)	Day 0 LE (Plano)	Day 3 LE (Plano)
R26_10	4.951	5.341	5.102	5.032
R26_11	4.979	5.247	4.986	5.039
R24_4	5.008	5.241	4.932	5.086
R24_6	4.927	5.397	4.915	4.988
R27_5	5.081	5.457	4.955	5.057
R27_6	5.057	5.378	5.073	5.139

Axial length / mm	Day 0 RE (-10D)	Day 3 RE (-10D)	Day 0 LE (Plano)	Day 3 LE (Plano)
R26_10	8.642	9.054	8.838	8.819
R26_11	8.726	8.837	8.701	8.72
R24_4	8.661	8.909	8.649	8.694
R24_6	8.47	8.905	8.137	8.571
R27_5	8.633	9.126	8.481	8.68
R27_6	8.751	8.975	8.64	8.676

Refractive errors /D	Day 0 RE (-10D)	Day 3 RE (-10D)	Day 0 LE (Plano)	Day 3 LE (Plano)
R26_10	3	-2.75	4	5

R26_11	4.5	-2.25	7	8
R24_4	5	-5.75	5.5	2
R24_6	1.5	-5.25	4.5	2
R27_5	3	-7	3.5	2
R27_6	4	-2.5	4	3

Vitreous chamber depth / mm	**Day 0**	**Day 3**	**Day 0**	**Day 3**
	RE (+10D)	**RE (+10D)**	**LE (Plano)**	**LE (Plano)**
R26_1	5.038	4.762	4.937	5.225
R26_4	4.934	4.656	4.912	5.071
R27_1	5.082	4.815	5.043	5.222
R27_2	4.775	4.315	4.698	4.655
R27_3	4.991	4.524	4.957	5.015

Axial length / mm	**Day 0**	**Day 3**	**Day 0**	**Day 3**
	RE (+10D)	**RE (+10D)**	**LE (Plano)**	**LE (Plano)**
R26_1	8.575	8.485	8.333	8.728
R26_4	8.438	8.28	8.465	8.628
R27_1	8.598	8.507	8.504	8.883
R27_2	8.537	8.38	8.522	8.364
R27_3	8.577	8.354	8.433	8.524

Refractive errors /D	**Day 0**	**Day 3**	**Day 0**	**Day 3**
	RE (+10D)	**RE (+10D)**	**LE (Plano)**	**LE (Plano)**
R26_1	3.5	9.5	3.5	3
R26_4	4	11	3	4.5
R27_1	4.5	13	4	3
R27_2	3	10	2.5	3
R27_3	3	11.5	4	4

Raw data of retinal cAMP concentration (in pmol/mg) after 3-day lens deprivation (Chapter 6)

	RE (-10D)	**LE (+10D)**
R27_9	0.586	1.294
R27_7	1.592	1.870
R27_12	0.995	2.912
R26_8	1.327	1.452
R21_15	2.521	3.755
R21_17	2.443	3.174
R21_18	2.977	4.525

	RE (-10D)	**LE (Plano)**
R27_5	1.345	1.448

R27_6	1.497	1.284
R26_10	1.031	1.265
R26_11	1.537	1.397
R24_4	1.431	1.011
R24_6	1.406	1.266

	RE (-10D)	**LE (Plano)**
R26_1	1.592	1.326
R26_4	1.618	1.468
R27_1	3.586	1.999
R27_2	2.908	2.631
R27_3	2.939	2.194

References

Altschul, R. and Herman, I. H. (1954). "Influence of oxygen inhalation on cholesterol metabolism." Arch Biochem Biophys **51**(1): 308-9.

Arber, S., Barbayannis, F. A., Hanser, H., Schneider, C., Stanyon, C. A., Bernard, O. and Caroni, P. (1998). "Regulation of actin dynamics through phosphorylation of cofilin by LIM-kinase." Nature **393**(6687): 805-9.

Arias-Carrion, O. and Poppel, E. (2007). "Dopamine, learning, and reward-seeking behavior." Acta Neurobiol Exp (Wars) **67**(4): 481-8.

Ashby, R., McCarthy, C. S., Maleszka, R., Megaw, P. and Morgan, I. G. (2007). "A muscarinic cholinergic antagonist and a dopamine agonist rapidly increase ZENK mRNA expression in the form-deprived chicken retina." Exp Eye Res **85**(1): 15-22.

Bachmann, K., Patel, H., Batayneh, Z., Slama, J., White, D., Posey, J., Ekins, S., Gold, D. and Sambucetti, L. (2004). "PXR and the regulation of apoA1 and HDL-cholesterol in rodents." Pharmacol Res **50**(3): 237-46.

Balazs, E. A., Toth, L. Z., Jutheden, G. M. and Collins, B. A. (1965). "Cytological and biochemical studies on the developing chicken vitreous." Exp Eye Res **4**(3): 237-48.

Barter, P., Gotto, A. M., LaRosa, J. C., Maroni, J., Szarek, M., Grundy, S. M., Kastelein, J. J., Bittner, V. and Fruchart, J. C. (2007). "HDL cholesterol, very low levels of LDL cholesterol, and cardiovascular events." N Engl J Med **357**(13): 1301-10.

Beresford, J. A., Crewther, S. G., Kiely, P. M. and Crewther, D. P. (2001). "Comparison of refractive state and circumferential morphology of retina, choroid, and sclera in chick models of experimentally induced ametropia." Optom Vis Sci **78**(1): 40-9.

Bernard, O. (2007). "Lim kinases, regulators of actin dynamics." Int J Biochem Cell Biol **39**(6): 1071-6.

Berthoud, V. M. and Beyer, E. C. (2009). "Oxidative stress, lens gap junctions, and cataracts." Antioxid Redox Signal **11**(2): 339-53.

Bertrand, E., Fritsch, C., Diether, S., Lambrou, G., Mueller, D., Schaeffel, F., Schindler, P., Schmid, K. L., van Oostrum, J. and Voshol, H. (2006). "Identification of Apolipoprotein A1 as a "STOP" signal for myopia." Mol Cell Proteomics.

Bertrand, E., Fritsch, C., Diether, S., Lambrou, G., Muller, D., Schaeffel, F., Schindler, P., Schmid, K. L., van Oostrum, J. and Voshol, H. (2006). "Identification of apolipoprotein A-I as a "STOP" signal for myopia." Mol Cell Proteomics **5**(11): 2158-66.

Birjmohun, R. S., Hutten, B. A., Kastelein, J. J. and Stroes, E. S. (2004). "Increasing HDL cholesterol with extended-release nicotinic acid: from promise to practice." Neth J Med **62**(7): 229-34.

Bitzer, M., Feldkaemper, M. and Schaeffel, F. (2000). "Visually induced changes in components of the retinoic acid system in fundal layers of the chick." Exp Eye Res **70**(1): 97-106.

Bitzer, M. and Schaeffel, F. (2002). "Defocus-induced changes in ZENK expression in the chicken retina." Invest Ophthalmol Vis Sci **43**(1): 246-52.
Bitzer, M. and Schaeffel, F. (2004). "Effects of quisqualic acid on retinal ZENK expression induced by imposed defocus in the chick eye." Optom Vis Sci **81**(2): 127-36.
Brand, C., Burkhardt, E., Schaeffel, F., Choi, J. W. and Feldkaemper, M. P. (2005). "Regulation of Egr-1, VIP, and Shh mRNA and Egr-1 protein in the mouse retina by light and image quality." Mol Vis **11**: 309-20.
Carlson, L. A. (2005). "Nicotinic acid: the broad-spectrum lipid drug. A 50th anniversary review." J Intern Med **258**(2): 94-114.
Casini, G. (2005). "Neuropeptides and retinal development." Arch Ital Biol **143**(3-4): 191-8.
Chambers, G., Lawrie, L., Cash, P. and Murray, G. I. (2000). "Proteomics: a new approach to the study of disease." J Pathol **192**(3): 280-8.
Chen, C. H. (2008). "Review of a current role of mass spectrometry for proteome research." Anal Chim Acta **624**(1): 16-36.
Chen, J., Godt, D., Gunsalus, K., Kiss, I., Goldberg, M. and Laski, F. A. (2001). "Cofilin/ADF is required for cell motility during Drosophila ovary development and oogenesis." Nat Cell Biol **3**(2): 204-9.
Chen, S. J., Ning, H., Ishida, W., Sodin-Semrl, S., Takagawa, S., Mori, Y. and Varga, J. (2006). "The early-immediate gene EGR-1 is induced by transforming growth factor-beta and mediates stimulation of collagen gene expression." J Biol Chem **281**(30): 21183-97.
Cheng, X., Ji, Z., Tsalkova, T. and Mei, F. (2008). "Epac and PKA: a tale of two intracellular cAMP receptors." Acta Biochim Biophys Sin (Shanghai) **40**(7): 651-62.
Chihara, E., Liu, X., Dong, J., Takashima, Y., Akimoto, M., Hangai, M., Kuriyama, S., Tanihara, H., Hosoda, M. and Tsukahara, S. (1997). "Severe myopia as a risk factor for progressive visual field loss in primary open-angle glaucoma." Ophthalmologica **211**(2): 66-71.
Chui, T. Y., Song, H. and Burns, S. A. (2008). "Individual variations in human cone photoreceptor packing density: variations with refractive error." Invest Ophthalmol Vis Sci **49**(10): 4679-87.
Cottriall, C. L., Truong, H. T. and McBrien, N. A. (2001). "Inhibition of myopia development in chicks using himbacine: a role for M(4) receptors?" Neuroreport **12**(11): 2453-6.
Crewther, D. P. (2000). "The role of photoreceptors in the control of refractive state." Prog Retin Eye Res **19**(4): 421-57.
Crewther, S. G., Murphy, M. J. and Crewther, D. P. (2008). "Potassium channel and NKCC cotransporter involvement in ocular refractive control mechanisms." PLoS One **3**(7): e2839.
Czepita, D., Zejmo, M. and Mojsa, A. (2007). "Prevalence of myopia and hyperopia in a population of Polish schoolchildren." Ophthalmic Physiol Opt **27**(1): 60-5.

de Rooij, J., Zwartkruis, F. J., Verheijen, M. H., Cool, R. H., Nijman, S. M., Wittinghofer, A. and Bos, J. L. (1998). "Epac is a Rap1 guanine-nucleotide-exchange factor directly activated by cyclic AMP." Nature **396**(6710): 474-7.

De Stefano, M. E. and Mugnaini, E. (1997). "Fine structure of the choroidal coat of the avian eye. Lymphatic vessels." Invest Ophthalmol Vis Sci **38**(6): 1241-60.

Ding, X., Patel, M. and Chan, C. C. (2009). "Molecular pathology of age-related macular degeneration." Prog Retin Eye Res **28**(1): 1-18.

Dongre, A. R., Opiteck, G., Cosand, W. L. and Hefta, S. A. (2001). "Proteomics in the post-genome age." Biopolymers **60**(3): 206-11.

Drew, B. G., Duffy, S. J., Formosa, M. F., Natoli, A. K., Henstridge, D. C., Penfold, S. A., Thomas, W. G., Mukhamedova, N., de Courten, B., Forbes, J. M., Yap, F. Y., Kaye, D. M., van Hall, G., Febbraio, M. A., Kemp, B. E., Sviridov, D., Steinberg, G. R. and Kingwell, B. A. (2009). "High-density lipoprotein modulates glucose metabolism in patients with type 2 diabetes mellitus." Circulation **119**(15): 2103-11.

Drew, B. G., Fidge, N. H., Gallon-Beaumier, G., Kemp, B. E. and Kingwell, B. A. (2004). "High-density lipoprotein and apolipoprotein AI increase endothelial NO synthase activity by protein association and multisite phosphorylation." Proc Natl Acad Sci U S A **101**(18): 6999-7004.

Dubey, R. K., Mi, Z., Gillespie, D. G. and Jackson, E. K. (1996). "Cyclic AMP-adenosine pathway inhibits vascular smooth muscle cell growth." Hypertension **28**(5): 765-71.

Edwards, M. H. (1999). "The development of myopia in Hong Kong children between the ages of 7 and 12 years: a five-year longitudinal study." Ophthalmic Physiol Opt **19**(4): 286-94.

Edwards, M. H. and Lam, C. S. (2004). "The epidemiology of myopia in Hong Kong." Ann Acad Med Singapore **33**(1): 34-8.

Edwards, M. H., Li, R. W., Lam, C. S., Lew, J. K. and Yu, B. S. (2002). "The Hong Kong progressive lens myopia control study: study design and main findings." Invest Ophthalmol Vis Sci **43**(9): 2852-8.

Ehrlich, D., Sattayasai, J., Zappia, J. and Barrington, M. (1990). "Effects of selective neurotoxins on eye growth in the young chick." Ciba Found Symp **155**: 63-84; discussion 84-8.

Fan, D. S., Cheung, E. Y., Lai, R. Y., Kwok, A. K. and Lam, D. S. (2004). "Myopia progression among preschool Chinese children in Hong Kong." Ann Acad Med Singapore **33**(1): 39-43.

Feldkaemper, M. P., Neacsu, I. and Schaeffel, F. (2009). "Insulin acts as a powerful stimulator of axial myopia in chicks." Invest Ophthalmol Vis Sci **50**(1): 13-23.

Fischer, A. J., McGuire, J. J., Schaeffel, F. and Stell, W. K. (1999). "Light- and focus-dependent expression of the transcription factor ZENK in the chick retina." Nat Neurosci **2**(8): 706-12.

Fitzgerald, M. E., Wildsoet, C. F. and Reiner, A. (2002). "Temporal relationship of choroidal blood flow and thickness changes during recovery from form deprivation myopia in chicks." Exp Eye Res **74**(5): 561-70.

Frohlich, T. and Arnold, G. J. (2006). "Proteome research based on modern liquid chromatography--tandem mass spectrometry: separation, identification and quantification." J Neural Transm **113**(8): 973-94.
Fruchart, J. C. and Duriez, P. (2006). "Mode of action of fibrates in the regulation of triglyceride and HDL-cholesterol metabolism." Drugs Today (Barc) **42**(1): 39-64.
Gao, Q., Liu, Q., Ma, P., Zhong, X., Wu, J. and Ge, J. (2006). "Effects of direct intravitreal dopamine injections on the development of lid-suture induced myopia in rabbits." Graefes Arch Clin Exp Ophthalmol **244**(10): 1329-35.
Gervois, P., Torra, I. P., Fruchart, J. C. and Staels, B. (2000). "Regulation of lipid and lipoprotein metabolism by PPAR activators." Clin Chem Lab Med **38**(1): 3-11.
Gonzalez-Flores, O., Gomora-Arrati, P., Garcia-Juarez, M., Gomez-Camarillo, M. A., Lima-Hernandez, F. J., Beyer, C. and Etgen, A. M. (2009). "Nitric oxide and ERK/MAPK mediation of estrous behavior induced by GnRH, PGE2 and db-cAMP in rats." Physiol Behav **96**(4-5): 606-12.
Graham, B. and Judge, S. J. (1999). "The effects of spectacle wear in infancy on eye growth and refractive error in the marmoset (Callithrix jacchus)." Vision Res **39**(2): 189-206.
Grossini, E., Molinari, C., Mary, D. A., Uberti, F., Ribichini, F., Caimmi, P. P. and Vacca, G. (2009). "Urocortin II induces nitric oxide production through cAMP and Ca2+ related pathways in endothelial cells." Cell Physiol Biochem **23**(1-3): 87-96.
Grossniklaus, H. E. and Green, W. R. (1992). "Pathologic findings in pathologic myopia." Retina **12**(2): 127-33.
Gruber, E. (1985). "Treatment of myopia with atropine and bifocals." Ophthalmology **92**(7): 985.
Haidar, B., Denis, M., Krimbou, L., Marcil, M. and Genest, J., Jr. (2002). "cAMP induces ABCA1 phosphorylation activity and promotes cholesterol efflux from fibroblasts." J Lipid Res **43**(12): 2087-94.
Haidar, B., Denis, M., Marcil, M., Krimbou, L. and Genest, J., Jr. (2004). "Apolipoprotein A-I activates cellular cAMP signaling through the ABCA1 transporter." J Biol Chem **279**(11): 9963-9.
Han, R., Lai, R., Ding, Q., Wang, Z., Luo, X., Zhang, Y., Cui, G., He, J., Liu, W. and Chen, Y. (2007). "Apolipoprotein A-I stimulates AMP-activated protein kinase and improves glucose metabolism." Diabetologia **50**(9): 1960-8.
Hasebe, S., Ohtsuki, H., Nonaka, T., Nakatsuka, C., Miyata, M., Hamasaki, I. and Kimura, S. (2008). "Effect of progressive addition lenses on myopia progression in Japanese children: a prospective, randomized, double-masked, crossover trial." Invest Ophthalmol Vis Sci **49**(7): 2781-9.
He, M., Zeng, J., Liu, Y., Xu, J., Pokharel, G. P. and Ellwein, L. B. (2004). "Refractive error and visual impairment in urban children in southern china." Invest Ophthalmol Vis Sci **45**(3): 793-9.
Hoffmann, M. and Schaeffel, F. (1996). "Melatonin and deprivation myopia in chickens." Neurochem Int **28**(1): 95-107.

Honda, S., Fujii, S., Sekiya, Y. and Yamamoto, M. (1996). "Retinal control on the axial length mediated by transforming growth factor-beta in chick eye." Invest Ophthalmol Vis Sci **37**(12): 2519-26.

Hoyt, C. S., Stone, R. D., Fromer, C. and Billson, F. A. (1981). "Monocular axial myopia associated with neonatal eyelid closure in human infants." Am J Ophthalmol **91**(2): 197-200.

Idres, N., Marill, J., Flexor, M. A. and Chabot, G. G. (2002). "Activation of retinoic acid receptor-dependent transcription by all-trans-retinoic acid metabolites and isomers." J Biol Chem **277**(35): 31491-8.

Ikeda, S., Cunningham, L. A., Boggess, D., Hawes, N., Hobson, C. D., Sundberg, J. P., Naggert, J. K., Smith, R. S. and Nishina, P. M. (2003). "Aberrant actin cytoskeleton leads to accelerated proliferation of corneal epithelial cells in mice deficient for destrin (actin depolymerizing factor)." Hum Mol Genet **12**(9): 1029-37.

Inaba, T., Yagyu, H., Itabashi, N., Tazoe, F., Fujita, N., Nagashima, S., Okada, K., Okazaki, M., Furukawa, Y. and Ishibashi, S. (2008). "Cholesterol reduction and atherosclerosis inhibition by bezafibrate in low-density lipoprotein receptor knockout mice." Hypertens Res **31**(5): 999-1005.

Irving, E. L., Sivak, J. G. and Callender, M. G. (1992). "Refractive plasticity of the developing chick eye." Ophthalmic Physiol Opt **12**(4): 448-56.

Ishida, B. Y., Duncan, K. G., Bailey, K. R., Kane, J. P. and Schwartz, D. M. (2006). "High density lipoprotein mediated lipid efflux from retinal pigment epithelial cells in culture." Br J Ophthalmol **90**(5): 616-20.

Iuvone, P. M., Tigges, M., Fernandes, A. and Tigges, J. (1989). "Dopamine synthesis and metabolism in rhesus monkey retina: development, aging, and the effects of monocular visual deprivation." Vis Neurosci **2**(5): 465-71.

Iuvone, P. M., Tigges, M., Stone, R. A., Lambert, S. and Laties, A. M. (1991). "Effects of apomorphine, a dopamine receptor agonist, on ocular refraction and axial elongation in a primate model of myopia." Invest Ophthalmol Vis Sci **32**(5): 1674-7.

Iwase, A., Araie, M., Tomidokoro, A., Yamamoto, T., Shimizu, H. and Kitazawa, Y. (2006). "Prevalence and causes of low vision and blindness in a Japanese adult population: the Tajimi Study." Ophthalmology **113**(8): 1354-62.

Jin, F. Y., Kamanna, V. S. and Kashyap, M. L. (1997). "Niacin decreases removal of high-density lipoprotein apolipoprotein A-I but not cholesterol ester by Hep G2 cells. Implication for reverse cholesterol transport." Arterioscler Thromb Vasc Biol **17**(10): 2020-8.

Jobling, A. I., Gentle, A., Metlapally, R., McGowan, B. J. and McBrien, N. A. (2009). "Regulation of scleral cell contraction by transforming growth factor-beta and stress: competing roles in myopic eye growth." J Biol Chem **284**(4): 2072-9.

Jobling, A. I., Nguyen, M., Gentle, A. and McBrien, N. A. (2004). "Isoform-specific changes in scleral transforming growth factor-beta expression and the regulation of collagen synthesis during myopia progression." J Biol Chem **279**(18): 18121-6.

Jobling, A. I., Wan, R., Gentle, A., Bui, B. V. and McBrien, N. A. (2009). "Retinal and choroidal TGF-beta in the tree shrew model of myopia: isoform expression, activation and effects on function." Exp Eye Res **88**(3): 458-66.

Junghans, B. M., Crewther, S. G., Liang, H. and Crewther, D. P. (1999). "A role for choroidal lymphatics during recovery from form deprivation myopia?" Optom Vis Sci **76**(11): 796-803.

Kang, G., Joseph, J. W., Chepurny, O. G., Monaco, M., Wheeler, M. B., Bos, J. L., Schwede, F., Genieser, H. G. and Holz, G. G. (2003). "Epac-selective cAMP analog 8-pCPT-2'-O-Me-cAMP as a stimulus for Ca2+-induced Ca2+ release and exocytosis in pancreatic beta-cells." J Biol Chem **278**(10): 8279-85.

Kilbourne, E. J., Widom, R., Harnish, D. C., Malik, S. and Karathanasis, S. K. (1995). "Involvement of early growth response factor Egr-1 in apolipoprotein AI gene transcription." J Biol Chem **270**(12): 7004-10.

Kinge, B., Midelfart, A., Jacobsen, G. and Rystad, J. (2000). "The influence of near-work on development of myopia among university students. A three-year longitudinal study among engineering students in Norway." Acta Ophthalmol Scand **78**(1): 26-9.

Kleinstein, R. N., Jones, L. A., Hullett, S., Kwon, S., Lee, R. J., Friedman, N. E., Manny, R. E., Mutti, D. O., Yu, J. A. and Zadnik, K. (2003). "Refractive error and ethnicity in children." Arch Ophthalmol **121**(8): 1141-7.

Koh, S. M. (2000). "VIP enhances the differentiation of retinal pigment epithelium in culture: from cAMP and pp60(c-src) to melanogenesis and development of fluid transport capacity." Prog Retin Eye Res **19**(6): 669-88.

Kopperud, R., Krakstad, C., Selheim, F. and Doskeland, S. O. (2003). "cAMP effector mechanisms. Novel twists for an 'old' signaling system." FEBS Lett **546**(1): 121-6.

Kroger, R. H., Hirt, B. and Wagner, H. J. (1999). "Effects of retinal dopamine depletion on the growth of the fish eye." J Comp Physiol A **184**(4): 403-12.

Latchman, D. S. (1997). "Transcription factors: an overview." Int J Biochem Cell Biol **29**(12): 1305-12.

Lawrence, M. S. and Azar, D. T. (2002). "Myopia and models and mechanisms of refractive error control." Ophthalmol Clin North Am **15**(1): 127-33.

Lee, J., Ko, M. and Joo, C. K. (2008). "Rho plays a key role in TGF-beta1-induced cytoskeletal rearrangement in human retinal pigment epithelium." J Cell Physiol **216**(2): 520-6.

Leung, J. T. and Brown, B. (1999). "Progression of myopia in Hong Kong Chinese schoolchildren is slowed by wearing progressive lenses." Optom Vis Sci **76**(6): 346-54.

Li, A., Guo, H., Luo, X., Sheng, J., Yang, S., Yin, Y. and Zhou, J. (2006). "Apomorphine-induced activation of dopamine receptors modulates FGF-2 expression in astrocytic cultures and promotes survival of dopaminergic neurons." Faseb J **20**(8): 1263-5.

Li, X. X., Schaeffel, F., Kohler, K. and Zrenner, E. (1992). "Dose-dependent effects of 6-hydroxy dopamine on deprivation myopia, electroretinograms, and dopaminergic amacrine cells in chickens." Vis Neurosci **9**(5): 483-92.

Liang, H., Crewther, D. P., Crewther, S. G. and Barila, A. M. (1995). "A role for photoreceptor outer segments in the induction of deprivation myopia." Vision Res **35**(9): 1217-25.
Liang, H., Crewther, S. G. and Crewther, D. P. (1995). "A model for the formation of ring mitochondria in retinal pigment epithelium." Yan Ke Xue Bao **11**(1): 9-15.
Liang, H., Crewther, S. G., Crewther, D. P. and Junghans, B. M. (2004). "Structural and elemental evidence for edema in the retina, retinal pigment epithelium, and choroid during recovery from experimentally induced myopia." Invest Ophthalmol Vis Sci **45**(8): 2463-74.
Lin, L. L., Shih, Y. F., Hsiao, C. K. and Chen, C. J. (2004). "Prevalence of myopia in Taiwanese schoolchildren: 1983 to 2000." Ann Acad Med Singapore **33**(1): 27-33.
Liu, C., Yao, J., de Belle, I., Huang, R. P., Adamson, E. and Mercola, D. (1999). "The transcription factor EGR-1 suppresses transformation of human fibrosarcoma HT1080 cells by coordinated induction of transforming growth factor-beta1, fibronectin, and plasminogen activator inhibitor-1." J Biol Chem **274**(7): 4400-11.
Longshore, M. A. and Makman, M. H. (1981). "Stimulation of retinal adenylate cyclase by vasoactive intestinal peptide (VIP)." Eur J Pharmacol **70**(2): 237-40.
Luft, W. A., Ming, Y. and Stell, W. K. (2003). "Variable effects of previously untested muscarinic receptor antagonists on experimental myopia." Invest Ophthalmol Vis Sci **44**(3): 1330-8.
Maciver, S. K. and Hussey, P. J. (2002). "The ADF/cofilin family: actin-remodeling proteins." Genome Biol **3**(5): reviews3007.
Mackness, M. I. and Durrington, P. N. (1995). "HDL, its enzymes and its potential to influence lipid peroxidation." Atherosclerosis **115**(2): 243-53.
Mao, J., Liu, S., Wen, D., Tan, X. and Fu, C. (2006). "Basic fibroblast growth factor suppresses retinal neuronal apoptosis in form-deprivation myopia in chicks." Curr Eye Res **31**(11): 983-7.
Marouga, R., David, S. and Hawkins, E. (2005). "The development of the DIGE system: 2D fluorescence difference gel analysis technology." Anal Bioanal Chem **382**(3): 669-78.
Mathis, U. and Schaeffel, F. (2007). "Glucagon-related peptides in the mouse retina and the effects of deprivation of form vision." Graefes Arch Clin Exp Ophthalmol **245**(2): 267-75.
Matsumura, H. and Hirai, H. (1999). "Prevalence of myopia and refractive changes in students from 3 to 17 years of age." Surv Ophthalmol **44 Suppl 1**: S109-115.
Maurice, D. M. and Mushin, A. S. (1966). "Production of myopia in rabbits by raised body-temperature and increased intraocular pressure." Lancet **2**(7474): 1160-2.
McBrien, N. A., Jobling, A. I. and Gentle, A. (2009). "Biomechanics of the sclera in myopia: extracellular and cellular factors." Optom Vis Sci **86**(1): E23-30.

McBrien, N. A., Moghaddam, H. O., Cottriall, C. L., Leech, E. M. and Cornell, L. M. (1995). "The effects of blockade of retinal cell action potentials on ocular growth, emmetropization and form deprivation myopia in young chicks." Vision Res **35**(9): 1141-52.

McBrien, N. A., Moghaddam, H. O. and Reeder, A. P. (1993). "Atropine reduces experimental myopia and eye enlargement via a nonaccommodative mechanism." Invest Ophthalmol Vis Sci **34**(1): 205-15.

McCarthy, C. S., Megaw, P., Devadas, M. and Morgan, I. G. (2007). "Dopaminergic agents affect the ability of brief periods of normal vision to prevent form-deprivation myopia." Exp Eye Res **84**(1): 100-7.

McFadden, S. A., Howlett, M. H. and Mertz, J. R. (2004). "Retinoic acid signals the direction of ocular elongation in the guinea pig eye." Vision Res **44**(7): 643-53.

McFadden, S. A., Howlett, M. H., Mertz, J. R. and Wallman, J. (2006). "Acute effects of dietary retinoic acid on ocular components in the growing chick." Exp Eye Res.

McGlinn, A. M., Baldwin, D. A., Tobias, J. W., Budak, M. T., Khurana, T. S. and Stone, R. A. (2007). "Form-deprivation myopia in chick induces limited changes in retinal gene expression." Invest Ophthalmol Vis Sci **48**(8): 3430-6.

Megaw, P., Morgan, I. and Boelen, M. (2001). "Vitreal dihydroxyphenylacetic acid (DOPAC) as an index of retinal dopamine release." J Neurochem **76**(6): 1636-44.

Megaw, P. L., Boelen, M. G., Morgan, I. G. and Boelen, M. K. (2006). "Diurnal patterns of dopamine release in chicken retina." Neurochem Int **48**(1): 17-23.

Megaw, P. L., Morgan, I. G. and Boelen, M. K. (1997). "Dopaminergic behaviour in chicken retina and the effect of form deprivation." Aust N Z J Ophthalmol **25 Suppl 1**: S76-8.

Mertz, J. R. and Wallman, J. (2000). "Choroidal retinoic acid synthesis: a possible mediator between refractive error and compensatory eye growth." Exp Eye Res **70**(4): 519-27.

Meyer, C., Mueller, M. F., Duncker, G. I. and Meyer, H. J. (1999). "Experimental animal myopia models are applicable to human juvenile-onset myopia." Surv Ophthalmol **44 Suppl 1**: S93-102.

Micheli, F. and Heidbreder, C. (2006). "Selective dopamine D3 receptor antagonists: a review 2001-2005." Recent Patents CNS Drug Discov **1**(3): 271-88.

Morgan, I., Kucharski, R., Krongkaew, N., Firth, S. I., Megaw, P. and Maleszka, R. (2004). "Screening for differential gene expression during the development of form-deprivation myopia in the chicken." Optom Vis Sci **81**(2): 148-55.

Morgan, I. G. (2003). "The biological basis of myopic refractive error." Clin Exp Optom **86**(5): 276-88.

Nagai, T., Tomizawa, T., Nakajima, K. and Mori, M. (2000). "Effect of bezafibrate or pravastatin on serum lipid levels and albuminuria in NIDDM patients." J Atheroscler Thromb **7**(2): 91-6.

Neele, D. M., de Wit, E. C. and Princen, H. M. (1999). "Inhibition of apolipoprotein(a) synthesis in cynomolgus monkey hepatocytes by retinoids

via involvement of the retinoic acid receptor." Biochem Pharmacol **58**(2): 263-71.
Nickla, D. L., Damyanova, P. and Lytle, G. (2009). "Inhibiting the neuronal isoform of nitric oxide synthase has similar effects on the compensatory choroidal and axial responses to myopic defocus in chicks as does the non-specific inhibitor L-NAME." Exp Eye Res **88**(6): 1092-9.
Nickla, D. L., Sharda, V. and Troilo, D. (2005). "Temporal integration characteristics of the axial and choroidal responses to myopic defocus induced by prior form deprivation versus positive spectacle lens wear in chickens." Optom Vis Sci **82**(4): 318-27.
Nickla, D. L. and Wildsoet, C. F. (2004). "The effect of the nonspecific nitric oxide synthase inhibitor NG-nitro-L-arginine methyl ester on the choroidal compensatory response to myopic defocus in chickens." Optom Vis Sci **81**(2): 111-8.
Nishida, T., Mukai, N., Solish, S. P. and Pomeroy, M. (1982). "Effects of cyclic AMP on growth and differentiation of rat retinoblastoma-like tumor cells in vitro." Invest Ophthalmol Vis Sci **22**(2): 145-56.
Norata, G. D., Callegari, E., Marchesi, M., Chiesa, G., Eriksson, P. and Catapano, A. L. (2005). "High-density lipoproteins induce transforming growth factor-beta2 expression in endothelial cells." Circulation **111**(21): 2805-11.
Norton, T. T. (1990). "Experimental myopia in tree shrews." Ciba Found Symp **155**: 178-94; discussion 194-9.
Norton, T. T. (1999). "Animal Models of Myopia: Learning How Vision Controls the Size of the Eye." Ilar J **40**(2): 59-77.
Obara, Y., Matsuzawa, T., Kuba, N. and Fujita, K. (1985). "Retinal damage in hatched chicks induced by formoguanamine. Decrease in ornithine aminotransferase activity and vitamin B6 content." Exp Eye Res **41**(4): 519-26.
Oishi, T. and Lauber, J. K. (1988). "Chicks blinded with formoguanamine do not develop lid suture myopia." Curr Eye Res **7**(1): 69-73.
Oram, J. F., Lawn, R. M., Garvin, M. R. and Wade, D. P. (2000). "ABCA1 is the cAMP-inducible apolipoprotein receptor that mediates cholesterol secretion from macrophages." J Biol Chem **275**(44): 34508-11.
Osorio, D., Vorobyev, M. and Jones, C. D. (1999). "Colour vision of domestic chicks." J Exp Biol **202**(Pt 21): 2951-9.
Over, R. and Moore, D. (1981). "Spatial acuity of the chicken." Brain Res **211**(2): 424-6.
Parsons, W. B., Jr. and Flinn, J. H. (1959). "Reduction of serum cholesterol levels and beta-lipoprotein cholesterol levels by nicotinic acid." AMA Arch Intern Med **103**(5): 783-90.
Patterson, S. D. and Aebersold, R. H. (2003). "Proteomics: the first decade and beyond." Nat Genet **33 Suppl**: 311-23.
Patton, W. F. (2002). "Detection technologies in proteome analysis." J Chromatogr B Analyt Technol Biomed Life Sci **771**(1-2): 3-31.

Pendrak, K., Nguyen, T., Lin, T., Capehart, C., Zhu, X. and Stone, R. A. (1997). "Retinal dopamine in the recovery from experimental myopia." Curr Eye Res **16**(2): 152-7.
Pendrak, K., Papastergiou, G. I., Lin, T., Laties, A. M. and Stone, R. A. (2000). "Choroidal vascular permeability in visually regulated eye growth." Exp Eye Res **70**(5): 629-37.
Percival, S. P. (1987). "Redefinition of high myopia: the relationship of axial length measurement to myopic pathology and its relevance to cataract surgery." Dev Ophthalmol **14**: 42-6.
Phillips, J. R. and McBrien, N. A. (2004). "Pressure-induced changes in axial eye length of chick and tree shrew: significance of myofibroblasts in the sclera." Invest Ophthalmol Vis Sci **45**(3): 758-63.
Quek, T. P., Chua, C. G., Chong, C. S., Chong, J. H., Hey, H. W., Lee, J., Lim, Y. F. and Saw, S. M. (2004). "Prevalence of refractive errors in teenage high school students in Singapore." Ophthalmic Physiol Opt **24**(1): 47-55.
Rada, J. A., Shelton, S. and Norton, T. T. (2006). "The sclera and myopia." Exp Eye Res **82**(2): 185-200.
Raviola, E. and Wiesel, T. N. (1985). "An animal model of myopia." N Engl J Med **312**(25): 1609-15.
Reis, R. A., Ventura, A. L., Kubrusly, R. C., de Mello, M. C. and de Mello, F. G. (2007). "Dopaminergic signaling in the developing retina." Brain Res Rev **54**(1): 181-8.
Rickers, M. and Schaeffel, F. (1995). "Dose-dependent effects of intravitreal pirenzepine on deprivation myopia and lens-induced refractive errors in chickens." Exp Eye Res **61**(4): 509-16.
Righetti, P. G. and Bossi, A. (1997). "Isoelectric focusing in immobilized pH gradients: an update." J Chromatogr B Biomed Sci Appl **699**(1-2): 77-89.
Robaei, D., Kifley, A., Rose, K. A. and Mitchell, P. (2006). "Refractive error and patterns of spectacle use in 12-year-old Australian children." Ophthalmology **113**(9): 1567-73.
Robbesyn, F., Auge, N., Vindis, C., Cantero, A. V., Barbaras, R., Negre-Salvayre, A. and Salvayre, R. (2005). "High-density lipoproteins prevent the oxidized low-density lipoprotein-induced epidermal [corrected] growth factor receptor activation and subsequent matrix metalloproteinase-2 upregulation." Arterioscler Thromb Vasc Biol **25**(6): 1206-12.
Rochette-Egly, C., Oulad-Abdelghani, M., Staub, A., Pfister, V., Scheuer, I., Chambon, P. and Gaub, M. P. (1995). "Phosphorylation of the retinoic acid receptor-alpha by protein kinase A." Mol Endocrinol **9**(7): 860-71.
Rohrer, B., Iuvone, P. M. and Stell, W. K. (1995). "Stimulation of dopaminergic amacrine cells by stroboscopic illumination or fibroblast growth factor (bFGF, FGF-2) injections: possible roles in prevention of form-deprivation myopia in the chick." Brain Res **686**(2): 169-81.
Rohrer, B., Spira, A. W. and Stell, W. K. (1993). "Apomorphine blocks form-deprivation myopia in chickens by a dopamine D2-receptor mechanism acting in retina or pigmented epithelium." Vis Neurosci **10**(3): 447-53.

Rosenberg, T. and Klie, F. (1996). "Current trends in newly registered blindness in Denmark." Acta Ophthalmol Scand **74**(4): 395-8.
Rymer, J. and Wildsoet, C. F. (2005). "The role of the retinal pigment epithelium in eye growth regulation and myopia: a review." Vis Neurosci **22**(3): 251-61.
Salgado-Pineda, P., Delaveau, P., Blin, O. and Nieoullon, A. (2005). "Dopaminergic contribution to the regulation of emotional perception." Clin Neuropharmacol **28**(5): 228-37.
Sasse, J. and Gallagher, S. R. (2004). "Staining proteins in gels." Curr Protoc Immunol **Chapter 8**: Unit 8 9.
Saw, S. M., Nieto, F. J., Katz, J., Schein, O. D., Levy, B. and Chew, S. J. (2000). "Factors related to the progression of myopia in Singaporean children." Optom Vis Sci **77**(10): 549-54.
Schaeffel, F., Bartmann, M., Hagel, G. and Zrenner, E. (1995). "Studies on the role of the retinal dopamine/melatonin system in experimental refractive errors in chickens." Vision Res **35**(9): 1247-64.
Schippert, R., Burkhardt, E., Feldkaemper, M. and Schaeffel, F. (2007). "Relative Axial Myopia in Egr-1 (ZENK) Knockout Mice." Invest Ophthalmol Vis Sci **48**(1): 11-17.
Schmid, K. L. and Wildsoet, C. F. (1996). "Effects on the compensatory responses to positive and negative lenses of intermittent lens wear and ciliary nerve section in chicks." Vision Res **36**(7): 1023-36.
Schmid, K. L. and Wildsoet, C. F. (1997). "The sensitivity of the chick eye to refractive defocus." Ophthalmic Physiol Opt **17**(1): 61-7.
Schmid, K. L. and Wildsoet, C. F. (2004). "Inhibitory effects of apomorphine and atropine and their combination on myopia in chicks." Optom Vis Sci **81**(2): 137-47.
Schweigert, F. J., Bathe, K., Chen, F., Buscher, U. and Dudenhausen, J. W. (2004). "Effect of the stage of lactation in humans on carotenoid levels in milk, blood plasma and plasma lipoprotein fractions." Eur J Nutr **43**(1): 39-44.
Seet, B., Wong, T. Y., Tan, D. T., Saw, S. M., Balakrishnan, V., Lee, L. K. and Lim, A. S. (2001). "Myopia in Singapore: taking a public health approach." Br J Ophthalmol **85**(5): 521-6.
Seino, S., Takahashi, H., Fujimoto, W. and Shibasaki, T. (2009). "Roles of cAMP signalling in insulin granule exocytosis." Diabetes Obes Metab **11 Suppl 4**: 180-8.
Seko, Y., Shimizu, M. and Tokoro, T. (1998). "Retinoic acid increases in the retina of the chick with form deprivation myopia." Ophthalmic Res **30**(6): 361-7.
Seltner, R. L. and Stell, W. K. (1995). "The effect of vasoactive intestinal peptide on development of form deprivation myopia in the chick: a pharmacological and immunocytochemical study." Vision Res **35**(9): 1265-70.
Sham, W. K., Dirani, M., Chong, Y. S., Hornbeak, D. M., Gazzard, G., Li, J. and Saw, S. M. (2009). "Breastfeeding and association with refractive error in young Singapore Chinese children." Eye.
Sharma, R., Mahajan, M., Singh, B., Bal, B. S. and Kant, R. (2006). "Apolipoprotein modifying effects of statins and fibrate in various age groups of coronary artery disease patients." J Indian Med Assoc **104**(9): 492-4, 496, 498.

Shen, W., Vijayan, M. and Sivak, J. G. (2005). "Inducing form-deprivation myopia in fish." Invest Ophthalmol Vis Sci **46**(5): 1797-803.
Sherman, S. M., Norton, T. T. and Casagrande, V. A. (1977). "Myopia in the lid-sutured tree shrew (Tupaia glis)." Brain Res **124**(1): 154-7.
Shih, Y. F., Fitzgerald, M. E., Norton, T. T., Gamlin, P. D., Hodos, W. and Reiner, A. (1993). "Reduction in choroidal blood flow occurs in chicks wearing goggles that induce eye growth toward myopia." Curr Eye Res **12**(3): 219-27.
Shih, Y. F., Fitzgerald, M. E. and Reiner, A. (1994). "The effects of choroidal or ciliary nerve transection on myopic eye growth induced by goggles." Invest Ophthalmol Vis Sci **35**(10): 3691-701.
Shih, Y. F., Hsiao, C. K., Chen, C. J., Chang, C. W., Hung, P. T. and Lin, L. L. (2001). "An intervention trial on efficacy of atropine and multi-focal glasses in controlling myopic progression." Acta Ophthalmol Scand **79**(3): 233-6.
Simo, R., Garcia-Ramirez, M., Higuera, M. and Hernandez, C. (2009). "Apolipoprotein A1 is overexpressed in the retina of diabetic patients." Am J Ophthalmol **147**(2): 319-325 e1.
Simon, P., Feldkaemper, M., Bitzer, M., Ohngemach, S. and Schaeffel, F. (2004). "Early transcriptional changes of retinal and choroidal TGFbeta-2, RALDH-2, and ZENK following imposed positive and negative defocus in chickens." Mol Vis **10**: 588-97.
Siripurkpong, P. and Na-Bangchang, K. (2009). "Effects of niacin and chromium on the expression of ATP-binding cassette transporter A1 and apolipoprotein A-1 genes in HepG2 cells." J Nutr Biochem **20**(4): 261-8.
Smith, E. L., 3rd and Hung, L. F. (2000). "Form-deprivation myopia in monkeys is a graded phenomenon." Vision Res **40**(4): 371-81.
Steinberg, T. H. (2009). "Protein gel staining methods: an introduction and overview." Methods Enzymol **463**: 541-63.
Stone, R. A., Laties, A. M., Raviola, E. and Wiesel, T. N. (1988). "Increase in retinal vasoactive intestinal polypeptide after eyelid fusion in primates." Proc Natl Acad Sci U S A **85**(1): 257-60.
Stone, R. A., Lin, T., Laties, A. M. and Iuvone, P. M. (1989). "Retinal dopamine and form-deprivation myopia." Proc Natl Acad Sci U S A **86**(2): 704-6.
Tarugi, P., Nicolini, S., Ballarini, G., Marchi, L., Duvigneau, C., Tartoni, P. and Calandra, S. (1996). "Synthesis and secretion of B-100 and A-I apolipoproteins in response to the changes of intracellular cholesteryl ester content in chick liver." J Lipid Res **37**(3): 493-507.
Tejedor, J. and de la Villa, P. (2003). "Refractive changes induced by form deprivation in the mouse eye." Invest Ophthalmol Vis Sci **44**(1): 32-6.
Tenenbaum, A., Motro, M., Fisman, E. Z., Tanne, D., Boyko, V. and Behar, S. (2005). "Bezafibrate for the secondary prevention of myocardial infarction in patients with metabolic syndrome." Arch Intern Med **165**(10): 1154-60.
Troilo, D. (1990). "Experimental studies of emmetropization in the chick." Ciba Found Symp **155**: 89-102; discussion 102-14.
Troilo, D., Gottlieb, M. D. and Wallman, J. (1987). "Visual deprivation causes myopia in chicks with optic nerve section." Curr Eye Res **6**(8): 993-9.

Tserentsoodol, N., Gordiyenko, N. V., Pascual, I., Lee, J. W., Fliesler, S. J. and Rodriguez, I. R. (2006). "Intraretinal lipid transport is dependent on high density lipoprotein-like particles and class B scavenger receptors." Mol Vis **12**: 1319-33.

Unlu, M., Morgan, M. E. and Minden, J. S. (1997). "Difference gel electrophoresis: a single gel method for detecting changes in protein extracts." Electrophoresis **18**(11): 2071-7.

Vessey, K. A., Rushforth, D. A. and Stell, W. K. (2005). "Glucagon- and secretin-related peptides differentially alter ocular growth and the development of form-deprivation myopia in chicks." Invest Ophthalmol Vis Sci **46**(11): 3932-42.

Wallman, J., Adams, J. I. and Trachtman, J. N. (1981). "The eyes of young chickens grow toward emmetropia." Invest Ophthalmol Vis Sci **20**(4): 557-61.

Wallman, J., Gottlieb, M. D., Rajaram, V. and Fugate-Wentzek, L. A. (1987). "Local retinal regions control local eye growth and myopia." Science **237**(4810): 73-7.

Wallman, J., Turkel, J. and Trachtman, J. (1978). "Extreme myopia produced by modest change in early visual experience." Science **201**(4362): 1249-51.

Wallman, J., Wildsoet, C., Xu, A., Gottlieb, M. D., Nickla, D. L., Marran, L., Krebs, W. and Christensen, A. M. (1995). "Moving the retina: choroidal modulation of refractive state." Vision Res **35**(1): 37-50.

Wang, P., Li, S., Xiao, X., Jia, X., Jiao, X., Guo, X. and Zhang, Q. (2009). "High myopia is not associated with the SNPs in the TGIF, lumican, TGFB1, and HGF genes." Invest Ophthalmol Vis Sci **50**(4): 1546-51.

Weiss, W. and Gorg, A. (2008). "Sample solublization buffers for two-dimensional electrophoresis." Methods Mol Biol **424**: 35-42.

Westbrook, A. M., Crewther, S. G., Liang, H., Beresford, J. A., Allen, M., Keller, I. and Crewther, D. P. (1995). "Formoguanamine-induced inhibition of deprivation myopia in chick is accompanied by choroidal thinning while retinal function is retained." Vision Res **35**(14): 2075-88.

Wiesel, T. N. and Raviola, E. (1977). "Myopia and eye enlargement after neonatal lid fusion in monkeys." Nature **266**(5597): 66-8.

Wildsoet, C. (2003). "Neural pathways subserving negative lens-induced emmetropization in chicks--insights from selective lesions of the optic nerve and ciliary nerve." Curr Eye Res **27**(6): 371-85.

Wildsoet, C. and Wallman, J. (1995). "Choroidal and scleral mechanisms of compensation for spectacle lenses in chicks." Vision Res **35**(9): 1175-94.

Wilkins, M. R., Sanchez, J. C., Gooley, A. A., Appel, R. D., Humphery-Smith, I., Hochstrasser, D. F. and Williams, K. L. (1996). "Progress with proteome projects: why all proteins expressed by a genome should be identified and how to do it." Biotechnol Genet Eng Rev **13**: 19-50.

Woessner, J. F., Jr. (1994). "The family of matrix metalloproteinases." Ann N Y Acad Sci **732**: 11-21.

Xing, D. and Bonanno, J. A. (2009). "Effect of cAMP on TGFbeta1-induced corneal keratocyte-myofibroblast transformation." Invest Ophthalmol Vis Sci **50**(2): 626-33.

Yalcin, A., Telang, S., Clem, B. and Chesney, J. (2009). "Regulation of glucose metabolism by 6-phosphofructo-2-kinase/fructose-2,6-bisphosphatases in cancer." Exp Mol Pathol **86**(3): 174-9.

Yan, J. X., Sanchez, J. C., Rouge, V., Williams, K. L. and Hochstrasser, D. F. (1999). "Modified immobilized pH gradient gel strip equilibration procedure in SWISS-2DPAGE protocols." Electrophoresis **20**(4-5): 723-6.

Yang, Z., Lan, W., Ge, J., Liu, W., Chen, X., Chen, L. and Yu, M. (2009). "The effectiveness of progressive addition lenses on the progression of myopia in Chinese children." Ophthalmic Physiol Opt **29**(1): 41-8.

Yoshino, M., Mizutani, T., Yamada, K., Tsuchiya, M., Minegishi, T., Yazawa, T., Kawata, H., Sekiguchi, T., Kajitani, T. and Miyamoto, K. (2002). "Early growth response gene-1 regulates the expression of the rat luteinizing hormone receptor gene." Biol Reprod **66**(6): 1813-9.

Zaiou, M., Azrolan, N., Hayek, T., Wang, H., Wu, L., Haghpassand, M., Cizman, B., Madaio, M. P., Milbrandt, J., Marsh, J. B., Breslow, J. L. and Fisher, E. A. (1998). "The full induction of human apoprotein A-I gene expression by the experimental nephrotic syndrome in transgenic mice depends on cis-acting elements in the proximal 256 base-pair promoter region and the trans-acting factor early growth response factor 1." J Clin Invest **101**(8): 1699-707.

Zannis, V. I., Chroni, A. and Krieger, M. (2006). "Role of apoA-I, ABCA1, LCAT, and SR-BI in the biogenesis of HDL." J Mol Med **84**(4): 276-94.

Zawilska, J. B., Bednarek, A., Berezinska, M. and Nowak, J. Z. (2003). "Rhythmic changes in metabolism of dopamine in the chick retina: the importance of light versus biological clock." J Neurochem **84**(4): 717-24.

Zha, Y., Leung, K. H., Lo, K. K., Fung, W. Y., Ng, P. W., Shi, M. G., Yap, M. K. and Yip, S. P. (2009). "TGFB1 as a susceptibility gene for high myopia: a replication study with new findings." Arch Ophthalmol **127**(4): 541-8.

Zhang, W., Zhao, J., Chen, L., Urbanowicz, M. M. and Nagasaki, T. (2008). "Abnormal epithelial homeostasis in the cornea of mice with a destrin deletion." Mol Vis **14**: 1929-39.

Zhao, Q., Tao, J., Zhu, Q., Jia, P. M., Dou, A. X., Li, X., Cheng, F., Waxman, S., Chen, G. Q., Chen, S. J., Lanotte, M., Chen, Z. and Tong, J. H. (2004). "Rapid induction of cAMP/PKA pathway during retinoic acid-induced acute promyelocytic leukemia cell differentiation." Leukemia **18**(2): 285-92.

Zheng, X. L., Matsubara, S., Diao, C., Hollenberg, M. D. and Wong, N. C. (2001). "Epidermal growth factor induction of apolipoprotein A-I is mediated by the Ras-MAP kinase cascade and Sp1." J Biol Chem **276**(17): 13822-9.

Zhu, X., Lin, T., Stone, R. A. and Laties, A. M. (1995). "Sex differences in chick eye growth and experimental myopia." Exp Eye Res **61**(2): 173-9.

Zhu, X., Park, T. W., Winawer, J. and Wallman, J. (2005). "In a matter of minutes, the eye can know which way to grow." Invest Ophthalmol Vis Sci **46**(7): 2238-41.

Zhu, X. and Wallman, J. (2009). "Opposite effects of glucagon and insulin on compensation for spectacle lenses in chicks." Invest Ophthalmol Vis Sci **50**(1): 24-36.

Zhu, X. and Wallman, J. (2009). "Temporal properties of compensation for positive and negative spectacle lenses in chicks." Invest Ophthalmol Vis Sci **50**(1): 37-46.

Zhu, Y., Wang, H. J., Chen, L. F., Fang, Q. and Yan, X. W. (2007). "Study of ATP-binding cassette transporter A1 (ABCA1)-mediated cellular cholesterol efflux in diabetic golden hamsters." J Int Med Res **35**(4): 508-16.